DISSERTATION

The Study of Amyloid beta (Aβ) induced ADF/cofilin Rods in Cultured Neurons: Implications in Alzheimer's disease and Neurodegeneration

Submitted by

Michael T. Maloney

Department of Biochemistry and Molecular Biology

In partial fulfillment of the requirements

For the Degree of Doctor of Philosophy

Colorado State University

Fort Collins, CO

Summer 2006

COLORADO STATE UNIVERSITY

June 20, 2006

WE HEREBY RECOMMEND THAT THE DISSERTATION PREPARED UNDER OUR SUPERVISION BY MICHAEL T. MALONEY ENTITLED THE STUDY OF AMYLOID BETA (Aβ) INDUCED ADF/COFILIN RODS IN CULTURED NEUORNS: IMPLICATIONS IN ALZHEIMER'S DISEASE AND NEURODEGENERATION BE ACCEPTED AS FULFILLING IN PART THE REQUIREMENTS FOR THE DEGREE OF DOCTOR OF PHILOSOPHY.

Committee on Graduate Work

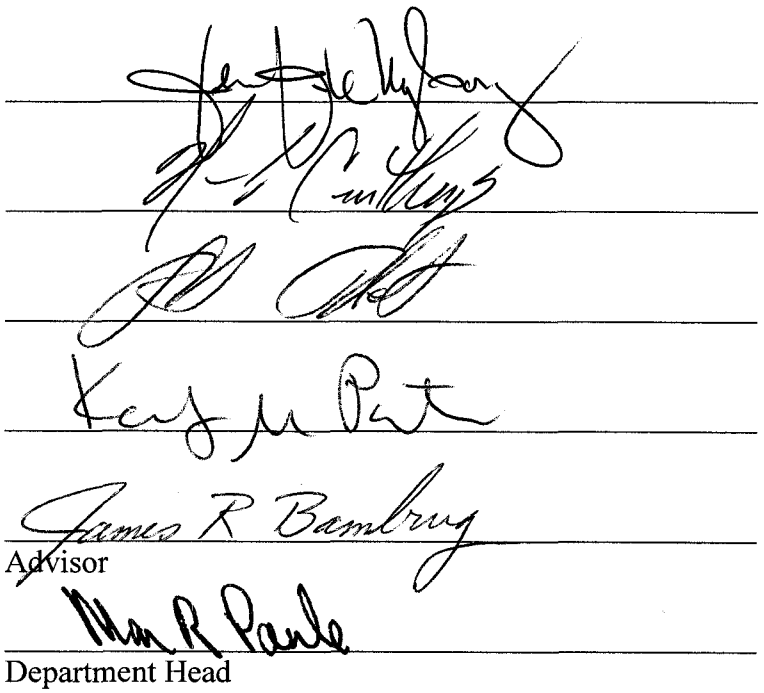

Advisor

Department Head

ABSTRACT OF DISSERTATION

The Study of Amyloid beta (Aβ) induced ADF/cofilin Rods in Cultured Neurons: Implications in Alzheimer's disease and Neurodegeneration

Rods are intracellular proteinaceous aggregates composed mainly of actin saturated with ADF/cofilin that form in response to stress. Neurodegenerative stress mimicked *in vitro* with ATP depletion, glutamate excitotoxicity and peroxide all are potent mediators of rod formation. In neurons, rods form in linear arrays within neurites and disrupt distal neurite function. Rods can become large enough to completely occlude the neurite and thereby disrupt distal microtubules interfering with anterograde and retrograde transport. Treatment of both organotypic hippocampal slice cultures and dissociated neuronal cultures with as little as 10 nM of soluble amyloid beta peptides ($A\beta_{1\text{-}42}$) induces rod formation. $A\beta_{1\text{-}42}$ induces rods in half the responding population of dissociated neurons within 6 hours and a maximal response of less than 20% of neurons with rods occurring by 24 hours. Thus $A\beta_{1\text{-}42}$ induced rods form rapidly in a sensitive sub-population of neurons. Transport defects are among the earliest abnormalities to occur in the brains of an AD mouse model (Tg-swAPP^{prp}) and synaptic pruning associated with cognitive decline begins to occur before overt neuronal loss. In cultured neurons accumulation of vesicles containing the amyloid precursor protein (APP), β-amyloid cleavage enzyme, and presenilin 1 (a member of the γ-secretase complex) occur

at rods. These trafficking defects may represent a site for increased amyloidogenic processing of APP into the Aβ peptides associated with Alzheimer's disease (AD) related senile plaques, extracellular deposits of aggregated Aβ peptide. In human AD brain nearly every senile plaque is associated with rod-like cofilin pathology. A feed foreword catalytic spiral is proposed wherein transient stress or Aβ induces rods leading to increased local Aβ production within stalled vesicles followed by increased extracellular Aβ, senile plaque deposition and further rod formation in the surrounding neuropil. Work included in this dissertation establishes a hippocampal slice culture system. Slice cultures will allow for continued investigations into the phenomenon of Aβ induced rod formation in an experimentally manipulatible system where neurons are kept in a more normal relationship with their surrounding cells. Such a system can be used to study the progression and pathology of Alzheimer's disease and other neurodegenerative amyloidopathies.

Michael T. Maloney
Department of Biochemistry
and Molecular Biology
Colorado State University
Fort Collins, CO 80523
Summer 2006

DEDICATION AND ACKNOWLEDGEMENTS

First and foremost, this work is dedicated to my mother Patricia L. Maloney whose personal struggle with early onset Alzheimer's disease has forever altered my path in life. In her memory and in memorial to all who have personally or indirectly suffered under the burden of a neurodegenerative disease, I present this dissertation in defense of my graduate research and education. This body of work represents my entrance into a lifelong pursuit for cures and therapies to neurodegenerative diseases.

I'd like to thank Dr. James R. Bamburg for guidance and direction. Dr. Bamburg has risen mentoring to an art form, continuously refining his craft. His dedication and love for teaching and fundamental research is an inspiration. I am blessed to have had the opportunity to work alongside such an accomplished scientist. Thanks also to Laurie Minamide, the lab manager, for teaching me nearly every technique used in my research today. Laurie is a pleasure to work with, an invaluable resource of knowledge, a great scientist and a good soul. Next I would like to thank Dr. Barbara W. Bernstein for her keen eye for experimental design and good sense. Barb has always kept an open mind during our countless scientific discussions and has been instrumental in guiding the direction of my research. As not to ramble I would simply like to thank the entire Bamburg lab staff past and present especially: Dr. Judy Boyle, Dr. Ravine Gungabissoon, Dr. Sankar Maiti, Dr. O'Neil Wiggan, Dr. Andy Kinley, Dr. Joe Fass, Dr. Lubna Tahtamouni, Alisa Shaw, Kevin Flynn, Janel Funk, Chi Pak, Hui Hung, Jennifer Durden, Rashmi Sampath, Denise Schafer, Katie McDermott and Hilary Bowden for being terrific. Additionally I would like to thank my advisory committee: Dr. Norm

Curthoys, Dr. Jenny Nyborg, Dr. Kathy Partin, and Dr. Stu Tobet for critical evaluation and guidance.

Finally I would like to thank my family beginning with my father John M. Maloney who is my moral compass and personal hero. Thank you brother Mark and sister Pamela for your friendship and support. A special thank you to my fiancée Janice Gonzalez, who I met in the Bamburg lab, for being my light in a dark world. Lastly sincere thanks go out to my friends and to the Gonzalez family.

TABLE OF CONTENTS

LIST OF FIGURES

TABLE OF ABBREVIATIONS

$\Delta\Psi_m$	mitochondrial membrane potential
Aβ	amyloid beta
$A\beta_{1-42}$	42 amino acid species of amyloid beta
AC	ADF/cofilin
AD	Alzheimer's disease
ADAM	a disintegrin and metalloproteinase domain
ADDL	Aβ derived diffusible ligands
ADF	actin depolymerizing factor
ADF-H	ADF homology domain
ADP	adenosine di-phosphate
AFM	atomic force microscopy
AICD	APP intracellular domain
ALS	amyotrophic lateral sclerosis
ANOVA	analysis of variance
APC	adenomatous polyposis coli
ApoE	apolipo protein E
APP	amyloid precursor protein
APPL	APP-like protein
ATP	adenosine tri-phosphate
BACE	β-amyloid cleavage enzyme
BFCN	basal forebrain cholinergic neuron
C83	83 amino acid C-terminal fragment of APP
C99	99 amino acid C-terminal fragment of APP
C-terminus	Carboxyl terminus
CA1	cornu ammonis region 1
CA3	cornu ammonis region 3
CFP	cyan fluorescent protein
CTF	C-terminal fragment
DAPI	4'-6-Diamidino-2-phenylindole
DG	dentate gyrus
div	days *in vitro*
DMSO	dimethylsulfoxide
DNaseI	Deoxyribonuclease I
DS	Down syndrome
EM	electron microscopy
ER	endoplasmic reticulum
f	fimbira
F-actin	Filamentous actin
FAD	familial Alzheimer's disease
FAK	focal adhesion kinase
G-actin	Globular actin
GBSS	Gey's balance salt solution
GFP	green fluorescent protein
GPCR	G-protein coupled receptor

GSK3	glycogen synthase kinase 3
HBSS	Hank's balanced salt solution
JIP1	c-Jun NH2-terminal kinase-interacting protein
JNK	c-jun-N-terminal kinase
LDL	low-density lipoprotein
LIMK	Lin-11, Isl-1, Mec-3 Kinase
LMW	low molecular weight
LTD	long-term depotentiation
LTP	long-term potentiation
MAPK	mitogen activated protein kinase a.k.a. microtubule associated protein kinase
na	numerical aperture
NFT	neurofibrillary tangle
NP	neuritic plaque
NMDA	N-methyl-d-aspartate
NMR	nuclear magnetic resonance
N-terminus	Amino terminus
NBM	nucleus basalis magnocellularis
NGF	nerve growth factor
OGD	oxygen-glucose deprivation
p(protein)	phosphorylated form of indicated protein
PAK	p21 activated kinase
PBS	Phosphate-buffered saline
PDGF	platelet derived growth factor
PHF	paired helical filament
P*i*	inorganic phosphate
PIP_2	phosphatidyl inositol 4,5 bisphosphate
PKC	protein kinase C
PS1/2	presenilin 1/2
RFP	red fluorescent protein
ROCK	rho kinase
ROS	reactive oxygen species
S2P	site 2 protease
S3D	amino acid 3 mutated from serine to aspartate
sAPPα	soluble N-terminus of APP following α-secretase cleavage
sAPPβ	soluble N-terminus of APP following β-secretase cleavage
S.D.	standard deviation
S.E.M.	standard error of means
SOD	super oxide dismutase
SSH	slingshot phosphatase
STS	staurosporine
TACE	TNF-α cleavage enzyme
TBS	Tris-buffered saline
TESK	testicular protein kinase
TGN	trans-Golgi network
Tg	transgenic

VDAC	voltage gated anion channel
Wnt	Wingless
wt	wild type
XAC	*Xenopus* ADF/cofilin
YFP	yellow fluorescent protein

Chapter One

Background and Introduction

Summary

Portions of this introduction were taken from a chapter on actin in disease to be published in 2006. The order of authors is as follows: Michael Maloney, Andy Kinley, Chi Pak and James Bamburg. The actin cytoskeleton is a network of filaments whose assembly and dynamics are regulated to a large degree by the ADF/cofilin family of proteins. Defects in actin structure and dynamics can be linked with a wide range of diseases and neurodegenerative conditions. Significant progress has been made in understanding the how the misregulation of actin and ADF/cofilin in response to neurodegenerative stress may represent an early feature of progressive degeneration in Alzheimer's disease (AD) and potentially in other neurodegenerative diseases as well.

History of AD

Alois Alzheimer first described nearly a century ago a neurodegenerative condition as, "an unusual illness of the cerebral cortex," that now bears his name (Alzheimer, 1907). Alzheimer was among the first individuals to posit that pathological changes in the post mortem brains of demented patients were tied to the progression of degenerative disorders responsible for abnormal behaviors. Among these pathological markers Alzheimer noted the presence of fibrils and miliary foci (amyloid) in the diseased damaged brain. Despite the long history, the cause of and treatments for AD have eluded physicians and scientists.

A positive diagnosis of AD requires selective neuron loss in specific brain regions, neuritic plaques composed of extracellular aggregates of β-Amyloid (Aβ), and neurofibrillary tangles (NFT's), composed of paired helical filaments (PHF's) of aggregated and hyper-phosphorylated tau protein (Iqbal & Grundke-Iqbal, 1996; James *et al.*, 1996; Wisniewski & Wegiel, 1992). Areas of the brain typically affected by amyloid plaques are the hippocampus, involved in learning and memory, and the neo-cortex, involved in higher brain functions. The symptoms of AD are believed to develop years after neurological damage has begun. Amyloid plaques are extracellular lesions composed of a core of fibrillar Aβ surrounded by dystrophic neurites and reactive glial cells. In 1991 missence mutations in the amyloid precursor protein (APP) were found linked to autosomal dominant, early onset familial AD (FAD) (Chartier-Harlin *et al.*, 1991a). These mutations occur in and around the Aβ region of the APP resulting in heightened production of the Aβ peptide, a proteolytic product derived from APP. The "amyloid hypothesis" states that the progressive accumulation and deposition of Aβ occurs in the brain over decades leading to neuronal dysfunction and eventually to clinical manifestation of AD (Chartier-Harlin *et al.*, 1991b; Goate *et al.*, 1991; Murrell *et al.*, 1991; Glenner & Wong, 1984b). Strong support for the amyloid hypothesis stems from the fact that Down syndrome individuals, trisomic for chromosome 21 (the genetic locus of APP), invariably develop AD pathology.

Amyloid Precursor Protein Processing

APP is a receptor-like trans-membrane glycoprotein consisting of an extra cellular amino-terminal domain, a single trans-membrane domain and a short cytoplasmic

carboxy-terminal domain (Fig 1.1). APP is expressed in a variety of cell types and tissues throughout the body (Mattson, 2004). The function of APP has not been fully characterized, however a *Drosophila* homologue APP-like (APPL) protein interacts with APPL-interacting protein 1 (APPL1) (Taru *et al.*, 2002). APPL1 shares high homology with JIP1 and 2, the mammalian MAPK family protein c-jun-N-terminal kinase (JNK) interacting proteins. Over expression of JIP1 and 2 in cells regulates the JNK dependent phosphorylation of APP (Taru *et al.*, 2002). Thus the JNK-JIP-APP interaction appears to be conserved and may play an important role in the metabolism and functioning of APP in higher eukaryotes.

Cleavage of APP occurs in its extra cellular domain by the proteases α- and β-secretase (Fig 1.1). Both α- and β-secretase cleavage generates an amino-terminal soluble fragment (sAPPα and sAPPβ) and an 83 (α-secretase) or 99 (β-secretase) residue carboxy-terminal fragment (C83 and C99) that remain membrane bound. α-Secretase is a metalloprotease that displays increased activity in response to phorbol esters that activate protein kinase C (PKC). β-Secretase, also known as β-amyloid cleavage enzyme (BACE) (Saunders *et al.*, 1999), localizes primarily to the Golgi and late endosomes, although it can also be detected in the plasma membrane.

Following α- or β-secretase cleavage, to produce C83 and C99 respectively, a second cleavage occurs within the trans-membrane domain by γ-secretase (Fig 1.1). C83 cleavage typically produces a soluble form of $A\beta_{1-40}$ whereas C99 cleavage produces the hydrophobic amyloidogenic $A\beta_{1-42}$ peptide (sequential cleavage of APP by β- and γ-secretases can give $A\beta_{1-39}$ to $A\beta_{1-43}$). Mutations found in FAD result in increased production and deposition of $A\beta_{1-42}$. To date no mutations have been identified in

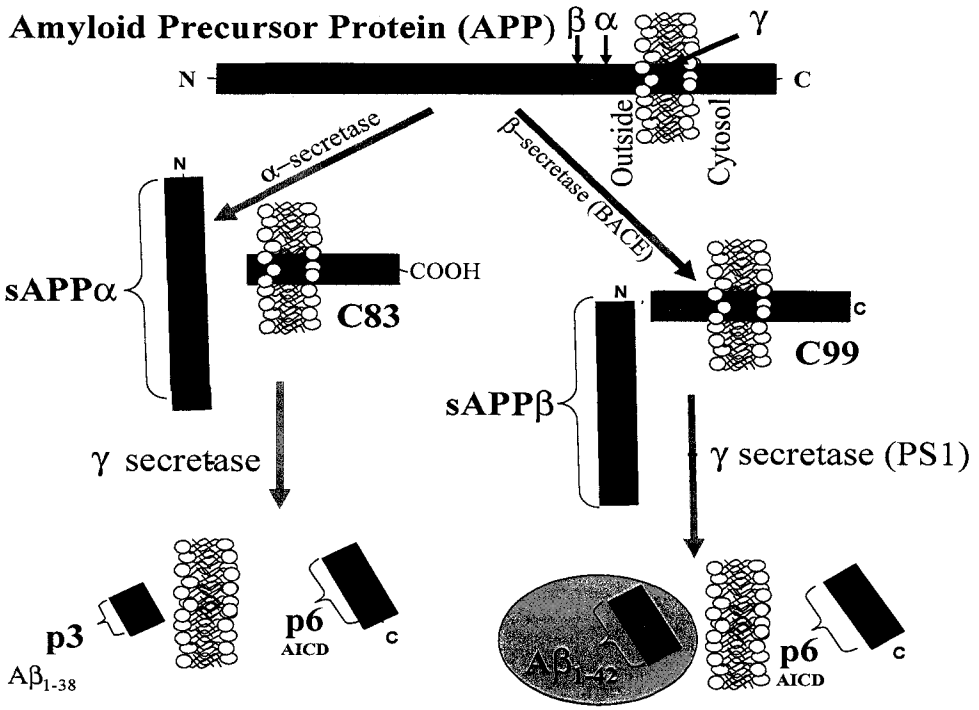

Figure 1.1: APP proteolytic processing. APP cleavage by α-secretase releases the soluble N-terminal fragment (sAPPα) and leaves the membrane bound C83 fragment. Subsequent cleavage of C83 by γ-secretase releases the p3 fragment and p6 APP intracellular domain (AICD). Alternatively APP cleavage by β-secretase releases the soluble N-terminal fragment (sAPPβ) and leaves the membrane bound C99 fragment. Subsequent cleavage of C99 by γ-secretase produces p6 AICD and the amyloidogenic $A\beta_{1-42}$ peptide.

BACE1, residing on chromosome 11, that correlate with an increased occurrence of AD, however a homologue, BACE2, has been identified on chromosome 21. This raises the possibility that BACE-like enzymatic activity may be partly responsible for the increased occurrence of AD in individuals with Down syndrome (Trisomy 21).

Alternative Processing and Interactions

γ-Secretase activity has also been implicated in proteolytic cleavage of Notch, a trans-membrane protein involved in cellular differentiation during nervous system development. The interaction of membrane bound proteins Delta, Jagged or Serrate, on one cell, with membrane bound Notch on another cell stimulates Notch cleavage. Following cleavage, the cytosolic tail of Notch translocates to the nucleus where it acts as a transcription factor. Cleavage of the cytosolic tails of both Notch and APP has been demonstrated to activate transcription. These similarities suggest that APP may play a role in signaling pathways similar to those of Notch (Selkoe, 2001).

In 1995 the catalytic subunit of the γ-secretase complex was isolated and identified as Presenilins 1 and 2 (PS1/2) (Levy-Lahad *et al.*, 1995; Rogaev *et al.*, 1995; Sherrington *et al.*, 1995). The genes encoding presenilins 1 and 2 are located on chromosome 14 and chromosome 1, respectively. Mutations in the presenilins have since been linked to increased production of $A\beta_{1-42}$, and are more prominent in FAD than are mutations in APP itself (Esler & Wolfe, 2001; Tsuda *et al.*, 1995). The presenilins are the catalytic components of the γ-secretases that process APP, therefore they are also likely to act as catalytic components of related proteases that clip transmembrane regions of Notch. SEL-12 is a PS1/2 homologue in *C. elegans* with 50% sequence homology.

SEL-12 functions as a co-receptor for the Notch receptor LIN-12 (Berezovska *et al.*, 1999). Defects in SEL-12 produce constitutive activation of LIN-12 that can be rescued by the introduction of human PS1/2 (Lenbaum & Levy-Lehad, 1998). This discovery raises the possibility that presenilins play a direct role in Notch signaling pathways. At first glance PS1 and 2 (γ-secretase) appear to be prime targets for therapeutic intervention, however the similarities between Notch and APP proteolytic processing raises strong concern regarding serious and unforeseen side effects likely to occur due to effects on Notch signaling *in vivo*.

Cleavage of APP by PS1 occurs largely in the endoplasmic reticulum (ER) and late endosomes. PS1's carboxy terminal fragment can be phosphorylated by PKC, though the physiological significance is not yet clear, this phosphorylation may regulate the PS1/2 turnover rate or interaction with other cellular factors (Fluhrer *et al.*, 2004). Alternative proteolysis of presenilins can occur at a site distal to their normal cleavage site mediated by a member of the caspase-3 family of apoptotic cysteine proteases. An FAD linked mutation has been found to make PS2 more susceptible to caspase-3 mediated alternative proteolysis. This finding suggests that mutations leading to the altered endoproteolysis of presenilins as well as mutations leading to the altered proteolytic processing of APP may also be involved in FAD.

Oxidative stress and AD

Mutant presenilins possess the constitutive ability to render neurons more vulnerable to a variety of neuronal injuries, including oxidative stress (Kim & Tanzi, 1997). Oxidative stress is a process in which the levels of oxygen free radicals (reactive

oxygen species or ROS) become elevated or antioxidant levels are decreased or both. Free radicals likely play a role in a variety of diseases such as AD, Parkinson's disease, cataracts and macular degeneration. The occurrence of oxidative stress increases with age, and is considered a part of the normal ageing process. ROS are produced by a stepwise monovalent reduction of O_2 to form super oxide (O_2^-), hydrogen peroxide (H_2O_2) or hydroxy free radicals (OH^-). Superoxide and peroxides are particularly nasty because they can readily permeate biological membranes, and hydroxy radicals can oxidize biological substrates, which then may become cross-linked. Oxidative damage occurs to lipids, proteins and DNA. Iron acts as a reducing agent via the Fenton reaction to produce destructive hydroxy radicals from super oxide and peroxide. The Fenton reaction is a univalent reduction of super oxide to produce H_2O_2 (Bryan, 1996). Cells utilize several enzymes to keep these activated oxygen species under regulation. Super oxide dismutase (SOD), also found on chromosome 21, forms peroxide and oxygen from super oxides within cellular compartments that produce activated oxygen. Catalase is an enzyme that catalyzes the dismutation of H_2O_2 to H_2O and O_2 (Bryan, 1996). Antioxidants, readily obtained from dietary sources, L-ascorbic acid (Vitamin C) and α-tocopheral (Vitamin E) both reduce oxygen free radicals (Bryan, 1996). Despite all of the body's hard work at managing activated oxygen species, the damage inflicted mounts over years and decades.

Several hypotheses link oxidative stress and neurodegeneration in AD brain with increased production and deposition of Aβ (Pike *et al.*, 1995a). Aβ can induce production of ROS in treated cells (Cafe *et al.*, 1996; Harris *et al.*, 1995; Ueda *et al.*, 1997), and is able to generate free radicals (Hensley *et al.*, 1996; Hensley *et al.*, 1994).

Synthetic Aβ fragments promote lipid peroxidation and increase protein carbonyl formation in neuronal cell cultures. Aβ induced oxidative stress is likely to impair mitochondrial function (Kaneko *et al.*, 1995) and decrease ATP production (Mark *et al.*, 1995; Mattson *et al.*, 1992; Zhang *et al.*, 1996). This Aβ mediated decrease in mitochondrial efficiency inevitably leads to increased release of ROS, which damage mitochondria and leads to more ROS production. It is this intimate link between Aβ, mitochondria and ROS makes it hard to determine where the degenerative spiral begins. Further studies are needed to determine if impaired energy metabolism or oxidative damage play a primary or secondary role in Aβ cytotoxicity (Aksenov *et al.*, 1998).

Cholesterol Metabolism and AD

Site 2 protease (S2P) is a polytopic membrane protein containing a zinc-coordinated active site, like that of the γ-secretases, responsible for processing a transcription factor involved in cholesterol metabolism (Wolfe *et al.*, 1999). α- and β-secretases are also membrane-anchored versions of known protease families and it is likely that these membrane-tethered forms, and their soluble relatives, are derived from common ancestral proteins. Sequence similarity around critical aspartate residues have been described between S2P-like proteases and presenilins (Wolfe *et al.*, 1999). Such similarities between proteins involved in cholesterol metabolism and APP processing suggest that these pathways may interact.

Apolipo protein E (ApoE) is the primary protein component of central nervous system lipoproteins. Possession of one or two ε-4 alleles of ApoE, normally involved in lipid transport, results in increase Aβ deposition in the brain before clinical symptoms of

AD arise thus implicating defects in cholesterol metabolism in the pathology of AD. Additional evidence for a link between cholesterol metabolism and neurodegenerative diseases is found in Niemann Pick Type C1 (NPCI) disease. NPC1disease is a cholesterol storage disorder, caused by mutations in the NPC1 gene, where Amyloid plaques are also noted in the pathology (Ohm *et al.*, 2003). Cholesterol metabolism and AD will be covered in greater detail in chapter four of this dissertation.

Focal Adhesions, Transcription Factors and AD

PS1 has been shown to interact with the catenin family of proteins, which are homologous to the *Drosophila* Armadillo family, involved in the Wnt-signaling pathway. In epithelial tissue in the absence of the Wnt ligand, β-catenin is bound to a complex of axin, adenomatous polyposis coli (APC), and glycogen synthase kinase 3β (GSK3β), the latter component which phosphorylates β-catenin targeting it for ubiquitination and proteosome destruction. In the presence of Wnt ligand, Wnt binds to Frizzled, a G-protein coupled receptor (GPCR), which activates Disheveled (Li *et al.*, 2006). Disheveled, working through FRAT, inhibits GSK3β, thus increasing the cytoplasmic pool of β-catenin. Activated β-catenin translocates to the nucleus where it acts as a transcription factor to signal cell division. β-Catenin is also known to be involved in epithelial adherens junctions, where it links the transmembrane cadherins to F-actin through interaction with α-catenin. In the brain PS1 interacts with the δ-catenin isoform. Both Notch and Wnt signaling pathways have been shown to be mutually inhibitory to one another and are functionally associated via convergence with the protein Disheveled (Grilli *et al.*, 2002). The human homologue of disheveled has been mapped to a region of

chromosome 3 inked to late-onset AD (Russ *et al.*, 2002). This evidence indicates that differential molecular interactions of the presenilins modulated in a tissue-specific or developmental stage specific manner may control different roles of the normal or mutant forms of the presenilins during development and in adulthood.

Effects of the Aβ Peptide

The Aβ peptides released by β- and γ-secretase cleavage of APP undergo a transition from non-aggregated Aβ (monomers) to oligomers and on to fibrils. This transition is marked by conformational changes in the peptide backbone. Monomeric non-aggregated $A\beta_{1-42}$ exists predominantly as a random-coil or it can adopt alpha helical motifs following treatment with fluorinated alcohols which are used to remove structural artifacts introduced during chemical synthesis (Dahlgren *et al.*, 2002). Folding intermediates on the pathway to fibril formation have been isolated thus demonstrating soluble oligomers possess a common conformation unique from those of monomeric and fibrillar $A\beta_{1-42}$ (Torok *et al.*, 2002; Walsh *et al.*, 1999). The different structures preferred by monomers, oligomers, and fibrils have been utilized to develop oligomeric specific antibodies (Kayed *et al.*, 2003). A central region of $A\beta_{1-42}$, spanning residues 31–35, is required for interacting with cellular membranes (Bond *et al.*, 2003). This membrane interaction surface is thought to be responsible for the heightened toxicity of oligomeric $A\beta_{1-42}$. Mature fibrils are dominated by beta sheet structures in which hydrophobic residues 17-20 are in contact with the toxic hydrophobic residues 31-35 (Lee *et al.*, 1995; Li *et al.*, 1999). Though assembly dynamics are still under investigation, it is believed that the burial of the reactive side chains in mature fibrils is in part responsible for their

reduced toxicity as compared to oligomeric structures (Chaney *et al.*, 1998; Petkova *et al.*, 2002).

Following their addition to cultured neurons, the $A\beta_{1-42}$ peptide aggregates remain stable and localize predominantly along the substrate (Pike *et al.*, 1992; Pike *et al.*, 1995b). Freshly prepared $A\beta_{1-40}$ or $A\beta_{1-42}$ both possess a random coil conformation and display little toxicity. It is only after undergoing changes induced by prolonged incubation to form fibrils, β-pleated sheet structure, that the $A\beta_{1-42}$ is found to damage cultured neurons (Pike *et al.*, 1993; Pike *et al.*, 1991a; Pike *et al.*, 1991b). Fibril preparations often consist of a spectrum of insoluble monomeric and oligomeric aggregates. High-speed centrifugation (100000 x g) of fibril preparations separates the insoluble fraction (fibrils) from soluble contaminants (monomers and oligomers). The purified fibrils will remain stable in cell culture conditions for extended periods of time (Kim *et al.*, 2003).

Correlations between fibrillar plaque density and the severity of dementia in AD brains are weak, whereas correlations between levels of soluble Aβ (oligomers) and the extent of synaptic loss and cognitive impairment are stronger (Dickson *et al.*, 1995; Lue *et al.*, 1999; McLean *et al.*, 1999; Terry *et al.*, 1991). Aβ oligomers inhibit neuronal viability ~10 fold more than fibrils and ~40 fold more than unaggregated peptide (monomers), with oligomeric $A\beta_{1-42}$-induced inhibition significant at 10 nM (Dahlgren *et al.*, 2002). Small diffusible Aβ oligomers (referred to ADDL, for Aβ derived diffusible ligands) kill mature neurons in organotypic central nervous system cultures at nanomolar concentrations (Lambert *et al.*, 1998). Aβ oligomers, in the absence of monomers and amyloid fibrils, disrupt synaptic plasticity *in situ* at concentration found in human brain

and cerebrospinal fluid. In addition, meta-stable intermediates in Aβ fibril formation (protofibrils) alter the electrical activity of neurons and cause neuronal loss.

Aβ selectively depresses excitatory synaptic transmission in neurons that overexpress APP, as well as in nearby neurons that do not (Ashenafi *et al.*, 2005). This depression depends on N-methyl-d-aspartate (NMDA) receptor activity and can be reversed by blockade of neuronal activity. The synaptic depression from excessive Aβ may contribute to cognitive decline during early AD. In addition it has been proposed that activity-dependent modulation of endogenous Aβ production may normally participate in a negative feedback to keep neuronal hyperactivity in check (Kamentz *et al.*, 2003). Disruption of this feedback system could also contribute to disease progression in AD.

$A\beta_{1-42}$ soluble oligomers have been reported to possess selective toxicity against the CA1 subfield of hippocampal neurons while having little or no toxicity against the CA3 subfield or cerebellar neurons (Kim *et al.*, 2003). In the same study fibrils were reported to be toxic to the entire hippocampus without subfield specificity as well as toxic against cerebellar neurons. ADDL have demonstrated selective toxicity against the CA3 subfield of the hippocampus. These contradictory results of oligomer vs. ADDL selective toxicity are currently unresolved. Understanding how and why the aggregated state of $A\beta_{1-42}$ delivers selective neurotoxicity is one of the questions under investigation in this dissertation.

A connection between tau pathology and amyloid plaques has been sought after for some time but to no avail. Platelet derived growth factor (PDGF) is a potent activator of APP β/γ-cleavage, giving rise to an increased generation of $A\beta_{1-42}$ through a pathway

involving the non-receptor tyrosine kinase Src and the small G-protein Rac 1 (Gianni *et al.*, 2003). Rac has been implicated in neurite outgrowth and axonal path finding (Ahmed *et al.*, 2006). Immediate downstream effectors of Rac1 are the PAK serene/threonine kinases, which become activated upon the binding of Rac-GTP or Cdc42-GTP to their N-terminal auto inhibitory domain. A second known effecter downstream of Rac1 is Cdk5 (Nikolic *et al.*, 1998). Cdk5 is one of the two kinases involved in the hyperphosphorylation of tau, a microtubule associated protein, in fibrillary tangles, suggesting that Rac 1 activation could, at the same time, increase Aβ generation and cause tau hyperphosphorylation.

The activities of the MAPK family members ERK1/2 were increased by treatment of cultured hippocampal neurons with fibrillar Aβ (Rapoport & Ferreira, 2000). Increased MAPK activity remained evident even after 4 days of treatment. $A\beta_{1-42}$ treated neurons showed increased hyperphosphorylation of tau. This hyperphosphorylation occurs on tyrosine residues and results in the appearance neuritic dystrophy (Rapoport & Ferriera, 2000). $A\beta_{1-42}$ treated neurons also showed an increased association of the tyrosine kinase Fyn with the non-receptor focal adhesion kinase (FAK). Fyn is a member of the Src family of tyrosine kinases. $A\beta_{1-42}$ treated neurons also show an increase in the activation of the MAP kinase family member ERK-2. Blocking of Src and PI3 Kinase activity by specific inhibitors can disrupt the tyrosine phosphorylation of Fyn and the subsequent activation of the MAPK signaling in $A\beta_{1-42}$ treated neurons. Thus, the FAK/Fyn/PI3K association is upstream of MAPK signaling in Aβ treated neurons. This cascade of signaling events are the earliest biochemical changes in neurons to be described in response to Aβ exposure.

Apoptosis is a highly regulated cellular death program. Various environmental insults lead to activation of apoptotic pathways. The process of intrinsic apoptosis begins with the release of cytochrome *c* from mitochondria, subsequent activation of the apoptosome and activation of a caspase cascade (Budd & Nicholls, 1998). $A\beta_{1-42}$ induced cell death has been characterized as apoptotic (Forloni *et al.*, 1993; Loo *et al.*, 1993). Activation of two families of proteases, the caspases and calpains, has been demonstrated following exposure to $A\beta_{1-42}$.

$A\beta_{1-42}$ was first shown to be neurotoxic to terminally differentiated rat hippocampal neurons in 1990 (Yankner *et al.*, 1990a; Yankner *et al.*, 1990b). Only 50% of cultured neurons remain viable after two days with 15 μM $A\beta_{1-42}$ fibrils (Pike *et al.*, 1992). Neurons susceptible to Aβ toxicity *in vitro* as well as neuronal population vulnerable to degeneration in AD display increased expression of immediate early genes, c-Jun and c-fos. Activation of these genes initiates the apoptotic neuronal death cascade. Apoptosis is characterized by formation of cell surface protuberances "blebs", complete chromatin condensation and nuclear shrinkage "pyknosis" followed by nuclear fragmentation "karyorrhesis" into multiple membrane-bound bodies. Aβ deposits *in vivo* are associated with neuritic plaques (NP) and dystrophic neurites that appear thickened with irregular swellings both along their length and terminal portions, and which occasionally exhibit fragmentation. Many dystrophic processes associated with NP also show a tortuous morphology and appear confined to the plaque environment.

The p38 MAP kinase is a member of the stress activated protein kinases found conserved throughout evolution in a wide variety of cell types (Cobb & Goldsmith, 1995; Marshall, 1994; Marshall, 1995; Sugden & Clerk, 1997). p38, activated via dual

phosphorylation, activates MAPKAP2, which then activates the small heat shock protein hsp27 via dual phosphorylation. Active hsp27 possesses actin-binding activity and plays a role in regulation of apoptosis. Activation of p38 MAPK is found to occur in most chronic neurodegenerative diseases, such as AD, Parkinson's disease and amyotrophic lateral sclerosis (ALS) (Koistinaho & Koistinaho, 2002). Immunohistochemical analysis of postmortem AD brains revealed increased levels of activated p38 MAPK as compared with age-matched controls (Hensley *et al.*, 1999). Acute brain injury such as stroke elicits a strong inflammatory reaction most likely initiated and sustained by MAPKs such as p38 (Yrjanheikki *et al.*, 1998). Activation of p38 has been demonstrated in response to transient middle cerebral artery occlusion-induced ischemia (Irving *et al.*, 2000; Wu *et al.*, 2000). Activation of p38 has also been demonstrated in response to glutamate–mediated hyper-activation of NMDA-receptors (Tikka & Koistinaho, 2001).

Actin

Eukaryotic cells contain three classes of cytoskeletal proteins: actin microfilaments, microtubules and intermediate filaments. Actin is a cytoskeletal protein with a molecular weight of ~43 kilo-Daltons (kDa) and an isoelectric point of 5.4 (Zechel & Weber, 1978). Various isoforms of actin account for anywhere from 2 to 20% of total cellular protein depending on the cell type (Korn, 1982). Neurons express only the β- and γ-cytoplasmic non-muscle isoforms (Kaech *et al.*, 1997). The actin cytoskeleton is essential for cell motility, some vesicle transport, cell division and a host of other functions (Kuhn *et al.*, 2000).

The regulation of actin assembly, dynamics and organization is carried out by many actin binding proteins, which govern everything from filament nucleation to branching, bundling and severing (Bamburg, 1999). A conservative count by dos Remedios *et al.*, (2003) netted no less than 162 distinct actin binding proteins and this number will undoubtedly continue to grow. Actin monomers (G-actin) polymerize into non-covalent filaments (F-actin) of 6 to 8 nm in diameter. The crystal structure of actin in complex with Deoxyribonuclease I (DNase I) has been solved (Federov *et al.*, 1997). This structure has led to further work in building a model of an actin filament including a high-resolution structure based on the monomer. Although a true high-resolution structure of F-actin has not yet been solved, cryo-electron microscopy and computational modeling reconstruction techniques have led to a low-resolution (~30 Å) model of F-actin (McGough, 1997) (Fig. 1.2). In a filament of actin, subunits are connected by a 167° rotation and a 2.7 nm axial rise. Filamentous actin aligns in a left-handed helical twist with a major repeat distance of 38 nm and ~13 subunits per repeat. F–actin helical turns result in a crossover every 35 nm.

Actin filaments are dynamic biopolymers that continually undergo cycles of assembly and disassembly. Monomers of actin can be added to or removed from a filament at both ends, however a polarity exits which influences the on/off rate of G-actin. This polarity is caused by the ability of an actin monomer to bind to adenine nucleotides, ATP and ADP. ATP-actin has a higher affinity for filament assembly than ADP-actin. The critical concentration C_c required for ATP-actin assembly into filaments is lower than the C_c for ADP-actin (Carlier & Pantaloni, 1997). Above the C_c actin monomers spontaneously bind to form filaments and below this C_c monomers

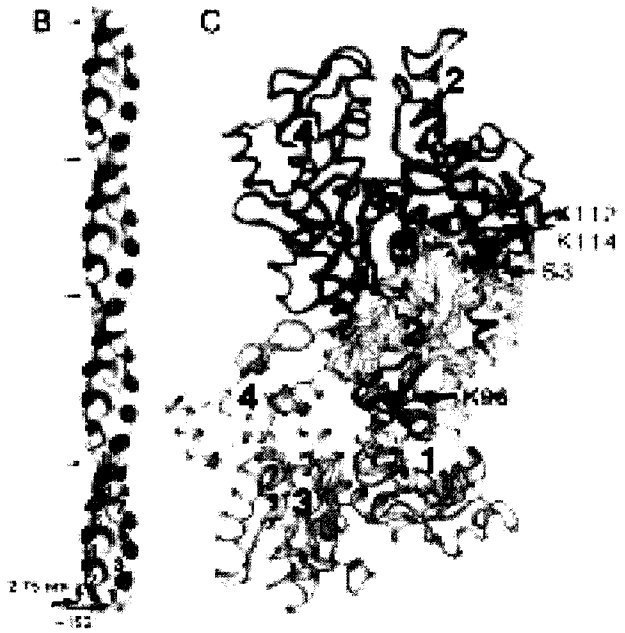

Figure 1.2: ADF/cofilin binding to F-actin. Low resolution structure of naked F-actin (A) and F-actin bound by ADF/cofilin (B) (A and B from Bamburg et al., 1995). ADF/cofilin binding changes the helical twist of the filament by about 5 degrees but does not change the rise per subunit. This binding arrangement stablizes lateral actin-actin bonds while destabilizing longitudinal bonds and eliminates phalloidin staining. Ribbon diagram of proposed ADF/cofilin binding to F-actin (C). The cofilin molecule (yellow) is depicted bound to two actin subunits in a filament (blue and gray) (C from Pope et al., 2004).

depolymerize from the filament end. After incorporation into a filament, the actin-bound ATP undergoes hydrolysis to ADP-P_i and eventually loses inorganic phosphate to become ADP-actin (Chen, 2001). Once an ADP-bound monomer is released from the minus end it must undergo a nucleotide exchange reaction before it can be added to the plus end of another filament (Fig 1.3). The protein profilin enhances the ADP-ATP nucleotide exchange rate (Pollard *et al.*, 2000), as does the Srv2/CAP1 protein (Mattila *et al.*, 2004). Profilin is a 15 kDa actin-binding protein that binds G-actin in a 1:1 molar ratio. Filamentous actin is a non-equilibrium polymer (Carlier & Pantaloni, 1997; Chen, 2001) meaning that at steady state, assembly occurs more rapidly at the "barbed" or plus (+) end of the filament while disassembly occurs more rapidly from the "pointed" or minus (–) end. The terms barbed and pointed originated from the characteristic arrowhead pattern, which develops when myosin heads decorate an actin filament. The polarity of an actin filament is critical to cellular functioning and motility, based on the direction-specific binding of many filament-binding proteins. When ATP actin addition to the (+) end equals the rate of ADP actin loss from the (–) end a steady state cycling of monomers occurs known as "treadmilling" (Wegner, 1976).

Treadmilling, the addition of subunits to the (+) end and loss of subunits from the (–) end, occurs 100 to 200 times faster in *vivo* than in *vitro*. The reported actin-based motility rate of 1-20 μm/min (7-130 subunits/sec/filament) is 1-2 orders of magnitude higher than the treadmilling rate measured in solutions of pure actin (Kuhn *et al.*, 2000). This difference in rates can be attributed to the multitude of actin binding proteins regulating filament turnover *in vivo*.

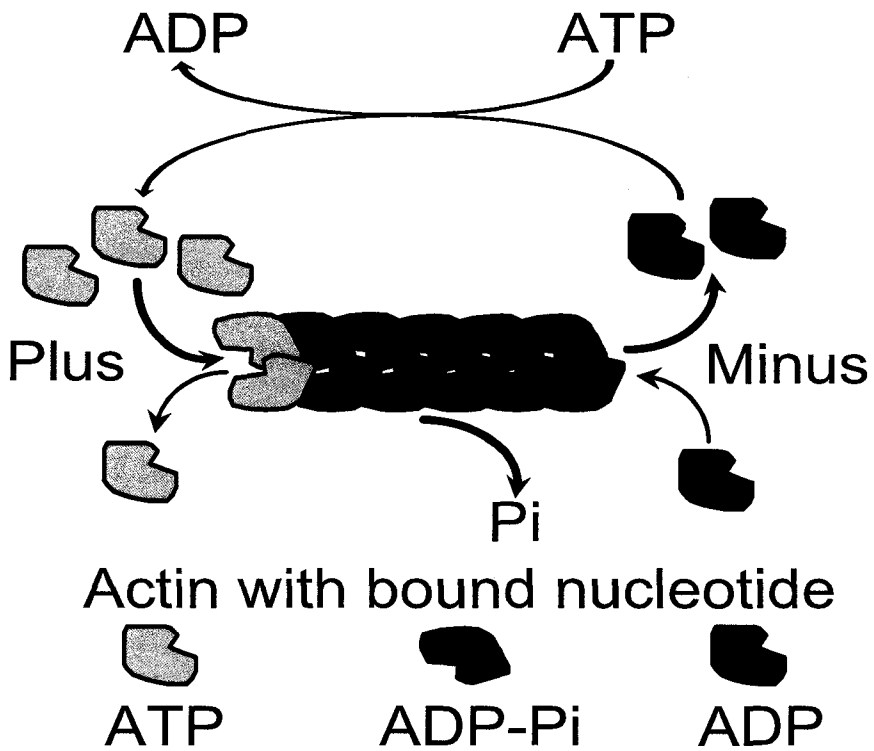

Figure 1.3: Actin treadmilling. At steady-state, actin filaments undergo treadmilling. ATP bound actin is added to the plus end of a growing filament followed by the hydrolysis of the γ-phosphate and release of inorganic phosphate (Pi). ADP-actin stabilizes a twisted conformation that allows for increased depolymerization from the minus end. Monomeric ADP-actin undergoes nucleotide exchange, removal of ADP and addition of ATP, enhanced by profilin.

Because actin is involved in so many important cellular activities, cells must possess a system for tight regulation of actin dynamics. Ca^{2+}, phospholipids and pH all affect the tension and relaxation of the actin cytoskeleton. To perform the various tasks of actin regulation, evolution has provided a variety of actin binding proteins each with specific function. Profilin enhances nucleotide exchange and can enhance the addition of subunits to the (+) ends of filaments, β-thymosin sequesters actin monomers, gelsolin severs F-actin and remains capped onto the barbed ends, Cap Z caps barbed ends of actin filaments, Arp2/3 enhances filament branching, α-actinin bundles filaments together and myosins bind to filaments, using them as cables to move vesicles and organelles throughout the cell, and ADF/cofilin severs F-actin and enhances filament disassembly from the (–) end (Paavilainen *et al.*, 2004). Barbed end capping proteins abolish actin dynamics at the (+) end. Capping a large proportion of the (+) ends increases the ATP G-actin pool, which then becomes funneled to the few uncapped filaments leading to accelerated protrusion.

ADF/cofilin

Members of the ADF/cofilin (AC) family are key regulators of actin assembly and turnover *in vivo* (Bamburg, 1999). Cofilin and Actin Depolymerizing Factor (ADF) are members of a 15–20 kDa actin-binding family of proteins ubiquitously expressed in eukaryotes from yeast to humans and share high sequence homology (Hatanaka *et al.*, 1996; Nishida, 1984). ADF, the first member of the family to be isolated, was purified from embryonic chick brain (Bamburg *et al.*, 1980). The nuclear magnetic resonance (NMR) structure for the human ADF homologue destrin was determined first followed by

the X-ray structure of yeast cofilin, actophorin and plant ADF. The X-ray crystal structure elucidated the architecture of the ADF-homology domain (ADF-H), a structural motif shared by the members of the AC family of proteins (Federov *et al.*, 1997). Cofilin possesses 70% sequence identity to ADF. Both ADF and cofilin modulate actin filaments in a pH dependent manner (Yonezawa *et al.*, 1985; Hawkins *et al.*, 1993; Hayden *et al.*, 1993), with ADF's regulation of actin being more greatly affected by pH than cofilin's (Bernstein *et al.*, 2000).

ADF and cofilin are typically found in cellular regions involved in high actin dynamics such as neuronal growth cones, ruffling membranes (Fig 1.4) and cleavage furrows. *Caenorhabiditis elegans* contains two AC family proteins unc60A/B. The unc60B isoforms is found specifically in muscle while unc60A is found throughout the body. Only the unc60A deletion mutant is lethal. *Drosophila melanogaster* and *Saccaromyces cervisia* both contain only a single AC family protein. A null mutant of this protein in both model systems is lethal. The lethality of AC family knockouts in all three animal models indicates that these proteins are fundamentally important in eukaryotes (Bamburg, 1999). ADF/cofilins have been shown to enhance treadmilling of F-actin *in vitro* by 25 fold (Carlier *et al.*, 1997). The rate of actin turnover increases 125 fold in the presence of both profilin and AC (Didry *et al.*, 1998; Chen, 2001). AC's bind ADP-G-actin with 30-80 fold higher affinity than for ADP-P_i or ATP G-actin at physiological ionic strength (Carlier *et al.*, 1997) suggesting the change in conformation of actin subunits within F-actin following P_i release enhances AC binding.

Interactions between AC and G- and F-actin have been studied extensively using a variety of techniques including electron microscopy, mutagenesis, biochemical assays,

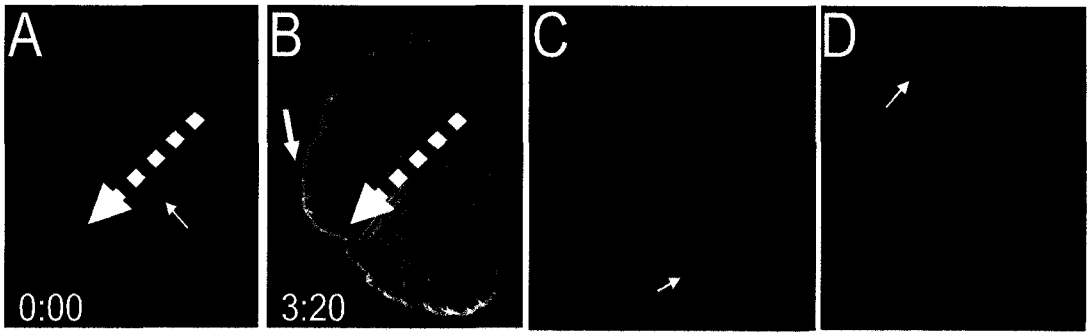

Figure 1.4: Major F-actin structures in non-muscle cells. Fluorescent phalloidin stained lamellipodium at leading edge of chick cardiac fibroblast with bold arrow showing direction of migration and small arrow showing graded polarity actin bundle (A). A second image of the cell shown in panel A, pseudocolored in green and overlayed on image in panel A to show new lamellipodial extension (arrow: bright green) that occured over the 3 min 20 sec time period (B). Filopodia (microspikes) on a neuronal growth cone (arrow in C). Stress fiber in a cultured non-polarized and non-migrating cell stained with Rhodamine phalloidin (arrow in D). (Images courtesy of Dr. Lubna Tahtamouni).

cross-linking, modeling, computational analysis and protein foot printing with synchrotron radiation (McGough *et al.*, 1997; Lappalainen, 1997; Moriyama *et al.*, 1992; Ono *et al.*, 2001; Sutton & Mabuchi, 1989; Guan *et al.*, 2002). The exact ADF/cofilin to F-actin binding interaction has still not been precisely determined because of difficulty in obtaining a stable structure of AC decorated F-actin imposed by AC's filament severing activity. ADF binds F-actin in a cooperative fashion such that the rate-limiting step is the binding of the first ADF molecule to a bare filament, then binding of subsequent ADF occurs more rapidly. AC induces a substantial change in the helical periodicity of F-actin upon binding (McGough *et al.*, 1997) (Fig 1.2). AC changes the twist per subunit by ~5° while maintaining a constant rise per subunit (i.e. the overall filament length remains unchanged). This binding arrangement stabilizes lateral actin-actin bonds while destabilizing longitudinal bonds and eliminates phalloidin binding. For some time AC induced severing of F-actin has been theorized to occur at the junction between decorated and naked actin (McGough *et al.*, 1997). However, a recent study by Bobkov *et al.*, 2006 indicates that fragmentation may occur at cofilin free regions of the filament weakened allosterically by nearby cofilin molecules. Filaments saturated with AC have a crossover of 27 nm, which is much shorter than the crossover of 35-38 nm seen in naked F-actin. ADF/cofilins are inhibited in actin binding by phosphorylation of Ser3 (Morgan *et al.*, 1993; Agnew *et al.*, 1995) and by binding to phosphatidyl inositol 4,5 bisphosphate (PIP_2). Phosphorylation is catalyzed by the protein kinases LIMK1, LIMK2 and TESK1 and TESK2 (Arber *et al.*, 1998; Yang *et al.*, 1998; Toshima *et al.*, 1995; Toshima *et al.*, 2001).

Phosphorylation reduces the affinity of ADF/cofilin for binding G- and F-actin by 20 fold (Bamburg, 1999). Stimulating increased filament turnover in cells does not always result in an altered ratio of phosphorylated to unphosphorylated ADF and cofilin, suggesting instead the half-life of the phosphate group on AC decreases, which has been demonstrated (Meberg *et al.*, 1998). This increase in the turnover of phosphorylated AC suggests that the pathways regulating the kinases and phosphatases bifurcate in at least some instances to keep them in balance. The increase in the rate of phosphorylation and dephosphorylation of AC is known as "phosphocycling".

Two isoforms of LIM kinase exist. Once activated both LIMK1 and LIMK2 undergo autophosphorylation as well as phophorylate ADF and cofilin, which are their major substrates. LIMK1 is activated by the p21 activated kinase (PAK) and Rho kinase (ROCK). In cultured fibroblasts, Cdc42 activation stimulates filopodial formation, Rac activation results in lamellipodial activation and Rho activation leads to stress fiber formation. Mutations in proteins involved in actin dynamics can be linked to a number of medical disorders such as Williams's syndrome. William's syndrome is caused by a deletion of a chromosomal region containing the gene for LIM kinase thus resulting in a hemizygosity of LIMK1 (Bamburg & Wiggan, 2002). The effects of Rho, Rac and Cdc42 are directed through intermediate proteins possessing a CRIB domain. The PAK family is one of the most extensively studied effectors of Cdc42 and Rac. PAK also activates the JNK and p38 stress kinase pathways and are targets of caspase–mediated proteolytic cleavage during apoptosis. The testicular protein kinases (TESK1 and 2) also phosphorylate AC proteins. The activation of TESK1 is regulated by its release from binding at focal adhesions through actopaxin (Lalonde *et al.*, 2005). ADF/cofilins are

activated when dephosphorylated by protein phosphatases in the Slingshot (SSH) family (Niwa *et al.*, 2000) or by chronophin (Gohla *et al.*, 2005). Slingshot is a phosphatase with a molecular weight of ~125 kDa. The phosphatase domain of SSH is distantly related to MAP kinase phosphatases. The phosphatase activity of the longform of Slingshot-1 (SSH-1L) is dependent upon F-actin binding *in-vitro* (Nagata-Ohashi *et al.*, 2004), is negatively regulated via PAK4 phosphorylation (Soosairajah *et al.*, 2005), and is activated via dephosphorylated by calcineurin (Nagata-Ohashi *et al.*, 2004; Wang *et al.*, 2005).

Neurodegenerative Stress and Rod Formation

The actin cytoskeleton is remodeled in response to various stimuli (Bershadsky *et al.*, 1980; Iida *et al.*, 1986; Nishida *et al.*, 1987). Micro-ischemia, glutamate excitotoxicity and oxidative stress are linked to age-related neurodegenerative disease (Lenaz, 1998; Nicholls & Budd, 1998; Richardson, 1997; Smith *et al.*, 1998). Exposure of cultured cells to ATP depletion, oxidative stress, or excitotoxicity for only a few minutes produces elongated filamentous actin aggregates known as rods (Minamide *et al.*, 2000) (Fig 1.5). Rod formation is associated with a rapid decrease in phosphorylated ADF/cofilin (pAC), resulting in activation of AC's actin binding/severing activity (Fig 1.6). This rapid decrease in phosphorylated AC occurs prior to and during rod formation (Minamide *et al.*, 2000).

Spontaneous rod formation results from the over-expression of wild type *Xenopus* ADF/cofilin-Green Florescent Protein (XAC-GFP) in hippocampal neurons (Bernstein *et al.*, 2006). The size of rods is proportional to the amount of AC expressed in neurons,

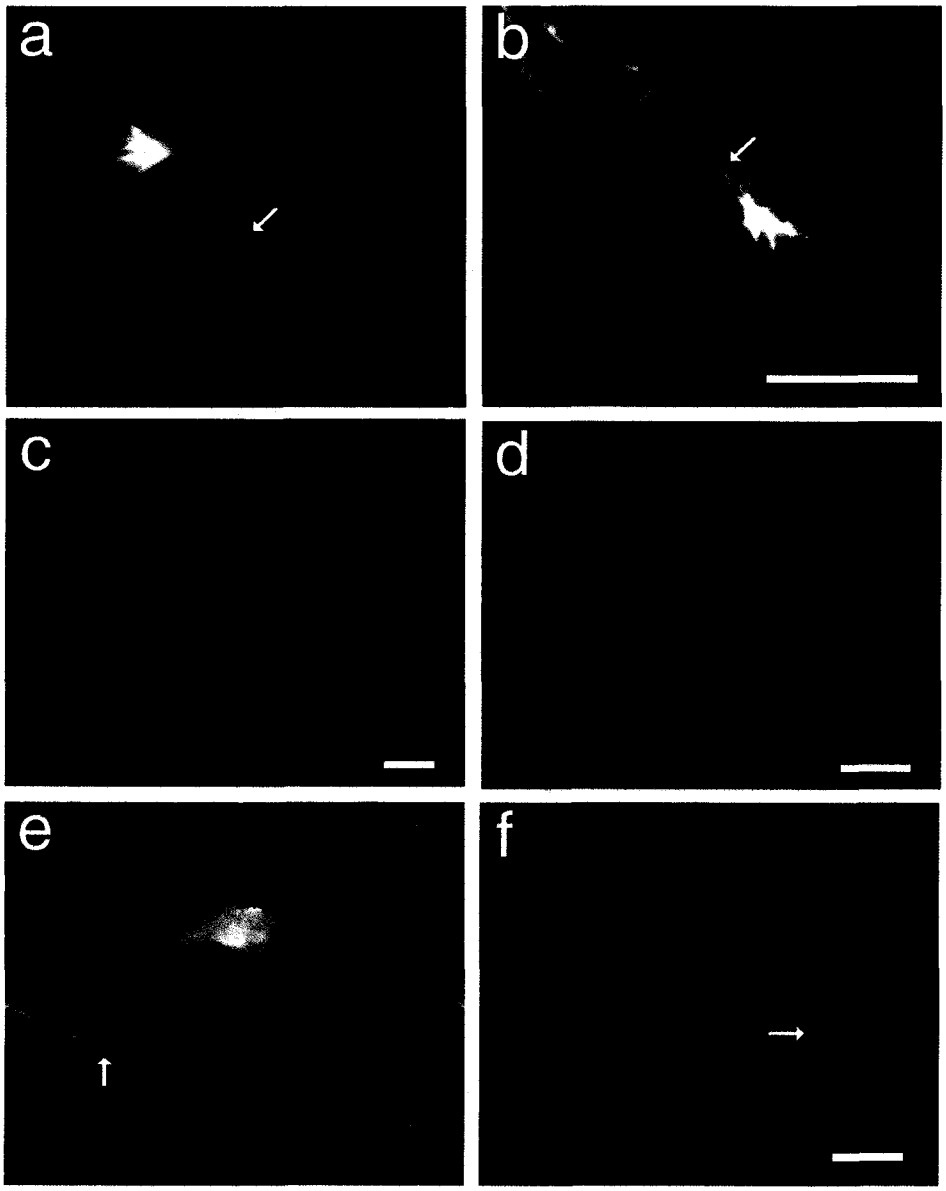

Figure 1.5: Rods immunostain for cofilin (green in a) and for actin (green in b), but do not stain with phalloidin (red in a and b). Rods sequester most endogenous cofilin (c), which is limiting. Doubling expression of cofilin (d) with XAC-GFP expression gives rods that are twice as long. Rods (red in e and f) form in neurofilament-H (NFH) positive (green in e and f) axons (e) and NFH negative dendrites (f). Scale bar = 10 mM. (From Minamide et al., 2000).

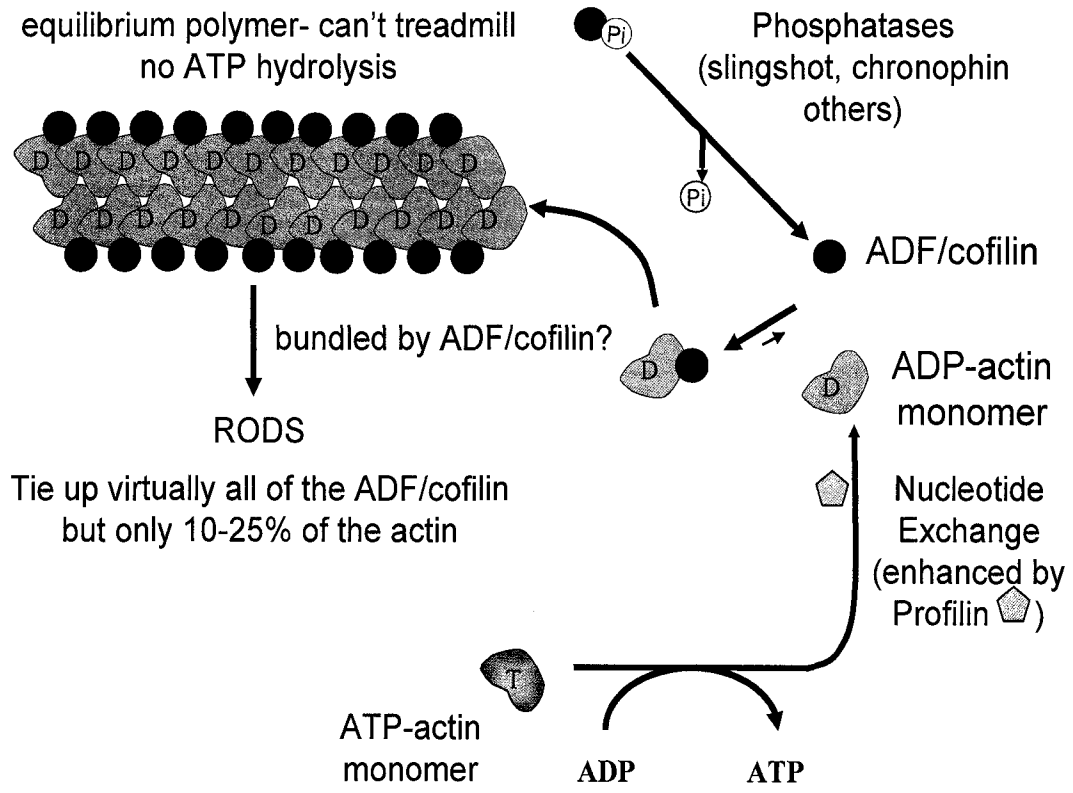

Figure 1.6: As ATP levels fall dephosphorylated ADF/cofilin and ADP-actin accumulate and form a complex that can assemble into filaments.

suggesting that the supply of AC is the limiting factor to rod length (Minamide *et al.*, 2000) (Fig 1.5). Though the exact protein content of rods is unknown, actin and proteins of the ADF/cofilin family are major constituents (Bamburg, 1999; Bamburg *et al.*, 1999).

Peroxide induces rod formation and promotes oxidative stress leading to widespread cellular damage within a short time span. Glutamate induces excitotoxicity in neurons and also leads to rapid rod induction. ATP depletion results in a rapid induction of rods. Rods formed following ATP depletion disappear completely within 30-60 min when cells are returned to standard culture conditions, but reappear in a subpopulation of neurons 24 hours later. Rod-like AC inclusions have been found in the hippocampus of AD brain but not in normal control human brain (Minamide *et al.*, 2000). Nearly 97% of 180 amyloid plaques from the frontal cortex and hippocampus of an AD brain showed AC aggregates over or around them (Minamide *et al.*, 2000).

Rapid rod formation has been observed in cultured neurons following insult. Glutamate and peroxide induce rods within thirty minutes, and ATP depletion within minutes of application (Minamide *et al.*, 2000). Rods represent the earliest, outwardly observable sign of neuronal stress, and have been hypothesized to act in neuroprotection (Bernstein *et al.*, 2006).

Rods in cellular defense

The translocation of cofilin to mitochondria has been documented in cells following treatment with the apoptotic agent staurosporine (STS) (Chua *et al.*, 2003). This translocation, which requires the activation of cofilin via dephosphorylation, typically begins within two hours and precedes cytochrome *c* release. Disruption of the

actin-binding domain of cofilin inhibits cytochrome *c* release but not translocation to mitochondria (Chua *et al.*, 2003). Thus the phenomena of ADF/cofilin translocation to mitochondria may represent a conserved and early step in the induction of apoptosis. One way rods may be protective is by sequestering cofilin thereby slowing mitochondrial translocation and subsequent activation of apoptosis. Actin turnover can consume up to 50% of the ATP in growing neurons (Bernstein & Bamburg, 2003). In XAC-GFP expressing neurons the presence of newly formed spontaneous rods in neurites retards both the loss of mitochondrial membrane potential and ATP as compared to neurites without rods or with older rods (Bernstein *et al.*, 2006). A second mechanism by which rods may be protective is in tying up large amounts of actin into non-dynamic aggregates. Thus, rods may help cells to preserve ATP during transient stress.

Further characterization of the role of rods in the early neuronal stress response is warranted and will be discussed in the conclusions/future directions chapter. Understanding of the early steps in neuronal stress, apoptosis and rod formation is key to gaining insight to the biochemical pathways directing neuronal survival during insult. We speculate that these components are all parts of a larger scheme directed at neuronal survival.

Conclusions and Focus of Dissertation

The deposition of Aβ into senile plaques is a hallmark of AD. Aβ peptides possess neurotoxic properties *in vivo* and *in vitro*. The shorter form of Aβ, $A\beta_{1\text{-}40}$, appears to be less toxic than the longer $A\beta_{1\text{-}42}$. $A\beta_{1\text{-}42}$ aggregation occurs in stages from monomers, to oligomers, and ultimately into fibrils. These various conformers possess

different degrees of neurotoxicity and in this dissertation we demonstrate that they also induce varying amounts of rod formation in a time- and concentration-dependent manner. We are beginning to understand the biological activity of $A\beta_{1-42}$ peptides by studying their effects on ADF/cofilin proteins in cultured neurons. Misregulation of ADF/cofilin induced by $A\beta_{1-42}$ can potentially impact cellular transport, APP processing, synaptic connectivity and neuronal survival. The aim of this research has been to understand how these effect on ADF/cofilin arise and thus, begin to answer fundamental questions that may lead the way towards developing strategies designed at preventing or delaying $A\beta_{1-42}$ mediated neurodegeneration and cognitive impairments.

The research presented in this dissertation builds largely upon the work of Minamide *et al.*, 2000 that demonstrated neurodegenerative stimuli induce rod formation in cultured neurons. From this point the initial finding that rods can also be induced by the exposure of cultured neurons to $A\beta_{1-42}$ led us to ask questions regarding the time- and concentration-dependence of this effect. Like any good scientific investigation this pursuit has only prompted more questions and helped in developing a hypothesis to explain how rods may be involved in the systematic failure of Alzheimer's disease. We have developed new tools including an adenoviral vector to express APP conjugated to Yellow fluorescent protein (APP-YFP) for following transport in live cells, and organotypic hippocampal slice cultures as a model system in which we can address questions regarding the specific effects of $A\beta_{1-42}$ on a sub-population of neurons. At the conclusion of this dissertation it will be clear that the pursuit of rods as contributors to neuronal dysfunction, and in protection, is relevant and requires further investigation.

Chapter Two

β-Secretase-cleaved APP accumulates at actin inclusions induced in neurons by stress or amyloid beta: a feed-forward mechanism for Alzheimer's disease.

Preface and Acknowledgement

The work presented in this chapter was published in the Journal of Neuroscience (Maloney *et al.*, 2005). The order and list of authors is as follows: Michael T. Maloney, Laurie S. Minamide, Andrew W. Kinley, Judith A. Boyle, and James R. Bamburg. We would like to thank Drs. Yunfeng Lu and Bruce Parkinson for assistance with atomic force microscopy, Hilary Bowden for assistance with microscopy, Drs. Barbara Bernstein, O'Neil Wiggan, Joe Fass and Mr. Kevin Flynn and Ms. Alisa Shaw for valuable suggestions and assistance. We especially thank Mr. Chi Pak for suggestions and critical reading of the manuscript. This work was supported by grants IIRG-01-2730 from the Alzheimer's Association, NS40371, NS43115 and GM35126 from the National Institute of Health, and a grant-in-aid from Sigma Xi.

Abstract

Rod-like inclusions (rods), composed of actin saturated with actin depolymerizing factor (ADF)/cofilin, are induced in hippocampal neurons by ATP-depletion, oxidative stress and excess glutamate and occur in close proximity to senile plaques in human Alzheimer's disease (AD) brain (Minamide *et al.*, 2000). Here we show rods are found in brains from transgenic AD mice. Soluble forms of amyloid beta ($A\beta_{1-42}$) induce the

formation of rods in a maximum of 19% of cultured hippocampal neurons in a time- and concentration-dependent manner. About half of the responding neurons develop rods within 6 h or with as little as 10 nM $A\beta_{1-42}$. $A\beta_{1-42}$ induces the activation (dephosphorylation) of ADF/cofilin in neurons that form rods. Vesicles containing amyloid precursor protein (APP), β-amyloid cleavage enzyme, and presenilin-1, a component of the γ-secretase complex, accumulate at rods. The β-secretase cleaved APP (either β-C-terminal fragment of APP or Aβ) also accumulates at rods. These results suggest that rods, formed in response to either Aβ or some other stress, block the transport of APP and enzymes involved in its processing to Aβ.. These stalled vesicles may provide a site for producing $A\beta_{1-42}$, which may in turn induce more rods in surrounding neurons, and expand the degenerative zone resulting in plaque formation.

Introduction

Hippocampal neurons exposed to neurodegenerative stimuli rapidly reorganize their actin cytoskeleton into rods, which are tapered cylindrical filamentous inclusions saturated with ADF/cofilin (Minamide *et al.*, 2000). Rods form in neurons transiently exposed to treatments that mimic oxidative stress, excitotoxicity and ischemia, and their formation is accompanied by a net dephosphorylation (activation) of ADF and cofilin, two closely related protein regulators of actin dynamics in eukaryotic cells (Bamburg & Wiggan, 2002). Rods can occlude the neurite, disrupting microtubules and causing distal neurite atrophy (Minamide *et al.*, 2000). Rod-like inclusions stained with ADF/cofilin antibody occur in human AD brain. Almost all amyloid-rich senile plaques were associated with rod-like inclusions, but over 40% of inclusions were not plaque-

associated. Thus, rods might occur in response to amyloid toxicity and/or they might participate in amyloid production.

Proteolytic cleavage of the full-length amyloid precursor protein (APP) by β-amyloid cleavage enzyme (BACE; also called β-secretase) and γ-secretase gives rise to Aβ peptides (Price *et al.*, 1995; Sisodia & Price, 1995; Hardy & Selkoe, 2002; Mattson, 2004; Tanzi & Bertram, 2005). Mutations leading to increased production of the more amyloidogenic $A\beta_{1-42}$ species are linked to early onset familial Alzheimer's disease (FAD) (Chartier-Harlin *et al.*, 1991a; Chartier-Harlin *et al.*, 1991b; Goate *et al.*, 1991; Murrell *et al.*, 1991; Price *et al.*, 1995). Treatment of cultured neurons with $A\beta_{1-42}$ inhibits fast axonal transport (Hiruma *et al.*, 2003). Furthermore, blockage of axonal transport is the earliest measured disturbance in brains of transgenic mice expressing mutant human APP (Stokin *et al.*, 2005).

$A\beta_{1-42}$ can exist as monomers, oligomers, fibrils and insoluble aggregates (Lambert *et al.*, 1998; Walsh *et al.*, 1999; Dahlgren *et al.*, 2002; Walsh *et al.*, 2002b; Chromy *et al.*, 2003; Kim *et al.*, 2003). These various species possess different degrees of neurotoxicity. Fibrils increase reactive oxygen species (Harris *et al.*, 1995; Cafe *et al.*, 1996), lipid peroxidation and free radicals (Hensley *et al.*, 1996; Lim *et al.*, 2005). Yet, soluble Aβ oligomers, including amyloid-derived diffusible ligands (ADDL), are more neurotoxic than fibrils and insoluble larger aggregates (Dahlgren *et al.*, 2002; Gong *et al.*, 2003). Soluble Aβ and ADDL at sub-micromolar concentrations are neurotoxic in organotypic cultures (Lambert *et al.*, 1998), alter neuronal electrophysiology (Hartley *et al.*, 1999), inhibit long-term potentiation (Walsh *et al.*, 2002a), and cause transient memory deficits (Cleary *et al.*, 2005). Together these findings suggest that rod

formation, initiated by Aβ peptides, might be the cause of transport blockage, which would affect synaptic function. Inhibition of transport also could enhance Aβ production, because the majority of β-secretase cleaved APP occurs in endosomes (Koo & Squazzo, 1994; Yamazaki *et al.*, 1995; Cordy *et al.*, 2003; Ehehalt *et al.*, 2003). Thus rods may both initiate neurodegeneration and amplify accumulating degenerative signals (e.g. Aβ).

Here we demonstrate that soluble $A\beta_{1-42}$ activates ADF/cofilin and induces the formation of rods in a sub-population of cultured hippocampal neurons in a time- and concentration-dependent manner. Rods are sites where vesicles containing APP and β-secretase-cleaved APP accumulate.

Materials and Methods

All chemicals are reagent grade and were obtained from Sigma-Aldrich Co. and all tissue culture reagents were from Life Technologies (Invitrogen™). β-Amyloid peptides ($A\beta_{1-42}$ and a scrambled peptide with the same amino acid composition) were purchased from Ana Spec, Inc. HAMS-F12 medium with L-glutamine and without phenol red was purchased from Caisson Laboratories Inc. (Rexburg, Idaho).

$A\beta_{1-42}$ preparations

Solubilization of the β-amyloid peptides and generation of the different $A\beta_{1-42}$ aggregates were performed as described previously (Dahlgren *et al.*, 2002; Stine *et al.*, 2003). Fibril preparations were centrifuged for 15 min at room temperature at 20,000 x g. The peptides in aliquots from supernatant and pellet fractions were extracted for dot blot analysis as described previously (Stine *et al.*, 2003). Primary antibody (FCA18;

Oncogene™ Research Products), recognizing the N-terminal amino acid of the $A\beta_{1-42}$, was used at 1:500 in blocking solution for 1 h at room temperature. Horseradish peroxidase-conjugated secondary antibody was used at 1:30,000 in Tris-buffered saline plus 0.05% Tween-20 (TBS-T) at room temperature for 1 h. Blots were developed using SuperSignal® West Pico or Extended Duration Chemiluminescent substrates (Pierce Biotechnology Inc.). Digitized images were captured using a Photometrics CH250 CCD camera (Photometrics LTD.) and spot intensity was quantified using MetaMorph software (version 6.1r5 Universal Imaging Corporation).

Cell culture and treatments

Hippocampal neuronal cultures were prepared as described previously (Bartlett & Banker, 1984; Mattson & Kater, 1988; Minamide *et al.*, 2000) with the following changes. Dissociated cells were plated on poly-D-lysine coated substrates in 8 well Lab Tek® Chamber Slides (Nalg Nunc International), and cultured under 400 µL Neurobasal medium supplemented with B27 and glutamine in a humidified 95% air/5%CO_2 incubator at 37°C. Dissociated cultures enriched in CA1 or CA3 neurons were prepared from 400 µm slices (McIlwein tissue chopper) of E18 rat hippocampi (Meberg & Miller, 2003). Prior to dissociation, slices were further dissected into CA1 and CA3 regions on a Nikon SMZ-U dissection microscope as shown in Supplementary Fig 2.1. Hippocampal neurons (6 days in vitro (div)) were treated with 10 nM, 100 nM or 1 µM $A\beta_{1-42}$ in the form of low molecular weight species, large oligomers, and fibrils/insoluble aggregates for 0.5-72 h. Controls included untreated neurons or neurons treated with 0.5% DMSO

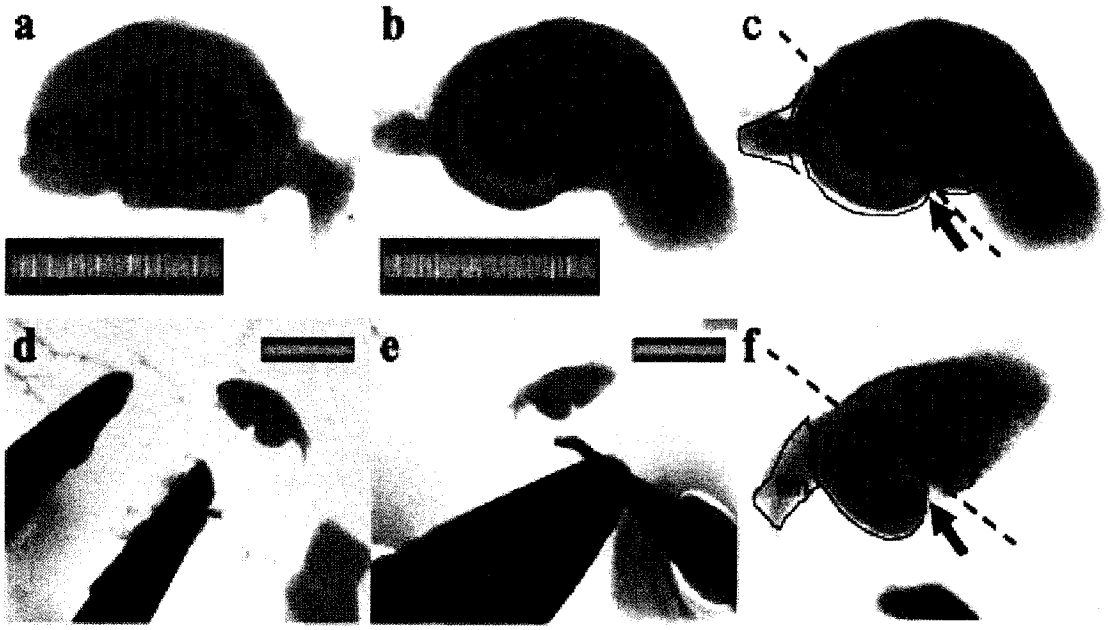

Supplementary Figure 2.1: Preparation of dissociated cultures enriched for CA1 or CA3 neurons. (a-c) Left and right hippocampal slices from brain showing the pyramidal cell layer of the hippocampus taken on a Nikon diaphot microscope with a 4 x objective. (d-f) Observations of the hippocampi from a Nikon SMZ-U Zoom 1:10 dissection microscope used for making the bisections of the CA1 and CA3 regions. Scale bars = 1 mm. CA1 = Cornu Amonis region 1, CA3 = Cornu Amonis region 3, DG = Dentate Gyrus, fim = fimbria. Black arrow points to hippocampal fissure.

(vehicle) or with 1 μM scrambled Aβ peptide that had been pre-incubated under conditions in which $A\beta_{1-42}$ forms fibrils.

For some studies rods were induced by transient (20 min) ATP depletion followed by washout of the ATP-depletion medium and 24 h recovery (Minamide *et al.*, 2000). Rods were also induced in some experiments by infecting 4 div hippocampal neuronal cultures with adenovirus for expressing the GFP chimera of wild type *Xenopus* ADF/cofilin (XAC-GFP) (Meberg & Bamburg, 2000). Spontaneous rods start to form in neurites of infected cells by 60 h post-infection (Bernstein *et al.*, 2006). Cells were fixed at 72 h post-infection.

Cells were fixed 30 min in cytoskeleton preservation buffer (10 mM MES, pH 6.1, 138 mM KCl, 3 mM $MgCl_2$, 2 mM EGTA, 0.32 M sucrose) containing 4% paraformaldehyde, pH 7.0. Cells were methanol (-20° C) permeabilized for 3 min and blocked in 2% goat serum/1% BSA in TBS before immunostaining with various antibodies. Primary antibodies include: affinity purified rabbit antiserum to chick ADF (2 ng/μL), which cross-reacts with mammalian ADF and cofilin (Minamide *et al.*, 2000), affinity purified rabbit anti-phospho ADF/cofilin (pAC; 0.02 ng/μL), which recognizes only the ser-3 phosphorylated forms of ADF/cofilin (Meberg *et al.*, 1998), protein A purified monoclonal mouse anti-cofilin (Mab22; 10 ng/μL IgG; Abe *et al.*, 1989), monoclonal anti-human β-amyloid Asp-1 (FCA18; 1:150; Oncogene™ Research Products), rabbit anti-BACE (M-83; 1:150; Santa Cruz Biotechnology, Inc.), rabbit anti-Presenilin 1 [residues 31-46] (Ab-1; 1:150; Oncogene™ Research Products), rabbit anti-β-Amyloid Precursor Protein (1:150; Zymed® Laboratories Inc). Secondary antibodies, all used at 1:450, include fluorescein goat anti-rabbit and goat anti-mouse and Texas-Red

goat anti-rabbit and goat anti-mouse (Invitrogen™ Molecular Probes™). DAPI (4'-6-Diamidino-2-phenylindole) was used at 1:1000 (Invitrogen™ Molecular Probes™). After blocking and staining, the rubber dividing chambers were removed and a 24 x 50 mm cover glass was mounted with Prolong Gold Antifade (Invitrogen™ Molecular Probes™).

The relative level of phosphorylated ADF/cofilin to total cofilin was determined by ratiometric analysis of fluorescence overlays from neurons immunostained with both pAC rabbit and mouse Mab22 primary antibodies and Texas Red and fluorescein secondary antibodies. Average pixel intensities were measured after background subtraction using MetaMorph software. All values were normalized to the ratio (set to 1) of pAC to total cofilin in untreated neurons.

Brain sections from transgenic (Tg2576) mice

A 4 month old transgenic mouse (Tg2576; Taconic Labs, Germantown, NY) was perfusion fixed (Bruijn *et al.*, 1997), the brain removed, post-fixed, and paraffin embedded. Sections (5 μm) were deparaffinized and immunostained for ADF/cofilin as previously reported for human AD brain (Minamide *et al.*, 2000).

Microscopy

Light microscopy: Phase-contrast and fluorescence micrographs were obtained using a 60x (1.4na) oil objective as previously described (Minamide *et al.*, 2000). Fluorescence measurements were made from non-saturating digital images all acquired under the same conditions with a CoolSnap ES CCD (Photometrics). Quantitative

analyses of some of these images were performed by obtaining average fluorescence intensities from the different cell regions (line scans) after subtracting background. MetaMorph v6.1 software (Universal Imaging) was used for all digital image processing. Slides were coded and scored blind to obtain percentages of neurons containing rods. At least 200 neurons per well were observed with a 40x oil (1.3 na) objective, and the percentages of neurons containing rods were recorded. To quantify the percentage of neurons that survived, the total number of neurons in 10 randomly selected fields (20x air objective) from Aβ-treated cultures was counted per well. This number was compared to the number of neurons surviving from untreated cultures plated from the same neuronal stock. Averages and standard deviations (S.D.) for identical treatments were obtained from multiple wells. Experiments were repeated 3 or more times to give standard error of means (S.E.M.). Analysis of Variance (ANOVA) was performed using SAS/LAB software (S.A.S. Institute Inc.).

Electron Microscopy (EM): $A\beta_{1-42}$ peptides: A 3 μL aliquot of $A\beta_{1-42}$ samples from each incubation condition was applied to a formvar-coated slot copper grid, blotted dry, negatively stained with 1% aqueous uranyl-acetate and examined on a JEOL 2000 T.E.M at 100 KV. Human AD brain: Postmortem human AD hippocampus (brain bank tissue) was fixed upon removal in 4% paraformaldehyde, 2% glutaraldehyde, postfixed in osmium, dehydrated, embedded in LR White resin, and uranyl acetate/lead citrate stained sections (90 nm) were observed with a JEOL-2000 TEM.

Atomic force microscopy (AFM): Peptides were prepared for AFM as previously described (Stine *et al.*, 2003). Images were obtained on NanoScope IIIa Scanning Probe Microscope equipped with MultiMode head, E-series piezoceramic scanner, and AFM

probe type of single-crystal silicon microcantilevers with 300 kHz resonant frequency and 40 N/m spring constant.

Results

Characterization of Aβ aggregates

To determine if any forms of $A\beta_{1-42}$ could induce rods in cultured hippocampal neurons we prepared and incubated stock solutions of synthetic $A\beta_{1-42}$ peptide under conditions previously shown to enrich preparations in low molecular weight (LMW) species, large oligomers, or fibrils with larger aggregates (Walsh *et al.*, 2002b). The composition of each prepared sample was analyzed by electron microscopy (EM) and by atomic force microscopy (AFM) (Fig. 2.2 Sup). Our three peptide preparations contain species that appear similar in size and distribution to those previously described (Lambert *et al.*, 1998; Walsh *et al.*, 1999; Dahlgren *et al.*, 2002; Walsh *et al.*, 2002b; Chromy *et al.*, 2003; Stine *et al.*, 2003). Overlap of $A\beta_{1-42}$ species occurs between preparations. Thus, we will define these samples as: (1) a LMW preparation containing small bead-like structures and aggregates, (2) a large oligomer preparation containing larger aggregates and short protofibrils, and (3) a fibril/insoluble aggregate preparation containing ribbon-like fibrils that remained in the supernatant following centrifugation at 20,000 x g for 15 min, as well as large amorphous aggregates that pelleted (Fig. 2.2 Sup). The insoluble aggregates of Aβ look remarkably similar in size and shape to the aggregates that comprise the dense core senile plaques of human AD brain (Fig. 2.2 Sup).

Rods, which are straight tapered bundles of F-actin saturated with ADF/cofilin, were identified by immunostaining for ADF/cofilin in E18 rat hippocampal neurons (6

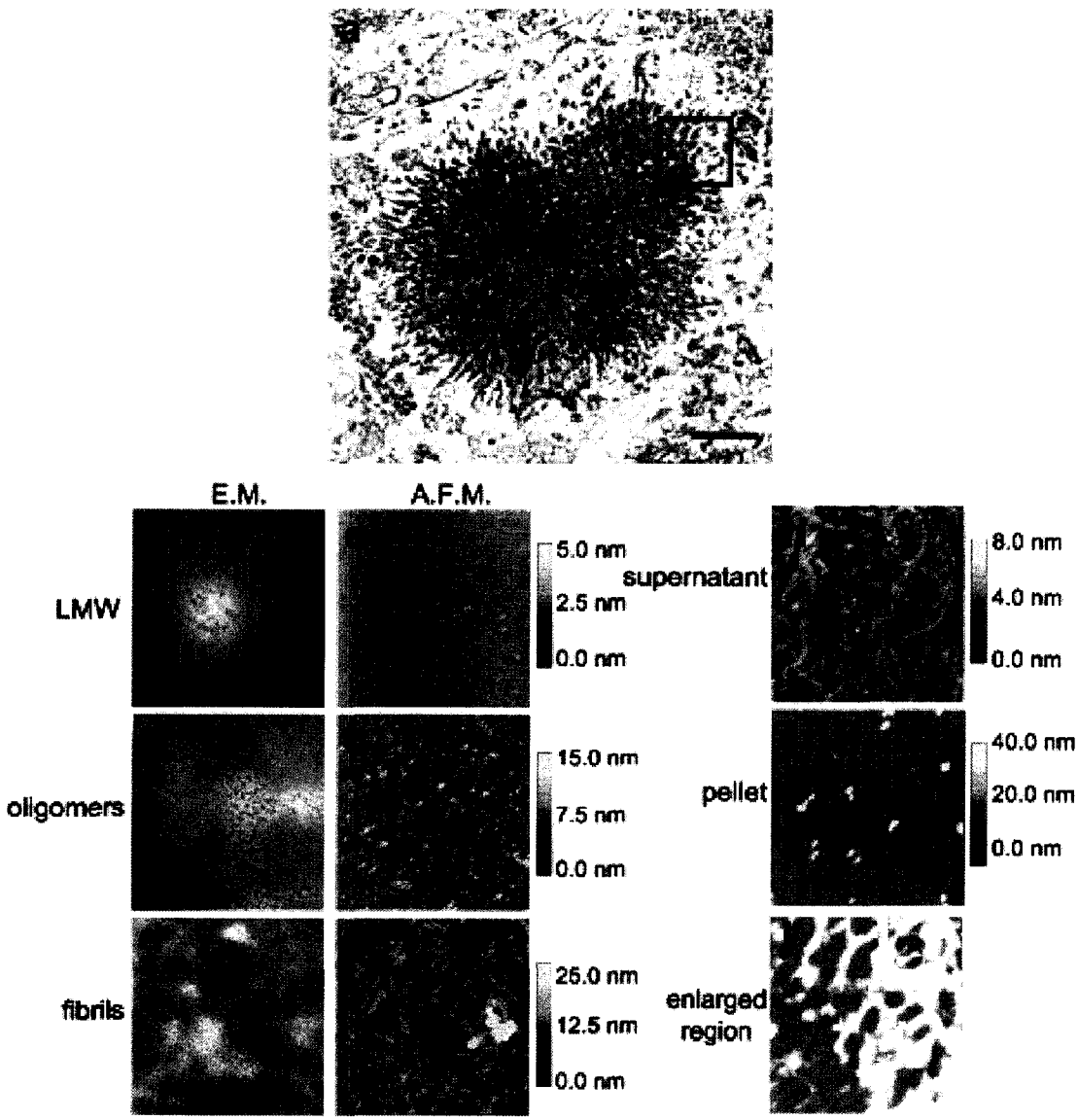

Supplementary Figure 2.2: AFM and EM images of Ab aggregates in vitro and amyloid plaque in human brain. (a) Negative stained EM photomicrograph of an amyloid plaque from human Alzheimer diseased brain (scale bar = 2 μm). (b-d) EM images (boxes are 2 x 2 μm). (e-i) AFM images (boxes are 2 x 2 μm). (h, i) Supernatant and pellet fractions from a fibril/insoluble aggregate preparation following centrifugation at 20,000 x g for 15 min. (j) Magnification of a 2 x 2 μm section from the amyloid plaque (a).

days in vitro (div)) treated 24 h with 1 μM of each of the different $A\beta_{1-42}$ samples (Fig. 2.1). Although neurites containing rods are contiguous, methanol permeabilization left phase dense regions where rods had formed (Fig. 2.1a, arrows), sometimes giving the neurites a fragmented appearance. In Triton X-100 extracted cultures (not shown), the neurite morphology is maintained and neurite fragmentation is not apparent (see Minamide *et al.*, 2000). Control neurons included those that were untreated, treated with vehicle alone (0.5% DMSO), or treated with 1 μM of scrambled $A\beta_{1-42}$ peptide that had been pre-incubated identically to the fibril fraction of $A\beta_{1-42}$. Cultures were also stained with the human anti-Aβ (FCA18 directed against the N-terminal asp) antibody to monitor the distribution of $A\beta_{1-42}$ associated with the affected neurons. $A\beta_{1-42}$ immunostaining was dispersed randomly (Fig. 2.1b, f, j, n), but each of the different Aβ preparations resulted in distinctive immunofluorescence staining. LMW species appeared as discrete puncta whereas large oligomers and fibrils/insoluble aggregates were more difficult to resolve in a single plane of focus. Tortuous and dystrophic neurites (Pike *et al.*, 1992; Grace *et al.*, 2002) were observed only in cultures treated with large oligomers and fibrils/insoluble aggregates (Fig. 2.1o).

The majority of extracellular Aβ is lost during fixation and immunostaining. However, large Aβ aggregates can be observed in cultures by phase microscopy (Fig. 2.3 Sup). Therefore, we analyzed the number of neurons in contact with visible Aβ aggregates by phase microscopy (20x objective) in live cultures. At any point in time we determined that 31-41% of the neurons contacted phase-visible aggregates of Aβ when added at 1 μM. Furthermore, if we evaporated the medium from a treated culture before fixing and immunostaining for Aβ, between 52-65% of the neurites visualized by tubulin

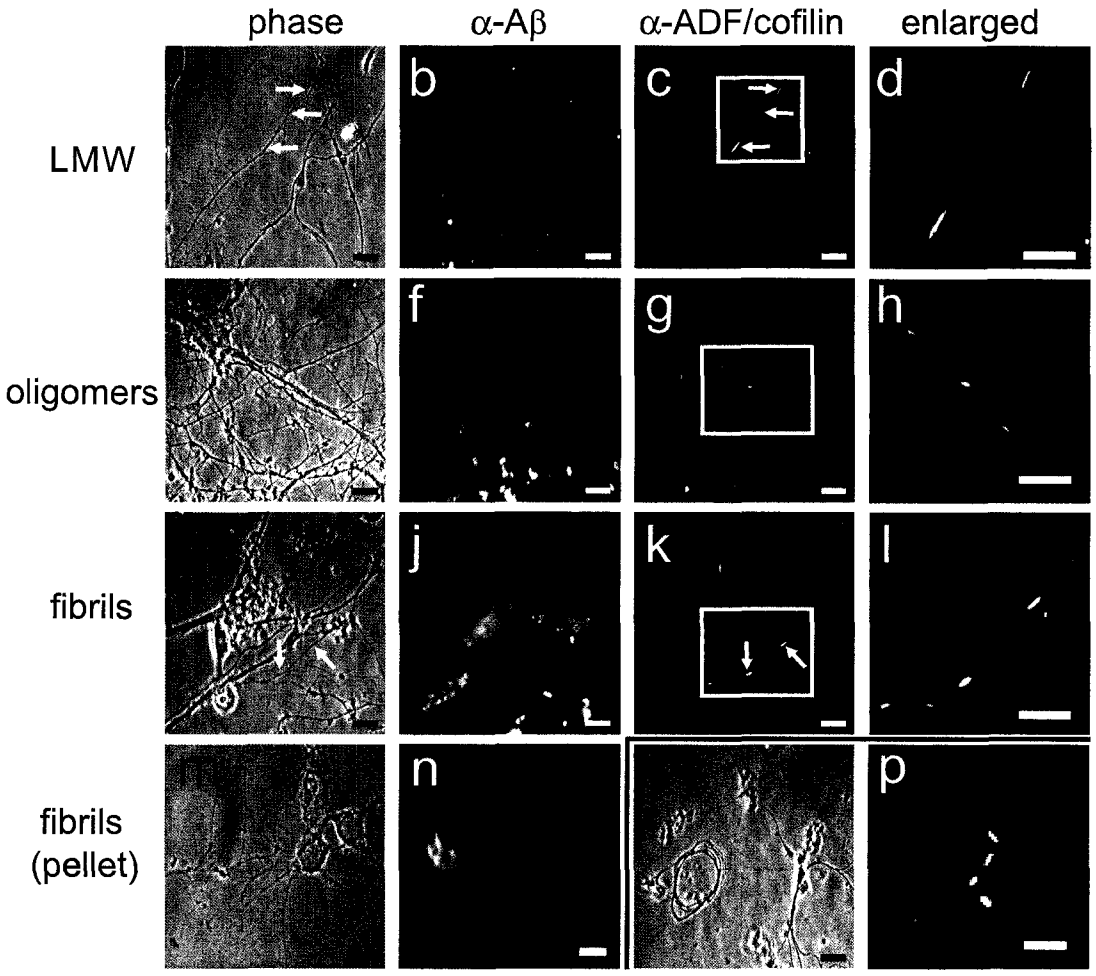

Figure 2.1: Aβ peptides induce rods in cultured neurons and in brains of transgenic mice. (a-l) Rods in hippocampal neurons treated with 1 μM of Ab1-42 low molecular weight (LMW), large oligomer (oligomers) or fibril/insoluble aggregate (fibrils) preparations. Arrows in panels (a, c), and (i, k) show the location of a rod in the phase and fluorescence image pairs. (m, n) Neurons treated with $A\beta_{1-42}$ pelleted from a fibril/insoluble aggregate preparation by centrifugation at 20,000 x g for 15 min. (n) Immunofluorescence of the pelleted $A\beta_{1-42}$ is more compact when compared to the whole fibril/insoluble aggregate preparations. (o) Example of a dystrophic neurite commonly found in fibril/insoluble aggregate-treated cultures. (p) Immunofluorescent rods stained for ADF/cofilin in the posterior cortex of a section of brain from a 4 month Tg2576 mouse. Scale bars = 10 μm (a-o). Scale bar = 5 μm (p).

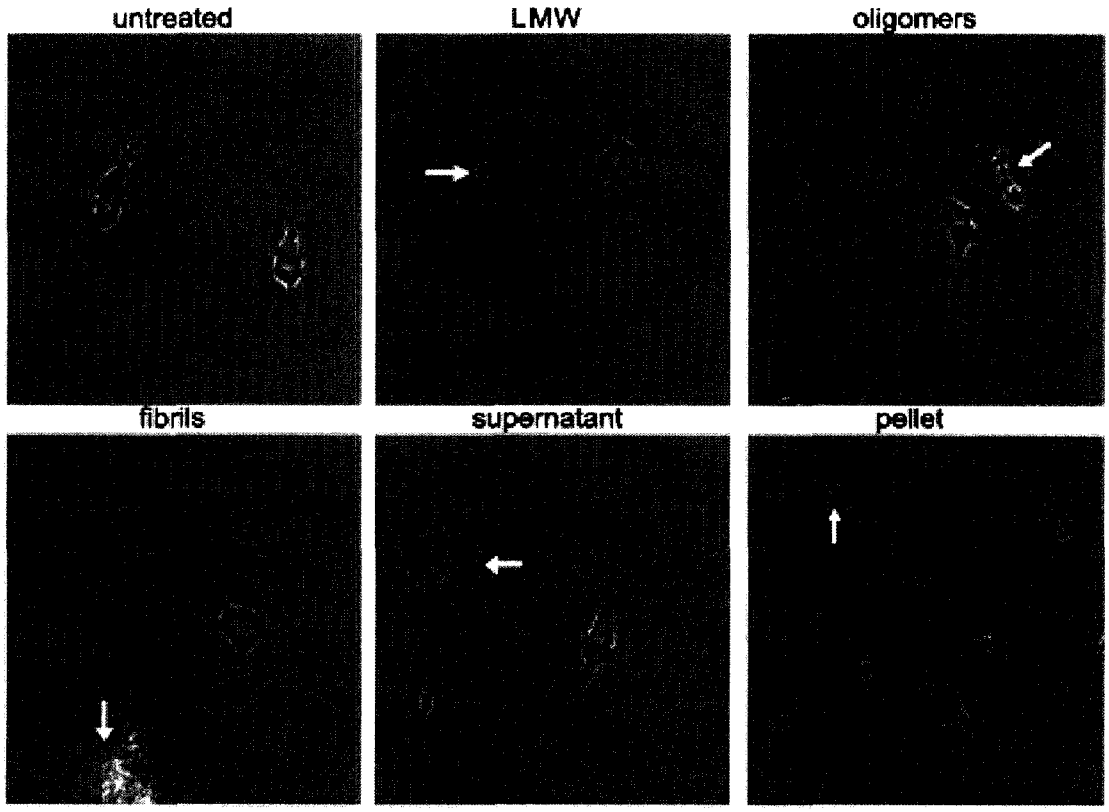

Supplementary Figure 2.3: Aβ aggregates are visible by phase microscopy. E18 rat hippocampal neurons 6 days *in vitro* were either untreated (a) or treated with: (b) 1 μM LMW, (c) 1 μM large oligomers, (d) 1 μM fibrils/insoluble aggregates, (e) 1.3 μM fibril supernatant, (f) 0.65 μM insoluble aggregate pellet. Arrows indicate peptide aggregates.

immunostaining were in direct contact with Aβ (Fig. 2.4 Sup). Because the large Aβ aggregates are freely moving in the culture medium, it is likely that all neurons spend at least some time in contact with Aβ aggregates *in vitro*.

Incubation conditions used to generate fibrils also generated insoluble aggregates (Lambert *et al.*, 1998; Walsh *et al.*, 1999; Dahlgren *et al.*, 2002; Walsh *et al.*, 2002b; Chromy *et al.*, 2003; Stine *et al.*, 2003). To determine whether fibrils or insoluble aggregates were the rod-inducing species in this Aβ fraction, we separated the two components by centrifugation at 20,000 x g. Portions of the supernatant and pellet fractions were solubilized in formic acid and the amount of Aβ in each fraction was determined by an immuno-dot blot assay. Nearly all of the rod-inducing activity of the fibril/insoluble aggregate preparation was associated with the supernatant fraction containing fibrils (Fig. 2.2a) and not with the pellet fraction containing insoluble aggregates.

To determine if excess Aβ production *in vivo* could also lead to neuronal rod formation, we examined the brain of a 4 month-old Tg2576 transgenic mouse for the presence of rods. Tg2576 mice express the Swedish mutation for human APP, which has been linked to familial Alzheimer's disease. A different strain of mouse expressing this same mutation of human APP generates excess Aβ peptides and has axonal transport deficits early in its development (Stokin *et al.*, 2005). Brain sections from the perfusion-fixed Tg2576 mouse show the presence of ADF/cofilin immunostained rods (Fig. 2.1p). Other studies have confirmed the formation of ADF/cofilin stained inclusions in neurons surrounding the regions of amyloid deposition in the Tg2576 mice (A. Mendoza-Naranjo,

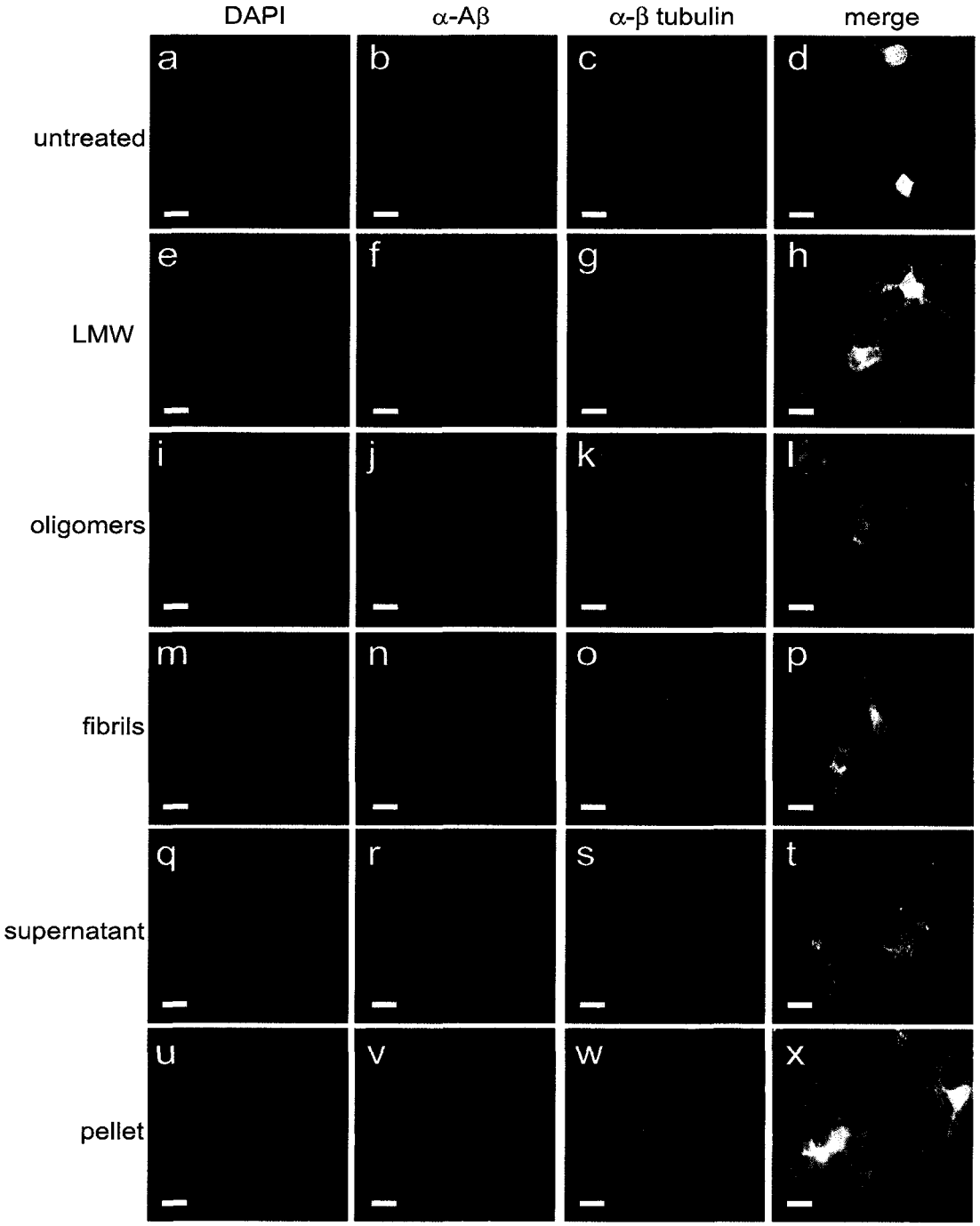

Supplementary Figure 2.4: Distribution of Aβ aggregates in cell culture. E18 rat hippocampal neurons 6 days *in vitro* were either untreated or treated with variously prepared Aβ peptides as labeled. Culture medium was evaporated and neurons and Aβ peptides stained as labeled. Abbreviations as in Figure 2.1.

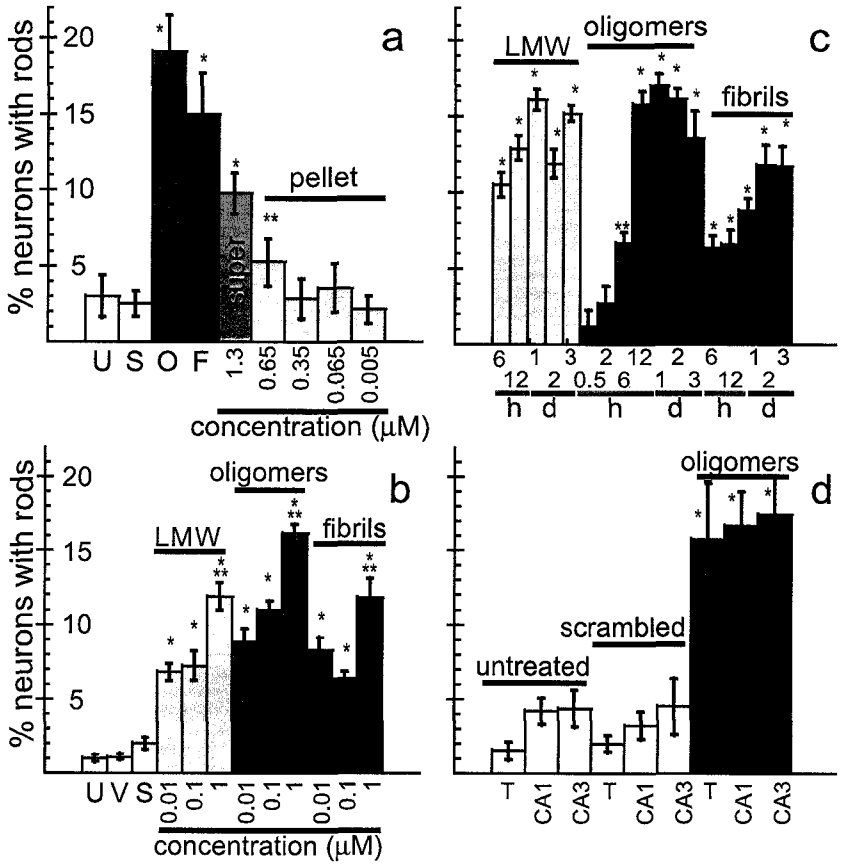

Figure 2.2: Effects of $A\beta_{1-42}$ on rod formation in cultured hippocampal neurons. (a) Percent of neurons with rods following 48 h of exposure to Aβ peptides. Differences are significant between control and experimental at $p < 0.0001$ (*) or $p < 0.01$ (**). Error bars (S.E6.M.). U = untreated; S = scrambled peptide; O = large oligomers; F = fibrils/insoluble aggregates. (b) Percent of neurons with rods following 48 h of exposure to soluble Aβ forms. Differences are significant between control and experimental at $p < 0.0001$ (*) or between control and other concentrations within its group at $p < 0.005$ (**). Error bars (S.E.M.). V = vehicle (0.5% DMSO). (c) Time course of 1 μM Aβ-induced rod formation. Time is in hours (h) or days (d). Differences are significant between control and experimental at $p < 0.0001$ (*), $p < 0.001$ (**). Error bars (S.E.M.). (d) Neurons forming rods in response to 48 h Ab treatment (1 μM oligomer) are distributed equally within CA1 and CA3 regions of hippocampus. Differences are significant between control and experimental at $p < 0.0001$ (*). Error bars (S.D.). T = total hippocampal neurons from a normal dissection.

C. Otth, J.R. Bamburg, R.B. Maccioni, C. Gonzalez-Billault, unpublished observations), similar to what has been observed in Alzheimer's brain (Minamide *et al.*, 2000).

$A\beta_{1-42}$ induces rods in a concentration- and time-dependent manner

To further characterize the rod-inducing activities of the $A\beta_{1-42}$ preparations, we examined their concentration-dependence on rod formation in 6 div hippocampal neurons. Controls were identical to those previously described. Less than 2% of neurons contained rods in all control groups (Fig. 2.2b). LMW, large oligomer and fibril/insoluble aggregate preparations of $A\beta_{1-42}$ between 10 nM and 1 μM induce a concentration-dependent increase in the percent of neurons containing rods with about 19% constituting the maximal response (Fig 2.2a, b). All three Aβ-preparations induced rods at 10 nM, the lowest concentration tested (Fig. 2.2b), although only about half of the maximal percent response was observed. At or below 1 μM $A\beta_{1-42}$, neuronal survival at 48 h remained high (>80%). Rod formation and survival were also analyzed in neurons treated with 2 μM and 10 μM $A\beta_{1-42}$ large oligomers. The percentage of neurons forming rods did not increase at concentrations above 1 μM; however, neuron survival declined considerably by 48 h following 2 μM treatment and all neurons were dead after treatment with 10 μM $A\beta_{1-42}$. These findings suggest that a subpopulation of hippocampal neurons is very sensitive to $A\beta_{1-42}$. $A\beta_{1-42}$ at concentrations as low as 10 nM will induce rods in about half the sensitive population, which plateaus at a maximum of about 19% for the highest non-lethal concentrations (1 μM).

Hippocampal neurons, 6 div, were treated with 1 μM $A\beta_{1-42}$ preparations and then fixed at various times and immunostained for rods. No more than 2% of the neurons in

untreated, vehicle-treated and scrambled peptide-treated control cultures contained rods at any time point. All Aβ samples induced significant rod formation by 6 h post-treatment, with maximal rod formation occurring by 12-48 h post-treatment (Fig. 2.2c). An increase in rod formation was observed in cultures exposed to 1 μM $A\beta_{1-42}$ large oligomer preparation as early as 2 h after treatment; however, due to the variability in the number of responding cells, this increase did not become significant over untreated controls until 6 h. In these experiments, neuronal survival seldom dropped below 80% at 72 h.

In response to ATP-depletion, greater than 80% of hippocampal neurons form rods immediately (Minamide *et al.*, 2000). In contrast, rod formation induced by $A\beta_{1-42}$ exposure occurred in a maximum of only 19% of cultured hippocampal neurons, even with Aβ at concentrations up to 10 μM or varying lengths of exposure (observed up to 3 days). Because neurons in specific sub-regions of the hippocampus show differential toxicity to $A\beta_{1-42}$ (Bahr *et al.*, 1998; Lambert *et al.*, 1998; Kim *et al.*, 2003), we determined whether rod formation simply reflected sub-region specific toxicity to $A\beta_{1-42}$. Accordingly, E18 rat hippocampal neurons (6 div) from the CA1 and CA3 regions (Fig. 2.1 Sup) were treated with 1 μM $A\beta_{1-42}$ large oligomers for 48 h. Controls included dissociated whole hippocampi or enriched CA1 and CA3 neuronal cultures that were either not treated or treated with 1 μM scrambled $A\beta_{1-42}$. No regionally localized population of hippocampal neurons appeared selectively responsive to rod induction by $A\beta_{1-42}$ large oligomers, as a maximum of only 17-18% of the neurons in both CA1 and CA3 enriched cultures contained rods 48 h post-treatment (Fig. 2.2d). This maximum percent response of rod induction for CA1 and CA3 enriched cultures is comparable to

the maximum percent response of rod induction seen for the dissociated, whole hippocampus. Although the percentage of neurons containing rods in control CA1 and CA3 cultures was more than twice the normal control value, we attribute this to the additional stress imposed by the lengthier dissection protocol required to isolate the CA1 and CA3 enriched regions.

Aβ induces ADF/cofilin activation only in neurons that form rods

The level of active (dephosphorylated) ADF/cofilin increases in neurons prior to and during rod induction by oxidative stress, excitotoxicity and ischemia (Minamide *et al.*, 2000). To determine if ADF/cofilin dephosphorylation also accompanies Aβ-induced rod formation, we compared the relative levels of phosphorylated ADF/cofilin (pAC) to total cofilin (pAC/total cofilin ratio) in untreated and Aβ-treated neurons. The ratio of the relative fluorescence was compared between the soma and neurites of neurons with and without rods. E18 rat hippocampal neurons 6 div were treated with 1 μM $A\beta_{1-42}$ large oligomers for 48 h to induce rods before fixing and immunostaining for total cofilin and pAC. In neurons which formed rods, there is a greater than 2-fold reduction in the pAC/total cofilin ratio in the soma of neurons containing rods as compared to neurons without rods (Fig. 2.3), indicating cofilin activation. Furthermore, neurons that do not respond to Aβ-treatment by forming rods show no significant change ($p>0.1$) in pAC/total cofilin ratio within their soma.

The pAC/total cofilin ratio was also measured within neurites from untreated neurons without rods, from Aβ-large oligomer treated neurons without rods, and from Aβ-large oligomer treated neurons with rods. In untreated neurons without rods, the

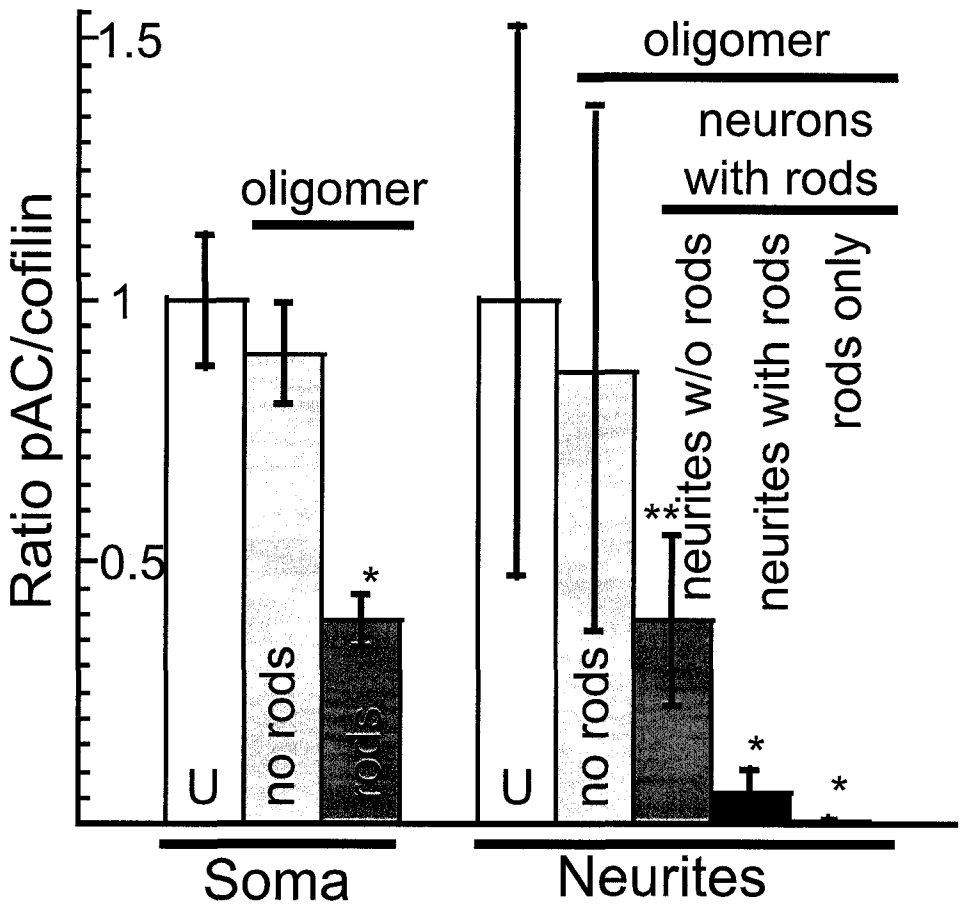

Figure 2.3: Ratios of phospho-ADF/cofilin to total cofilin staining in neurons in response to treatment with Aβ large oligomers. Rod formation is accompanied by an activation of the available ADF/cofilin pool as indicated by decreasing pAC levels. All values were normalized to the ratio of pAC to total cofilin in untreated neurons (set to 1). Error bars (S.D.). Differences are significant between control and experimental at $p < 0.0001$ (*) or $p < 0.05$ (**). Neurons with rods in right panel were analyzed in three ways. Ratios were taken from neurites that did not contain rods, from neurites that contained rods but from a non-rod region, and from neurites that contained rods from the region of the rod. U = untreated neurons, no rods = Ab-treated neurons that did not form rods.

pAC/total cofilin ratio remained comparable to controls. Similarly, treated neurons without rods also do not exhibit a significant change in the pAC/total cofilin ratio (Fig 2.3, columns labeled no rods). In treated neurons with rods, we examined within the same neuron, two groups of neurites, those containing rods and those not containing rods. Within neurites without rods from treated neurons that contained rods elsewhere, a 2.5-fold decline in the pAC/cofilin ratio was observed, similar to what was observed for their soma. However, within neurites containing rods, this ratio declined nearly 7-fold compared to untreated controls (Fig. 2.3). Furthermore, we observed a greater than a 60-fold decline in the pAC/cofilin ratio in the region occupied by the rods (Fig. 2.3). These data indicate that rod formation and dephosphorylation (activation) of ADF/cofilin in response to Aβ treatment occurs within the same neuronal population.

Localization of endogenous APP, BACE, PS1 and β-secretase cleaved APP to rods

To determine whether rods affect the transport of APP-containing vesicles and the enzymes which process APP into Aβ peptides, we immunostained E18 rat hippocampal neurons with antibodies to the midregion of the APP ectodomain (Koo & Squazzo, 1994; Yamazaki *et al.*, 1996) and to ADF/cofilin. In untreated cells, ADF/cofilin localized predominantly to growth cones and the cell body (Fig. 2.4a, j). APP was found in the cell body, but immunostaining was stronger in neurites (Fig. 2.4b), consistent with previous studies (Yamazaki *et al.*, 1995). Rods were induced either by transient (20 min) ATP-depletion followed by washout and overnight recovery (Fig. 2.4d-f) or by adenoviral mediated over-expression of *Xenopus* ADF/cofilin (XAC)-GFP, which induced spontaneous rod formation by 60 h after infection (Bernstein *et al.*, 2006). Minamide *et*

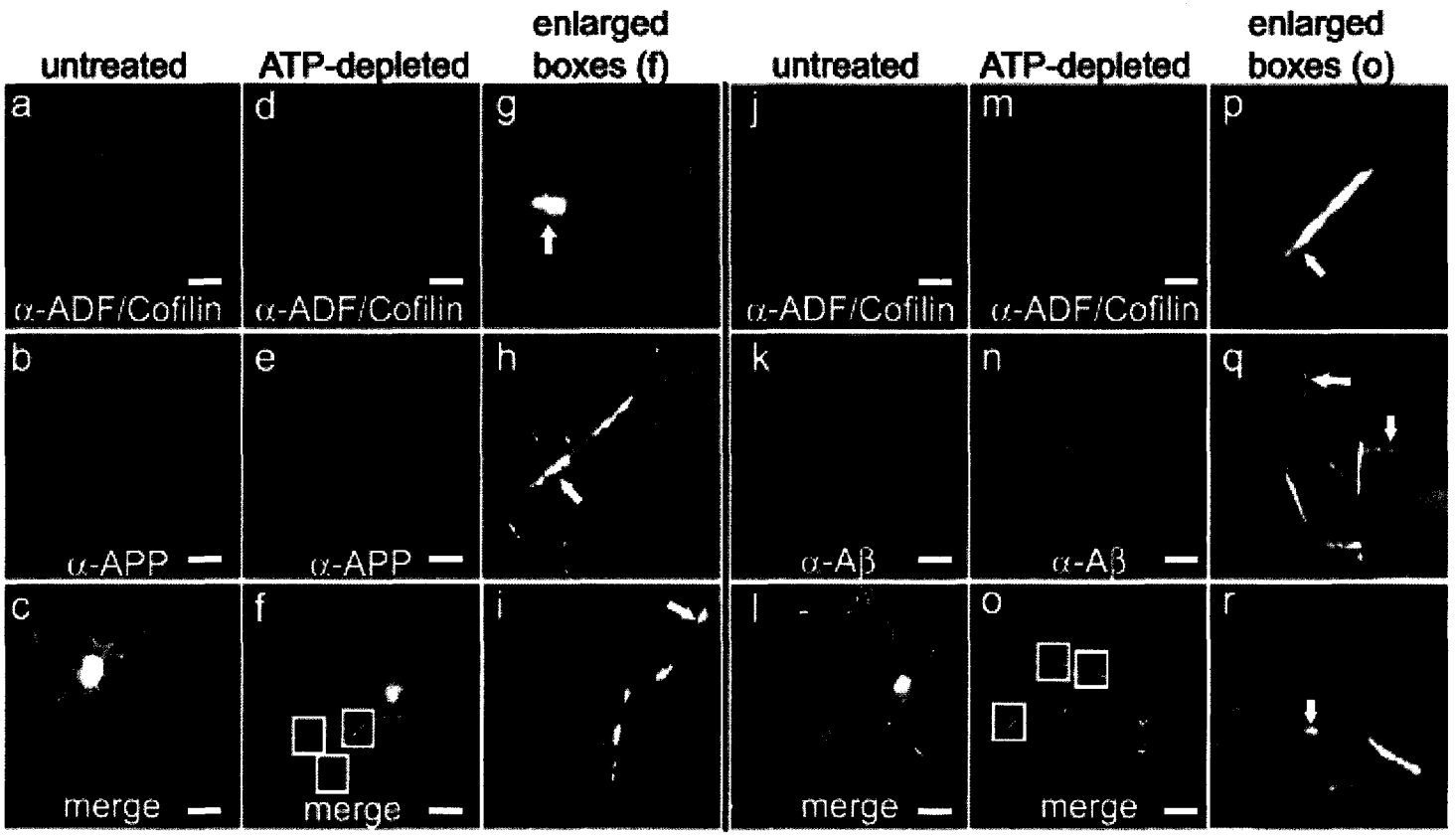

Figure 2.4: Vesicles containing APP and the β-secretase cleaved APP (β-CTF or Aβ) accumulate at ADF/cofilin-containing rods in neurites. Untreated E18 rat hippocampal neurons and 20 min ATP-depleted neurons that had undergone a 24 h recovery were fixed 7 days *in vitro* and immunostained as labeled. Scale bars = 10 mm.

al. (2000) showed that in ATP-depleted neurons, ATP levels returned to normal within 30 min following wash out, but rods reformed during the next 24 h in some neurites from about 30% of the neurons. ADF/cofilin accumulated in rods (Fig 2.4d, g-i), which were also the major site for APP accumulation in a vesicular (punctate) staining pattern (Fig. 2.4e). APP immunostaining either localized along the sides of the rods or was enriched at the distal ends of rods, suggesting accumulation of retrogradely transported vesicles (Fig. 2.4f-i). The β-secretase cleaved APP (β-CTF and/or Aβ-immunostained using an antibody to the N-terminal asp residue of the Aβ peptide, was similarly localized (Fig. 2.4j-r). In untreated cells, β-secretase cleaved APP was distributed within the cell body and neurites (Fig. 2.4k). In neurites with rods, β-secretase cleaved APP accumulated either throughout the rods proper or predominantly at one end (Fig. 2.4o-r).

BACE and presenilin 1 (PS1) immunostaining localized throughout the soma and neurites in vesicle-like puncta in untreated neurons (Fig. 2.5 Sup). In neurons with rods, PS1 and BACE localize near rod ends, particularly the distal end and along the side of rods in vesicular-like clusters (Fig. 2.5 Sup). These data suggest that ADF/cofilin-actin rods are a site for the accumulation of cargo containing APP, BACE, and PS1. We cannot be certain that the biochemical machinery required for Aβ production is completely contained within the same vesicle population. However, from the presence of the β-secretase cleaved APP in the same location we can infer that BACE is within the APP-containing vesicles and thus rod-induced disruption of transport might provide an environment where β-cleavage of APP can occur and accumulate.

We quantified, in three separate experiments, the immunofluorescence staining intensities of APP and β-secretase cleaved APP associated with the rods and in regions

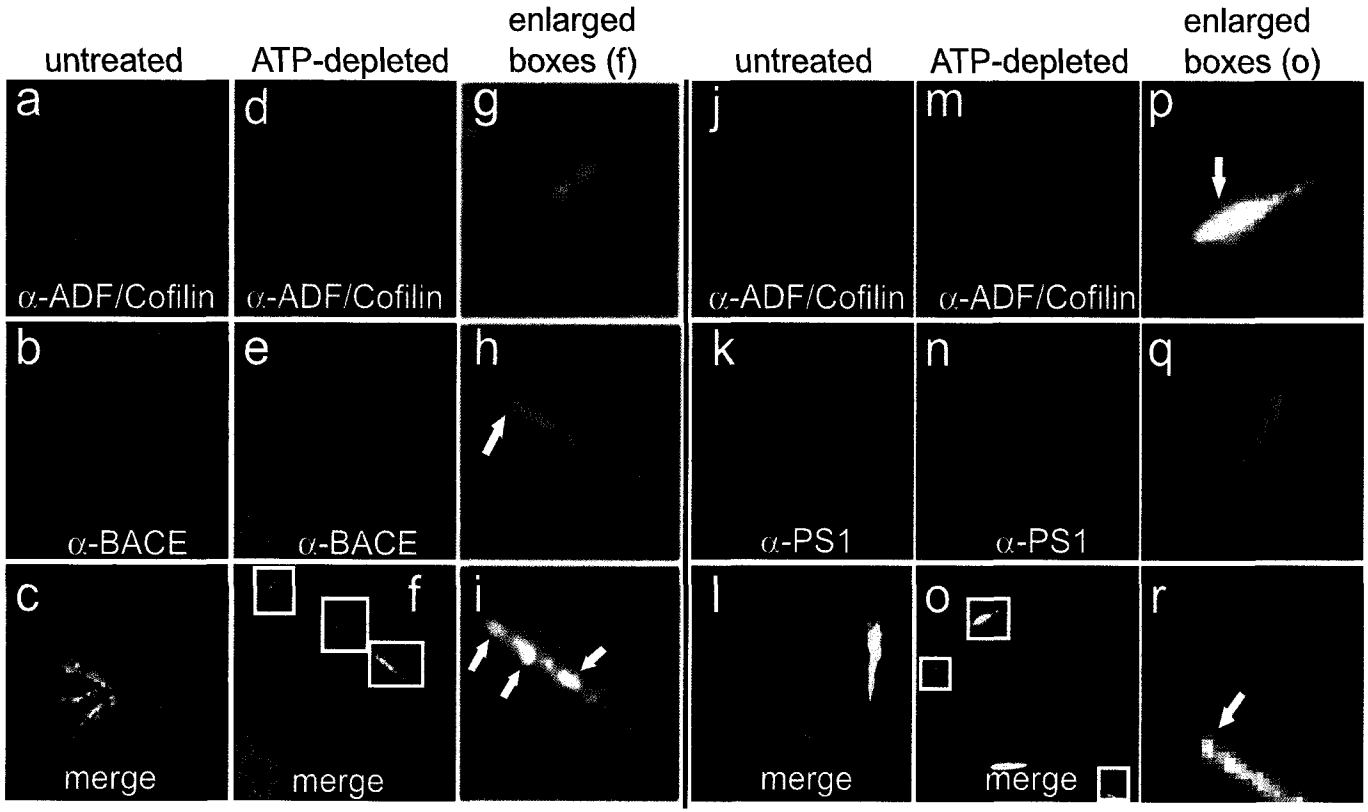

Supplementary Figure 2.5: Vesicles containing BACE and PS1 accumulate at ADF/cofilin-containing rods in neurites. Untreated E18 rat hippocampal neurons and 20 min ATP-depleted neurons that had undergone a 24 h recovery were fixed 7 days *in vitro* and immunostained as labeled.

distal to or between the rods, as well as in neurites without rods. Two of these experiments used transient ATP depletion with overnight recovery to induce rods and the third used rods that spontaneously formed from XAC-GFP overexpression. Results from the three experiments were similar indicating that the amount of APP and β-cleaved APP accumulation at rods is not dependent on the mechanism of rod formation (i.e. whether rods are induced by ATP depletion or by XAC-GFP overexpression). When compared to the staining intensity of neurites without rods for images captured under identical conditions, there is almost a 5-fold increase in the APP and a 2.3-fold increase in β-secretase cleaved APP associated with the rods and about a 40% reduction in the APP and a 60% reduction in β-secretase cleaved APP in regions between or distal to the rods (Fig. 2.5).

Discussion

Actin pathology often accompanies neurodegenerative changes in the brain. Two common actin-containing structures reported in AD brain are Hirano bodies and ADF/cofilin-actin rods. Hirano bodies are large paracrystaline aggregates that contain actin and immunostain for epitopes of ADF/cofilin (Maciver & Harrington, 1995), many actin binding proteins and tau (Hirano, 1994). ADF/cofilin-actin rods are much smaller inclusions that often occur in linear arrays. Although it is not known if the ADF/cofilin-actin rods can recruit additional proteins and give rise to Hirano bodies over time, the two structures are clearly separate entities in fixed AD brain sections (Minamide *et al.*, 2000).

$A\beta_{1\text{-}42}$ concentrations as low as 10 nM induce ADF/cofilin-actin rod formation in half of the hippocampal neurons that respond to higher concentrations (half maximum

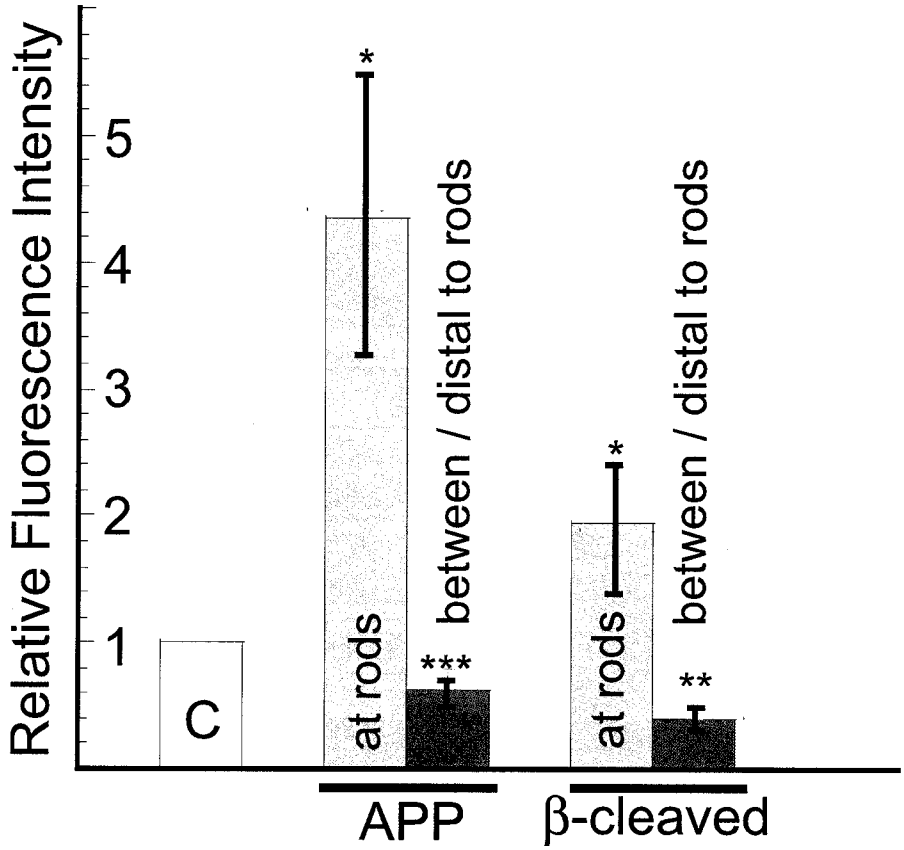

Figure 2.5: In cultured hippocampal neurons both APP and β-secretase-cleaved APP accumulate at rods and decline in regions between or distal to rods. Quantitative measurements of average immunofluorescence intensity were obtained for immunostained APP and β-secretase cleaved APP (FCA18 antibody) in cells without rods and cells in which rods were formed either through transient ATP depletion and 24 h recovery (two experiments), or from overexpression of XAC-GFP (one experiment). All images within the same experiment were captured using the same objective, camera and exposure settings. The fluorescence intensity values for the APP and β-secretase cleaved APP were set to 1 for the neurites containing no rods (C = control) and relative fluorescence values over the position of the rods (at rods) or between and distal to the rods were measured and plotted relative to the controls. Error bars are S.E.M. Differences shown are significant between control and experimental at $p < 0.0001$ (*), $p < 0.002$ (**), or $p < 0.09$ (***) as indicated.

percent response), as low a concentration as has been shown to have a physiological effect on neurons (Lambert *et al.*, 1998; Dahlgren *et al.*, 2002; Walsh *et al.*, 2002a; Hiruma *et al.*, 2003; Kim *et al.*, 2003; Takahashi *et al.*, 2004; Cleary *et al.*, 2005). The amount of soluble Aβ extracted from the frontal cortex of control human brains is 0.09±0.05 μg/g and from AD brain is 0.29±0.25 μg/g (McLean *et al.*, 1999). Estimating 200 μL/g interstitial volume (or 800 μL/g total volume) of water, interstitial concentrations of soluble Aβ are 44-155 nM in control brain and 44-598 nM in AD brain. If Aβ is equally distributed intra- and extracellularly, the concentrations are 5-39 nM in control brain and 5-150 nM in AD brain. Reports of decreased soluble Aβ within the cerebral spinal fluid of AD patients imply that much of the increased total soluble Aβ-pool in brain is intracellular (Blennow *et al.*, 2001). In either case an approximately 3.5-fold increase of soluble Aβ in AD brain could apply a significant stress on a selective population of sensitive neurons. Rods were not observed in control human brain tissues (Minamide *et al.*, 2000), even though the estimated Aβ amount in these brains is above the minimum concentrations we found necessary to induce rods in cultured hippocampal neurons. This finding suggests that either the form of Aβ in control human brain is different (perhaps a less toxic monomer; Kim *et al.*, 2003), or alternatively that neurons from control brain are less stressed by other factors (e.g. excess glutamate) that also contribute to rod formation.

Our findings of ADF/cofilin rods in the perfusion fixed Tg2576 mice are significant in that previous studies showing these inclusions in human AD brain could only be performed on brain samples obtained 2-12 h postmortem. Here the animals were

rapidly sacrificed and perfusion-fixed making it much more unlikely that rods formed only as a result of postmortem changes.

Actin dynamics in cultured embryonic neurons uses ~50% of cellular ATP (Bernstein & Bamburg, 2003) and thus rods have been proposed to represent an early neuroprotective mechanism during times of transient stress by sequestering virtually all of the ADF/cofilin into non-dynamic polymers of ADF/cofilin-ADP-actin (Bernstein *et al.*, 2006). The reduction of pAC levels in both soma and neurites of Aβ-treated neurons containing rods is indicative of a global activation of ADF/cofilin proteins within the Aβ-sensitive neuronal population, which may suggest that this sub-population of neurons has activated a neuroprotective pathway that they were unable to reverse.

The reason for Aβ-induced rod formation in only a sub-population of cultured hippocampal neurons is still uncharacterized. All cultured hippocampal neurons are responsive to $A\beta_{1\text{-}42}$, as treatment with high concentrations of $A\beta_{1\text{-}42}$ large oligomers (10 μM) results in complete lethality. Therefore, lower concentrations of $A\beta_{1\text{-}42}$ that trigger rod formation must work in a more specific manner on a particularly sensitive group of neurons. There are a number of plausible and potentially interesting mechanisms at work, which may explain this phenomenon. Aβ selectively binds to an undetermined sub-population of neurons in culture, which represents only 30-50% of the total population (Lacor *et al.*, 2004), providing one possible explanation for the limited pool of sensitive neurons. In addition, a subset (30-40%) of cultured hippocampal neurons, susceptible to nerve growth factor induced apoptosis, expresses the p75 receptor without expression of the cognate Trk receptors (Friedman, 2000). The p75 receptor has been

implicated in Aβ-mediated cell death (Perini *et al.*, 2002), thus Aβ binding to such a sub-population of neurons may explain the selective response of rod formation.

The aggregation state of Aβ may dictate the substrate binding preference, as suggested by differential binding to NMDA vs. non-NMDA receptors (Ye *et al.*, 2004), further narrowing this pool of sensitive neurons. Alternatively, Aβ may affect the activity of upstream regulators of ADF/cofilin. Low levels of $A\beta_{1-42}$ induce rapid Rac1 activation in PC12 cells (Chromy *et al.*, 2003). Hippocampal neurons treated with soluble Aβ fibrils also show activation of Rac1/Cdc42, Pak1 and dephosphorylation of AC proteins enhanced by the phosphatase slingshot, resulting in actin reorganization (A. Mendoza-Naranjo, C. Otth, J.R. Bamburg, R.B. Maccioni, C. Gonzalez-Billault, unpublished observations). Therefore, Aβ peptides may induce activation of specific signaling pathways in a sub-population of normal neurons that result in enhanced ADF/cofilin activity. In addition, Aβ has been shown to have detrimental effects on mitochondria (Grant *et al.*, 1999; Anandatheerthavarada *et al.*, 2003; Lustbader *et al.*, 2004; Mattson, 2004) and there may exist a neuronal sub-population in which mitochondria are extremely sensitive to Aβ. The ability to visualize rod-containing neurons in live cells expressing fluorescent protein chimeras of ADF/cofilin offers an opportunity to isolate and characterize this selective neuronal population.

In cultured neurons, $A\beta_{1-42}$ peptides induce rods that become sites for the accumulation of vesicles containing APP and its proteolytic processing machinery. In brains of transgenic mice expressing the Swedish mutation of human APP, one of the earliest defects observed is an accumulation of vesicular and organelle cargoes and formation of axonal varicosities at sites of transport blockage (Stokin *et al.*, 2005).

Maximal production of Aβ from APP in cultured neurons requires the endocytosis of APP (Koo & Squazzo, 1994; Cordy *et al.*, 2003; Ehehalt *et al.*, 2003). Inhibition of endocytosis in hippocampal neurons by expression of dominant interfering forms of dynamin, a GTPase required for endocytosis, dramatically decreases the amount of Aβ peptides that are secreted into the cell culture medium (Ehehalt *et al.*, 2003). The accumulation of APP, BACE, and PS1 in vesicles accumulating at rods may be a mechanism by which rods could enhance production of Aβ peptides. It is particularly noteworthy that the APP-containing vesicles either reside evenly distributed along the rods or accumulate at the distal end of the rod, suggesting that retrogradely transported endosomes accumulate. Aβ oligomers occur in vesicles localized along neurites and at synaptic compartments in both cultured neurons and in the brains of Tg2576 mice (Takahashi *et al.*, 2004). Rods provide an attractive mechanism to describe a variety of pathological and experimental data implicating the blockage of cargo transport in neurodegenerative diseases.

From the combined data presented herein and from the findings of others, we propose a hypothetical feed forward model (Fig. 2.6 Sup) for neurodegeneration and senile plaque growth in Alzheimer's disease and potentially in other amyloidogenic disorders, such as Down Syndrome (Head & Lott, 2004; Nixon, 2005). A specific neuronal sub-population may be adversely susceptible to the accumulation of Aβ, such as in familial Alzheimer's disease, or to other stress-inducers such as ischemia, oxidative stress, or excitotoxicity, which may be involved in sporadic AD. These insults can result in rod formation within neurites, thereby blocking vesicle transport and leading to the continued generation of Aβ within stalled endosomes, and subsequent secretion at these

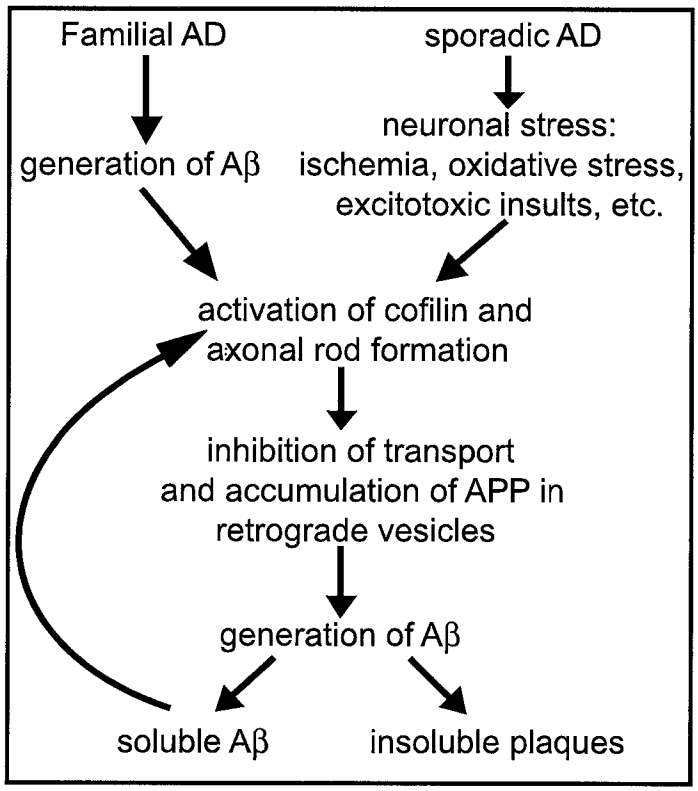

Supplementary Figure 2.6: Hypothetical model for a convergent feed-forward mechanism of plaque formation and neurodegeneration in familial and sporadic Alzheimer's disease. Inherited mutations, as in FAD, lead to increased Ab that can induce rod formation in a sensitive population of neurons. Other forms of neuronal stress, such as ischemic injury, excitotoxicity or oxidative stress induce rod formation and may lead to sporadic AD. Disruption of APP-, BACE- and PS1-containing vesicles by rods may lead to locally elevated Aβ production in neurites. Aβ can either be sequestered into insoluble plaques or soluble Aβ can induce further rod formation in the surrounding neuropil exacerbating the neurodegenerative cycle.

focal sites. Locally elevated Aβ can give rise to additional rod formation in the surrounding neuropil further exacerbating the neurodegenerative cycle.

Chapter Three

Anoxia and Amyloid-β induce ADF/cofilin Rod formation in Hippocampal Organotypic Slice Cultures

Preface and Acknowledgement

Thanks are in order to Marcia Podlisny and Dennis Selkoe for providing the cell derived Aβ conditioned medium utilized in the experiments presented herein.

Abstract

With advancing age the brain becomes increasingly susceptible to ischemic insults resulting from mitochondrial rundown and stroke. Mini-strokes, transient loss of blood flow to a region of the brain, often results in irreparable damage. Exposure of dissociated E-18 rat hippocampal neurons to conditions mimicking ischemia produces a rapid reorganization of the cytoskeletal proteins ADF/cofilin and actin into tapered cylindrical aggregates known as rods. Rods disrupt distal neurite functioning and may be involved in synaptic loss and cognitive or functional impairment. Using organotypic hippocampal slice cultures we demonstrate that ADF/cofilin-actin rod formation occurs within minutes of ATP rundown induced either by ATP-depletion medium, excess glutamate, peroxide, oxygen-glucose deprivation or by anoxia. Rod formation also occurs in slice cultures following exposure to nanomolar concentrations of soluble $A\beta_{1-42}$ similar to what we reported in dissociated neurons. We have used the slice cultures to identify regions within the hippocampus that appear to be most susceptible to $A\beta_{1-42}$-

induced rods. These regions appear to localize along the blade of the dentate gyrus where cells of the molecular layer receive input from the cholinergic cell bodies residing in the septum.

Introduction

Hippocampal slice cultures provide an excellent *in vitro* model system for studying neurodegenerative conditions (Holopainen, 2005). A major advantage of slice cultures is the maintenance of *in vivo* like cytoarchitecture and synaptic connectivity (Stoppini *et al.,* 1991). The hippocampus, the major region of the brain involved in learning and memory, becomes functionally impaired in a number of human diseases including vascular dementia and Alzheimer's disease (AD). Ischemia can occur when the cerebral vasculature becomes partially or completely occluded (stroke) thereby depriving neurons of oxygen. The brain has a high metabolic activity making it susceptible to ischemic damage, furthermore the hippocampus is especially susceptible to ischemic injury (Schmidt-Kastner & Freund, 1991). Following transient oxygen-glucose deprivation (OGD; model for ischemia), organotypic hippocampal slice cultures experience selective apoptotic neuronal death (Mattson *et al.,* 2000; Rami *et al.,* 2003; Eldadah & Faden, 2000; Graham & Chen, 2001) in the CA1 region (Chen *et al*, 1998) largely resulting from glutamate excitotoxicity (Hewitt & Corbett, 1992). OGD induces morphological changes in CA1 neurons including swollen neurons with vacuolated cytoplasm (Lushnikova *et al.,* 2004). In vivo studies using transient ischemia (10 min) induced by clamping the carotid artery caused elevated intracellular Ca^{2+}, activation of calpain, cytoskeletal alterations, and cell death (Lee *et al.,* 1991). Selective calpain

inhibition is neuroprotective in hippocampal slice cultures following OGD (Brana *et al.,* 1999).

Misregulation of neuronal actin and ADF/cofilin is associated with a range of cognitive impairments and degenerative conditions (Maloney *et al.,* 2006). Exposure of dissociated hippocampal cultures to oxidative stress, excitotoxic levels of glutamate, ATP-depletion medium, or $A\beta_{1-42}$ induces the rapid formation of ADF/cofilin-actin rods (Minamide *et al.,* 2000; Maloney *et al.,* 2005). In cultured *Aplysia kurodai* neurons, the overexpression of cofilin induces rods responsible for synaptic loss and impaired synaptic plasticity (Jang *et al.,* 2005). Thus, stress-induced rods have the potential to explain cognitive and functional impairment associated with cerebro-vascular diseases.

The neuronal actin cytoskeleton is a tightly regulated network of filaments that places a high demand on cellular energy. Under resting conditions actin-ATP hydrolysis consumes nearly 50% of neuronal ATP (Bernstein & Bamburg, 2003). Adenoviral mediated overexpression of *Xenopus* ADF/cofilin conjugated to green fluorescent protein (XAC-GFP) induces the formation of rods in neurites, the presence of which retards the loss of mitochondrial membrane potential ($\Delta\Psi_m$) and ATP when compared to neurites without rods (Bernstein *et al.,* 2006). Short-term exposure to OGD makes organotypic hippocampal slice cultures resistant to subsequent prolonged anoxia (Xu *et al.,* 2002; Valentim *et al.,* 2003) a characteristic termed ischemic preconditioning (Lushnikova *et al.,* 2004). Stress induced actin-rod formation sequesters nearly all available ADF/cofilin into non-dynamic aggregates (Minamide *et al.,* 2000; Bernstein *et al.,* 2006). Thus, rods may play a neuroprotective role by shutting down actin dynamics to preserve ATP during transient neuronal insult.

Rod-like cofilin pathology is found associated with amyloid plaques in human AD brain but not in normal control brains (Minamide *et al*, 2000). Additionally rod-like cofilin aggregates have been found in the brains of transgenic mice (Tg2576) (Maloney *et al.*, 2005) expressing a mutant form of APP associated with increased $A\beta_{1-42}$ production and human familial AD. Here we report the formation of rod-like cofilin aggregates in organotypic hippocampal slice cultures following transient exposure to anoxia, ATP-depletion, glutamate, peroxide, OGD, and soluble $A\beta_{1-42}$. This work builds upon our previous studies in dissociated rat hippocampal neurons by demonstrating rod formation in this highly organized and physiologically relevant culture system. Furthermore by bridging the gap between rods in dissociated primary neuronal cultures and rod-like cofilin pathology in diseased human brain, we are taking a key step in establishing an *in vitro* system for evaluating the role of rods in neurodegenerative disease.

Materials and Methods

All chemicals are reagent grade and were obtained from Sigma-Aldrich Co. and all tissue culture reagents were from Life Technologies (Invitrogen™). β-Amyloid peptide ($A\beta_{1-42}$ and a scrambled peptide with the same amino acid composition) were purchased from Ana Spec, Inc.

Cell culture and treatments

Hippocampal slice cultures were prepared from P7-P9 Sprague Dawley rat pups essentially as described previously (Stoppini *et al*, 1991). Briefly, hippocampi were quickly dissected into filter sterilized ice-cold (4° C) Gey's Balanced Salt Solution

(GBSS) plus 4% glucose solution, then sliced to a thickness of 400 μm on a McIlwain tissue chopper. Finally 3-6 intact slices are arranged onto 0.4 μm Transwell® Polyester membranes inserted into 6 well culture plates (Corning Costar® 3450). Beneath the membrane is added 1.7 mL of filter sterilized slice culture medium (50 mL horse serum, 50 mL Hank's Balanced Salt Solution (HBSS), 100 mL Minimal Essential Medium (MEM), 500 μL 1.25 mM L-glutamine, 4 mL 25% glucose, 1 mL 100 U/mL Penicillin-Streptomycin). MEM is HEPES and bicarbonate buffered. Slice culture medium is aspirated and replaced with 1.5 mL on day 3 and every 2-3 days thereafter as required. For all experiments slices on membranes were cultured for 10 days in a 95% air/5%CO_2 incubator at 37° C. For live cell imaging slices were prepared as described above then 1-2 hippocampi were placed onto 12 x 22 coverslips and imbedded in 20 μL of chicken plasma (Cocalico Biologicals, Inc.) and clotted with 6 μL thrombin (150 NIH units/mL in H_20; MP Biomedicals, Inc.). Slides with imbedded hippocampi were placed into flat bottom test tubes (Nunclon Delta Tubes; Nunc™) and 700 μL of slice culture medium was added. Tubes were placed at a 6° angle in a rolling incubator system (0.6 r.p.m) at 35° C and medium was replaced every 2-3 days. Imaging was performed on day 10.

For peroxide, glutamate, and $A\beta_{1-42}$ peptide treatments (all on day 8) respectively, hydrogen peroxide was added to the medium to a final concentration of 10 μM, glutamate was added to the medium to a final concentration of 250 μM, and $A\beta_{1-42}$ peptide was added to the medium to final concentrations of 10 nM, 1 μM or 2 μM. A small amount of the treated medium was layered over each slice then the cultures were placed back in the 95% air/5%CO_2 incubator at 37° C for 1h (peroxide and glutamate) or for 48 h ($A\beta_{1-42}$ peptide), before having the medium removed and replaced with fresh medium. For ATP

depletion experiments, the slice culture medium was aspirated and replaced with ATP depletion medium [6 mM 2-deoxyglucose, 10 mM NaN_3 in Phosphate Buffered Saline (PBS)] and cultures were place into a humidified air incubator at 37° C for 1 h before being immediately fixed or having the medium removed and replaced with fresh medium. Oxygen/glucose deprivation of slices was performed as described previously (Cimarositi *et al.,* 2001; Strasser & Fischer, 1995). Briefly slices were rinsed once in controlled salt solution (CSS) (120mM NaCl, 5.4mM KCl, 0.8mM $MgCl_2$, 1.8 mM $CaCl_2$, 25 mM Tris pH 7.2, 15 mM glucose) on day 8 followed by treatment with OGD medium (CSS with sucrose substituted for glucose and bubbled with N_2). Slices were sealed in a chamber flushed with N_2 and placed in an incubator at 37° C for 1 h before removing the OGD medium, rinsing 2X with CSS, and replacing the medium with fresh slice culture medium. For expression of *Xenopus* ADF/cofilin tagged with green (XAC-GFP) or red (XAC-mRFP) fluorescent proteins (Meberg & Bamburg, 2000), ~10^6 adenoviral particles were placed directly onto each slice on a membrane and the cultures were returned to the 95% air/5%CO_2 incubator at 37° C for 12 h before the medium was removed and replaced with fresh slice culture medium. For rolling cultures, ~1.0 x 10^7 adenoviral particles were placed directly into the medium on day 7 and left in culture until viewing. Slices were made anoxic on day 10 in culture by placing them face down onto a glass microscope slide and quickly sealing the edges with paraffin.

Solubilization of the β-amyloid peptides and generation of the soluble $A\beta_{1-42}$ aggregates were performed as described previously (Dahlgren *et al.,* 2002; Stine *et al.,* 2003). Cell-derived conditioned medium (CDCM) was obtained from control Chinese hamster ovary (CHO) cells or those expressing a human mutant form of amyloid

precursor protein (7PA2) (Podlisny *et al.,* 1995). CDCM was diluted to 2X in slice culture medium then syringe filter sterilized. On day 2, medium was removed and replaced with either slice culture medium, 2X CHO (control) conditioned medium, or 2X 7PA2 (Aβ) conditioned medium. On days 5 and 8 this process was repeated such that a set of slices was exposed to the CHO or 7PA2 medium for 2, 5 or 8 days. Size exclusion chromatography (SEC) purified Aβ monomers or dimer-trimer fractions of 7PA2 cell-derived conditioned medium was diluted to 0.5X in slice culture medium, bubbled with CO_2 before adjusting to pH 7.2 and syringe filtered. On day 2, medium was removed and replaced with either control monomer (ncM), control dimer-trimer (ncDT), Aβ monomer (AβM), or Aβ dimer-trimer (AβDT) conditioned medium. On days 5 and 8 this process was repeated such that a set of slices was exposed to ncM, ncDT, AβM, or AβDT for 2, 5 or 8 days. All slices were fixed on day 10.

Slices were fixed for 4 h at room temperature in 4% paraformaldehyde in PBS adjusted to pH 7.0. Slices were methanol (-20° C) permeabilized for 10 min and blocked in 2% goat serum/1% Bovine Serum Albumin Fraction V (BSA) in Tris Buffered Saline (TBS) before immunostaining with various antibodies. In experiments where fluorescent phalloidin was used to stain actin filaments, slices were permeabilized with 0.1% Triton X-100 in PBS for 10 min. Primary antibodies include: affinity purified rabbit antiserum to chick ADF (1439; 2 ng/μL), which cross-reacts with mammalian ADF and cofilin (Minamide *et al.,* 2000), protein A purified monoclonal mouse anti-cofilin (Mab22; 10 ng/μL IgG; Abe *et al.* 1989), monoclonal anti-human β-amyloid Asp-1 (FCA18; 1:150; CalBiochem®), rabbit anti-β-Amyloid Precursor Protein (1:150; Invitrogen™). Secondary antibodies, all used at 1:450, include fluorescein goat anti-rabbit and goat anti-

mouse and Texas-Red goat anti-rabbit and goat anti-mouse (Invitrogen™ Molecular Probes™). Texas Red -X phalloidin (Molecular Probes™) was used at 1:50 in PBS. DAPI (4'-6-Diamidino-2-phenylindole) was used at 1:1000 (Invitrogen™ Molecular Probes™). After blocking and staining slices were carefully cut out of the membrane inserts and mounted on 22 x 22 mm cover glass with Prolong Gold Antifade (Invitrogen™ Molecular Probes™).

Microscopy: Phase-contrast and fluorescence micrographs were obtained using 4x [0.13 numerical aperture (NA)], 10x (0.25 NA), 20x (0.75 NA) air objectives or 40x (1.3 NA), 60x (1.4 NA), 100x (1.4 NA) oil objectives as previously described (Minamide *et al.*, 2000). For experiments using SEC fractionated monomer and dimer-trimer Aβ fractions in conditioned medium, the total number of rods per field was counted using a 60x oil objective. Slices were scanned in a grid pattern to sample the entire area of the slice. By mapping the rod counts per 60x field onto a low power (4x) image of the slice, the location of the high-power field within the slice was ascertained. This mapping was aided by the bleaching of background fluorescence in the region examined at high power, which showed up as a dark circle on the low power image of the slice. A contour map was then generated from the rod counts using a gradient scale where 0 rods = black, 1-5 rods = blue, 5-10 rods = green, 10-15 rods = yellow, 15-20 rods = red and >20 rods per field = white. Colored overlays were integrated using Adobe Photoshop v.7.0 Filter/texture/stained glass function and setting the cell size to 12, border thickness to 1, and light intensity to 1. This map is then overlayed onto a low power (4x) image of the

slice with dotted lines drawn in to represent the pyramidal cell layers of the Dentate Gyrus and Cornu Amonis based on DAPI staining.

For live cell imaging, XAC-GFP or XAC-mRFP infected slices were made anoxic as described above and immediately imaged at 20x on a Nikon inverted microscope. Fluorescence images were acquired with a CoolSnap ES CCD (Photometrics). MetaMorph v6.1 software (Universal Imaging) was used for all digital processing. Time lapse images were collected every 20 sec for 10 min then the slice was scanned for rod formation.

Results

Rod formation in slice cultures parallels that of dissociated neurons

In response to ATP depletion rod like aggregates form rapidly in organotypic hippocampal slice cultures infected with adenovirus expressing XAC-GFP (Fig. 3.1). Rod-like aggregates labeling with an ADF/cofilin antibody also are observed in uninfected slices following ATP depletion, and in slice cultures treated with 10 μM H_2O_2 for 1 h, 250 μM glutamate for 1 h, OGD for 1 h, or 2 μM soluble $A\beta_{1-42}$ for 48 h (Fig. 3.2). In untreated control slices, ADF/cofilin labeled rod-like aggregates are observed sporadically and infrequently. Preliminary evidence indicates that these rod-like aggregates observed in slices are similar to cofilin-rods reported to form in dissociated neurons under identical conditions. Though these cofilin labeled inclusions appear rod-like in shape, further characterization remained necessary and was pursued.

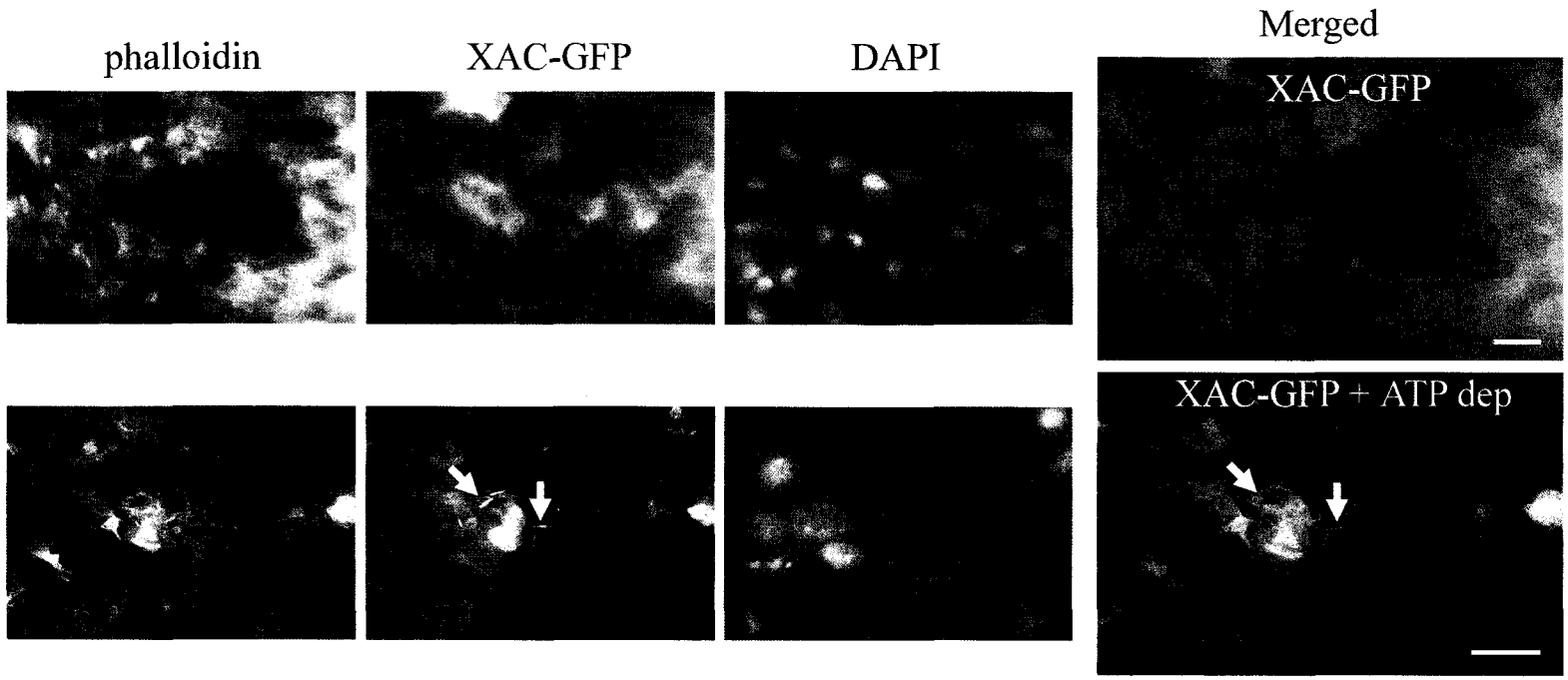

Figure 3.1: Rods in slices infected with XAC-GFP following ATP depletion are refractory to phalloidin staining. Arrows indicate the location of rods in XAC-GFP and merged images. Scale bars = 10 μm.

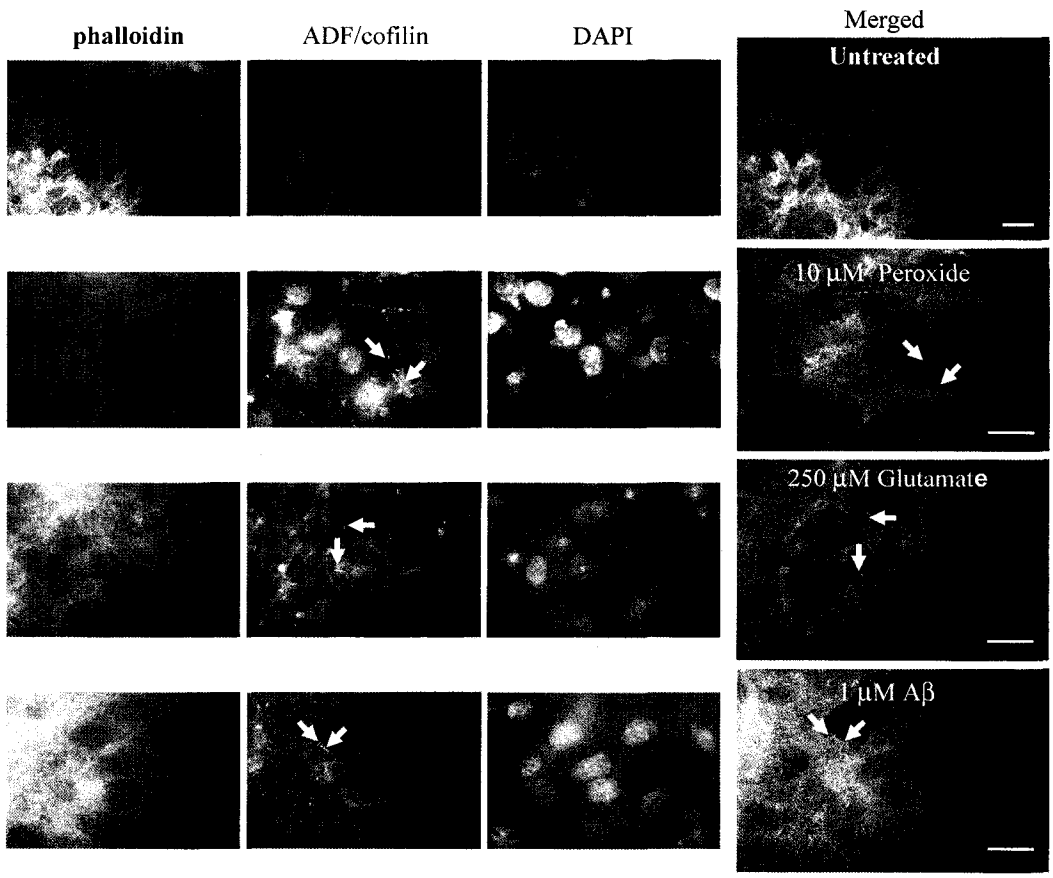

Figure 3.2: Rods in slices treated with peroxide, glutamate and Aβ are refractory to phalloidin staining. Arrows indicate the location of rods in the ADF/cofilin and merged images. Scale bars = 10 μm.

Defining a rod

Rods can be uniquely classified from other cytoskeletal inclusions by their immunostaining with antibodies to both actin and ADF/cofilin, but when well fixed, their inability to be labeled with fluorescent phalloidin (Minamide *et al.,* 2000). For the purpose of cofilin-rod characterization, organotypic slices were infected with XAC-GFP or XAC-mRFP or treated with peroxide, ATP depletion medium, excess glutamate, OGD, or 1 μM $A\beta_{1-42}$ to induce rods. Treated slices were fixed and immunostained with antibodies against ADF/cofilin, and some slices were stained with fluorescent phalloidin. To be classified as rods they must co-stain with actin and ADF/cofilin antibodies, but should not stain with fluorescent phalloidin. Because actin is such an abundant protein, staining tissue with actin antibodies makes it difficult to observe specific actin-containing structures including rods due to a high background signal. Thus, we rely upon the ADF/cofilin and phalloidin labeling characteristics to define the rod-like aggregates observed in slices.

ADF/cofilin labeled rod-like aggregates were refractory to phalloidin labeling in slices treated with all neurodegenerative stimuli (Fig 3.1 and 3.2). Thus, the rod-like aggregates observed in organotypic hippocampal slice cultures following exposure to all of the previously tested neurodegenerative stimuli and with OGD fit the definition of rods that form in identically treated dissociated primary cultured neurons (Minamide *et al.,* 2000, Maloney *et al.,* 2005). From this point foreword we will refer to all ADF/cofilin stained "rod-like" aggregates as rods.

Time Course of Anoxia Induced Rod Formation

The time course of rod formation was studied in organotypic hippocampal slices infected with adenovirus expressing XAC-GFP or XAC-mRFP. Slices were made anoxic by placing them face down on a glass microscope slide and sealing the edges with paraffin. Immediately after making the slices anoxic XAC-GFP or XAC-mRFP expression is diffuse within cells (Fig 3.3) and no rods were detected. Images were collected at a randomly selected locations in the slices every 20 s for 10 min during which time no rod formation was observed. However, a subsequent scan of the slice revealed abundant XAC-GFP or XAC-mRFP containing rods had formed in various areas of the slice. Time-lapse observation of rod containing regions detected no new rod formation indicating that rods form rapidly and abundantly within 10 min of anoxia and reach a maximum number within this time (Fig 3.3). This experiment was repeated on five slices with identical outcomes. Sub-regional preferences for rod formation were not identified because live slice observations were severely limited in terms of depth of focus and the absence of DAPI staining made locating slice regions difficult.

Concentration Dependence of $A\beta_{1-42}$ Induced Rod Formation

Rod formation has been reported to occur in dissociated neurons treated with 10 nM soluble $A\beta_{1-42}$ (Maloney *et al.*, 2006). In kind, hippocampal slice cultures were treated with 10 nM soluble $A\beta_{1-42}$ and 1 μM $A\beta_{1-42}$ for 48 h beginning on day 8. Slices were fixed and immunostained with an ADF/cofilin antibody to observe rods on day 10. Rods were observed in cultures treated both 10 nM and 1 μM soluble $A\beta_{1-42}$. These data

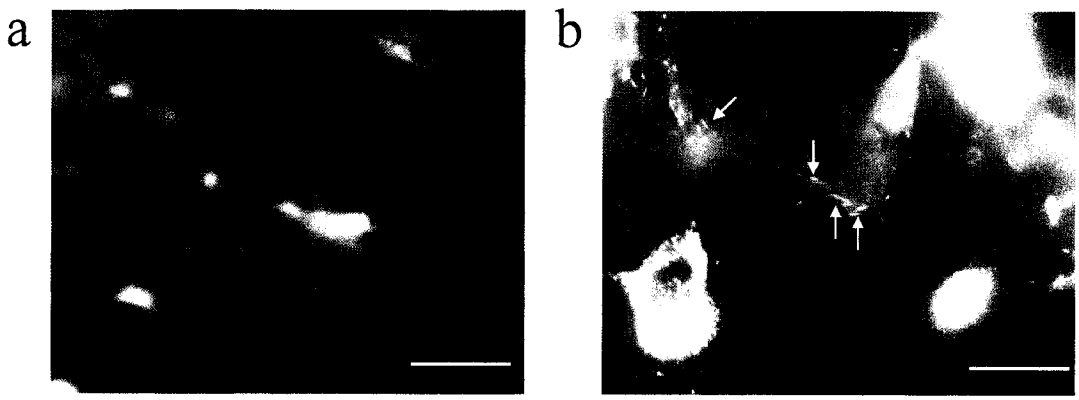

Figure 3.3: Anoxia induces rod formation in organotypic slice cultures. Organotypic slice cultures were infected with XAC-mRFP for three days in culture then made anoxic by placing them onto a glass microscope slide and sealing the coverslip with paraffin. mRFP is diffusely distributed in slices immediately upon viewing (a). mRFP positive rods form rapidly (complete within 10 min) following anoxic conditions (arrows b). Scale bars = 50 μm. Arrows indicate the location of a few rods. Images captured at 20x.

demonstrate that soluble $A\beta_{1-42}$ induces rods in organotypic slice cultures at low nanomolar concentrations as reported to occur in dissociated cultures (Maloney *et al.*, 2005).

Rod formation occurs in localized regions of hippocampal slice cultures

An initial examination of slices treated with 10 nM, 1 μM, and 2 μM soluble $A\beta_{1-42}$ indicated that rod formation may occur preferentially in and around the region of the dentate gyrus (DG) and to a lesser degree in CA1 and CA3 regions (Fig 3.4). This finding prompted a closer investigation of the regional distribution of rods within Aβ treated slice cultures. Hippocampal slice cultures were treated with 1 μM soluble $A\beta_{1-42}$ for 48 h starting on day 8 of culture. On day 10, slices were fixed and rods were immunostained using an ADF/cofilin antibody. Slices were then systematically scanned using a 60x objective and the total number of rods per field was scored. Rod formation was found to occur in regional hot spots within the slice, with a large percentage of all rod formation occurring in and around the DG (Fig 3.5). This regional distribution of rods was not observed in untreated control slices or in slices that were ATP depleted and fixed immediately or after a 48 h recovery (Fig 3.6). Sporadic rod formation was observed in untreated control slices with rods distributed randomly across the tissue. Slices fixed immediately following ATP depletion without a recovery period contain abundant rods that are widely distributed across the tissue with no regional hot spots. ATP depletion followed by 48 h recovery resulted in low numbers of rods similar to those observed in the untreated control slices.

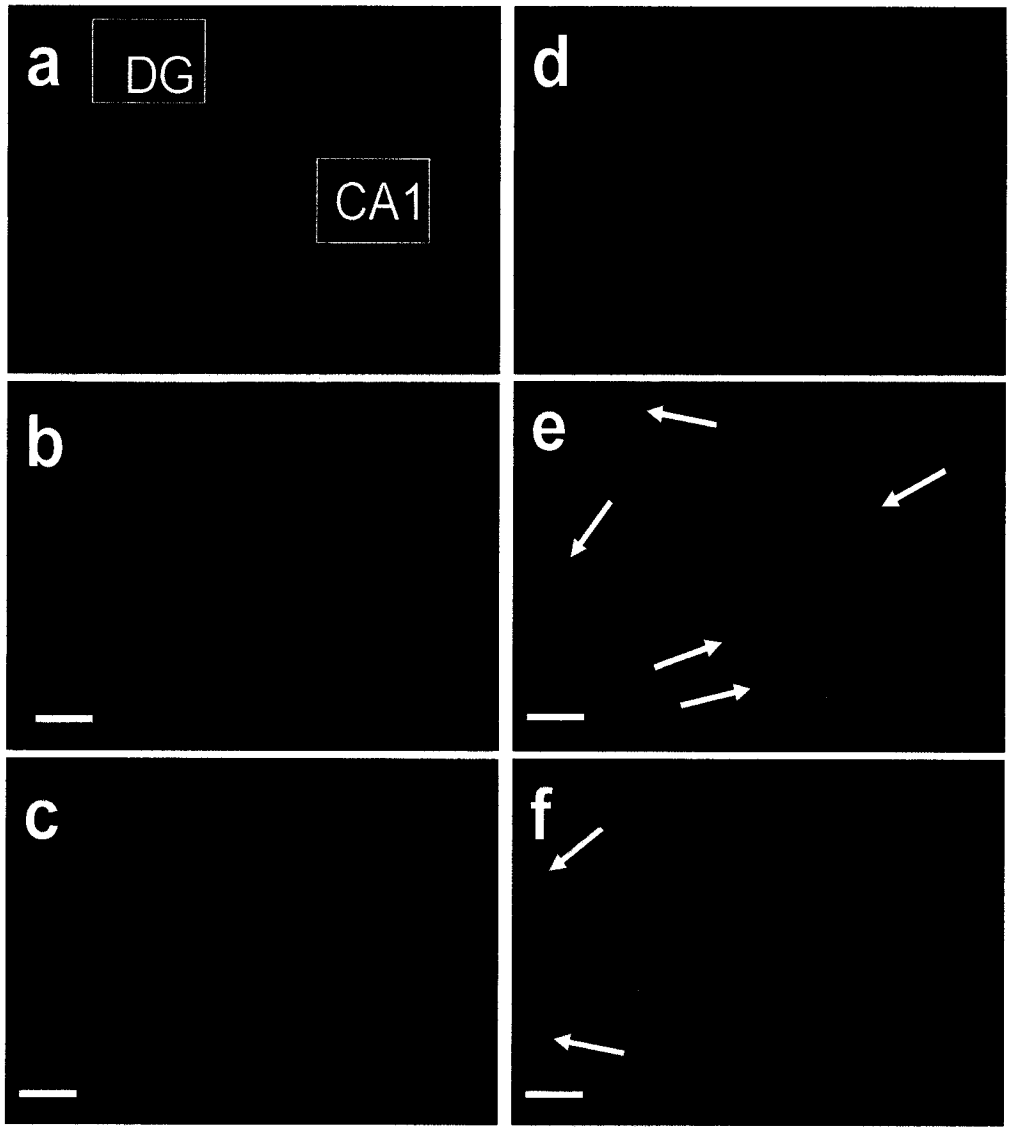

Figure 3.4: Aβ-oligomers induce rod formation in neurons of 10 day organotypic slices from rat hippocampus. Immunostaining for Aβ is in green (a, b, c) and immunostaining for cofilin is in red (d, e, f). Low magnification (4x) image (a) shows boxed area of dentate gyrus (DG) and CA1 which are magnified in (e) and (f) respectively. Many rods in linear arrays are found within the DG suggesting they form within neurites and in a regional subpopulation of neurons in slice culture treated with soluble Aβ. Rods are present, but significantly lower in CA1. Scale bars = 10 μm.

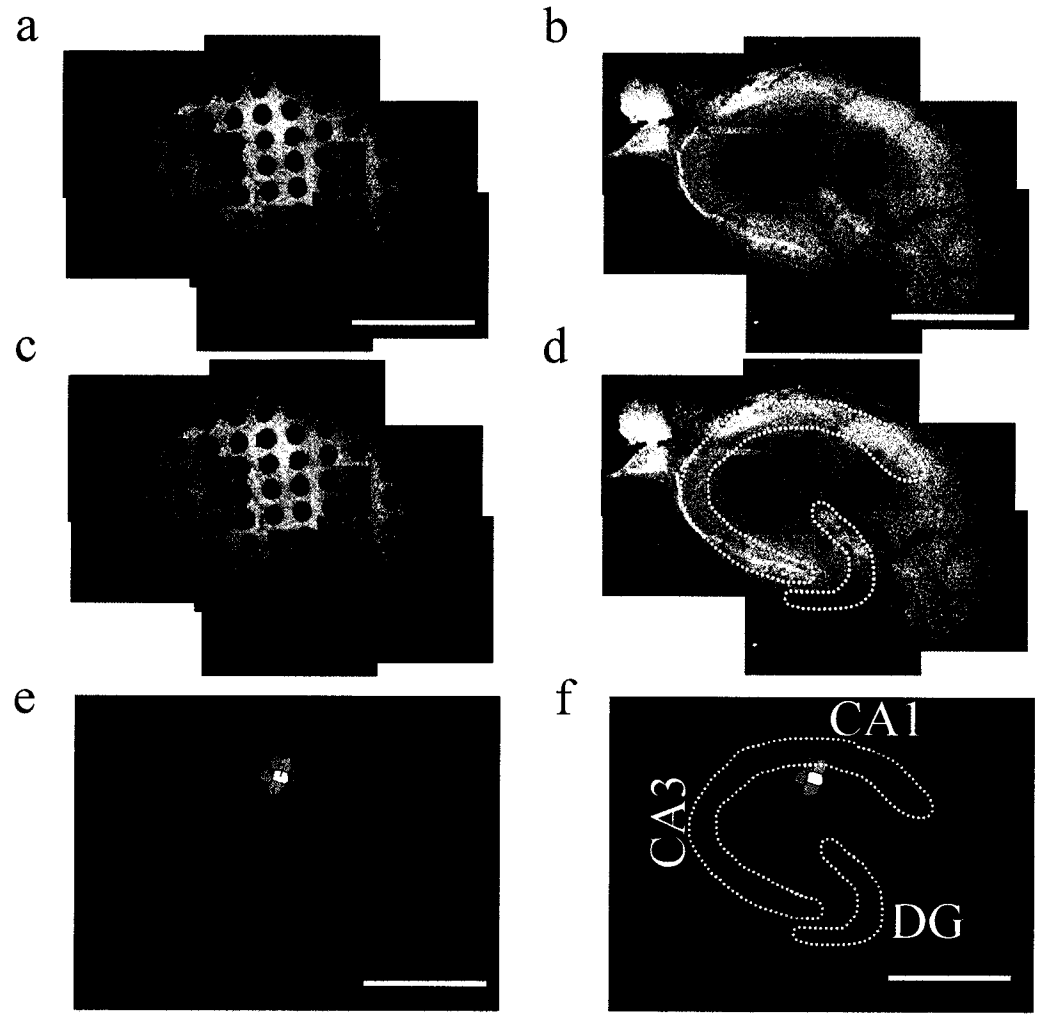

Figure 3.5: Topographical map of rods. Low power (4x) images were taken of each slice in the Texas Red channel (a) and DAPI channel (b) folowing systematic rod count at 60x. Bleached circles on the Texas Red image indicate the regions observed at 60x and the number of rods is indicated for each spot (c). The dentate gyrus (DG) and pyramidal cell layers of the CA1 and CA3 are outlined and overlayed onto the DAPI image (d). A topographical map of rod abundance was created by assigning a color gradient to each numerical value where 0 rods = black, 1 - 5 rods = blue, 6 - 10 rods = green, 11 - 15 rods = yellow, 15 - 20 rods = red and > 20 rods = white (e). Colors were intergrated using Adobe Photoshop as described in material and methods. The outline of cell layers from the DAPI image is overlayed on the countour map to locate the regions of highest rod formation (f). Scale bars = 50 μm. Images of the entire hippocampus were stitched together from overlapping images collected at 4x. This slice was treated with 1 μM Aβ for 48 h. All topographical maps were created using this method.

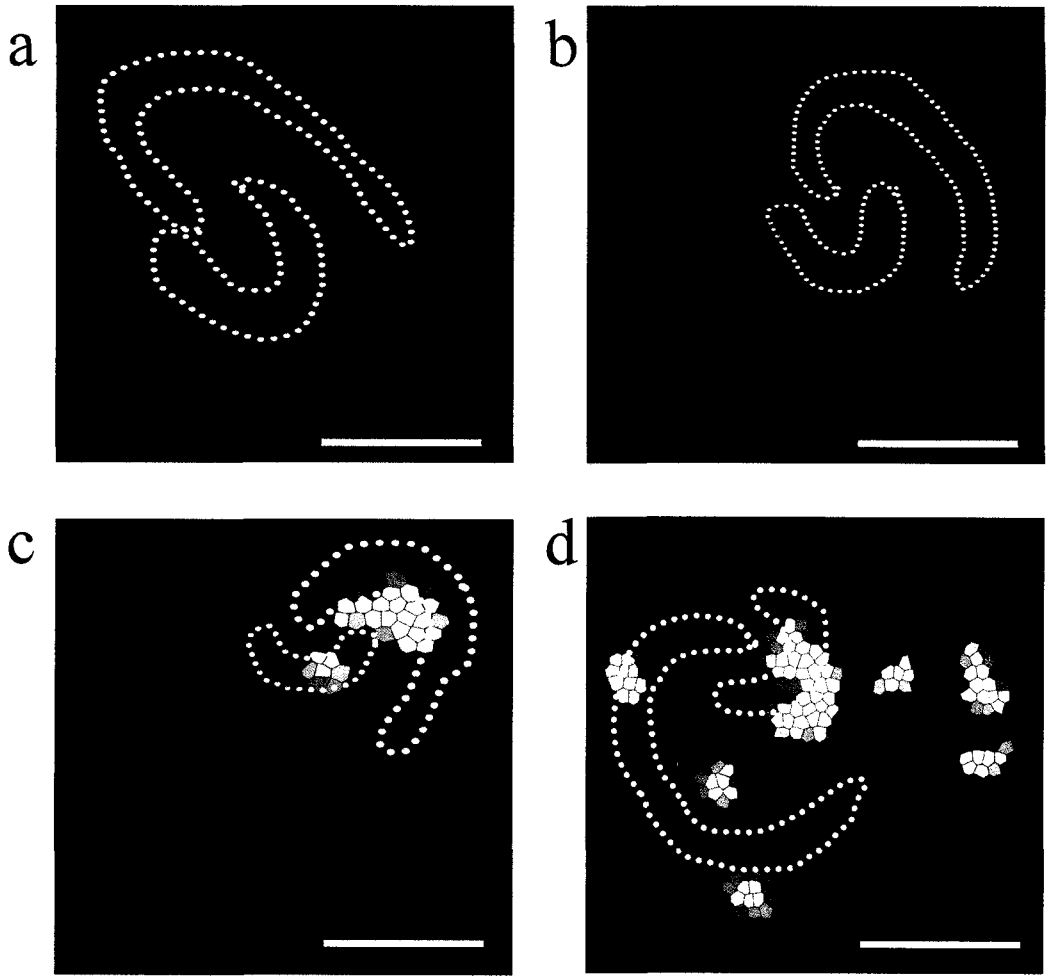

Figure 3.6: Topographical maps of rod formation in organytypic slice cultures. Rods are observed infrequently and with no regional distribution in slices treated with ATP depletion for 1 h on day 8 and allowed 48 h recovery (a, b). Rod formation is elevated in slices treated with 1 μM Aβ and the majority of rods are found in a region adjacent to the dentate gyrus (c, d). Variation in the size of slices is due to the region of the hippocampus from which they were cut on the McIlwain tissue chopper. Slices taken from the middle of the hippocampus proper are larger than slices cut from either end. Scale bars = 50 μm.

Cell derived Aβ induces rods

The study of Aβ peptide effects on neurons using commercially available synthetic peptides is limited by difficulties in controlling the size and aggregation state under *in-vitro* incubation conditions (Cleary *et al.,* 2005). To address this concern we employed the use of human amyloid-β peptides produced by Chinese hamster ovary (CHO) cells stably expressing a mutated form of APP known to be involved in human AD (Podlisny *et al.,* 1995). 7PA2 (CHO cells expressing human APP mutant V717F) cells secrete sub-nM to nM concentrations of low-*n* oligomeric Aβ into the culture medium (Podlisny et al, 1998; Walsh *et al.,* 2005). 7PA2 conditioned medium contains monomeric and oligomeric Aβ peptides in the absence of large insoluble species (Walsh *et al.,* 2002a). These cell derived Aβ peptides have been demonstrated to disrupt cognitive function when injected intracerebroventricularly (i.c.v.) into Sprague Dawley rats (Cleary *et al.,* 2005). Cell derived Aβ was used to test the hypothesis that soluble, low-*n* oligomers of Aβ, in the absence of larger aggregates or insoluble species and fibrils, are responsible for the rod inducing effects observed in synthetic Aβ treated cultured neurons.

Slice cultures were chronically treated with 7PA2-conditioned medium or medium from untransfected control cells (CHO). The CHO and 7PA2 conditioned media are collected at 1X concentration and subsequently concentrated by freeze drying to a 10-12X stock concentration. The concentrated stock was diluted into neuronal cell culture medium and used at a final concentration of 2X. Cell derived Aβ-conditioned medium was added to slices on days 2, 5 and 8 in culture and all slices were fixed on day 10. Untreated slices provided a negative control for rod formation and a positive control were

slices that had undergone ATP-depletion. Post-fixation slices were immunostained with an ADF/cofilin antibody to identify rods. Rod formation was observed in all slices treated with 7PA2-conditioned medium prompting a more detailed examination into the species of Aβ that may be responsible for rod formation.

Size exclusion chromatography was used to fractionate 7PA2-conditioned medium into monomeric Aβ (AβM) and dimer-trimer Aβ (AβDT). Slice cultures were treated with AβM, AβDT, control monomer (ncM) or control dimer-trimer (ncDT) derived fractions at a final concentration of 0.5X. Aβ and control fractions were added to slices on days 2, 5 and 8 in culture and all slices were fixed on day 10. An examination of slices treated chronically from day 2 to day 10 with 0.5X AβM or AβDT revealed low levels of rod formation, but with a small increase of rods in a regional distribution adjacent to the dentate gyrus in AβDT-treated cells. Significantly, the monomeric fraction was inactive. Low levels of rod formation were also recorded in slices treated chronically from day 8 to day 10 with 0.5X AβM. Slices treated chronically with AβDT from day 8 to day 10 displayed elevated numbers of rods per field with a hot spot of rod formation in the same region as observed with other treatments. Therefore, naturally produced oligomers of Aβ target the same cell population as the synthetic Aβ.

Discussion

Organotypic hippocampal slice cultures have already proven invaluable in the continuing study of Aβ induced rods. We have demonstrated that rods form in organotypic hippocampal slice cultures under identical conditions previously demonstrated to produce rods in dissociated neurons (Maloney *et al.*, 2005; Minamide *et*

al., 2000). The rods formed in slice cultures are refractory to phalloidin staining and readily label with antibodies to ADF and cofilin.

Of interest is the rapidity with which rod form in slices in response to anoxia, ATP depletion and the observation that rods form as a result of transient treatment with OGD and high levels of glutamate. These four neurodegenerative stimuli can be used to model ischemia or stroke in organotypic slice culture. In the case of OGD, neuronal cell loss in the CA1 region has been attributed to excitotoxic levels of glutamate (Hewitt & Corbett, 1992). The presence of rods in dissociated neurons has been demonstrated to disrupt transport in neurites and lead to the accumulation of vesicles containing the amyloid precursor protein (APP), β-amyloid cleavage enzyme, presenilin 1 (a component of the γ-secretase complex) and β-cleaved APP (the immediate precursor to Aβ) (Maloney *et al.*, 2005). APP, BACE and PS1 all accumulate in axonal swellings, associated with increased levels of Aβ that form during normal brain aging or after head trauma (Kawarabayashi *et al.*, 1993; Roberts *et al.*, 1994; Smith *et al.*, 2003; Chen *et al.*, 2004; Maloney *et al.*, 2005, Stokin & Goldstein, 2006). Swellings have also been reported to form within cholinergic axons of the nucleus basalis magnocellularis in early stage human AD brain (Stokin *et al.*, 2005). The cause of early onset familial Alzheimer's disease has been linked to a handful of mutations found in the genes encoding APP and PS1/2 that lead to increased production of the 42 amino acid species of Aβ ($A\beta_{1-42}$). These mutations account for fewer than 5% of all diagnosed cases of AD. The majority of AD is sporadic and occurs in individuals with little or no genetic commonalities. The incidence of mini-vascular events (mini-strokes) is a leading cause of multi-infarct dementia (MID). The formation of rods as a result of such events could

establish a degenerative cycle of transport defects and locally elevated Aβ production and eventually deposition into senile plaques and help to explain at least some of the incidence and pathology of sporadic AD.

Sub-regions of the hippocampus display heightened sensitivity to soluble and fibrillar forms of Aβ (Bahr *et al.,* 1998; Lambert *et al.,* 1998; Kim *et al.,* 2003). Regional differences in rod formation induced by soluble Aβ may also help to explain cognitive decline without overt neuronal loss observed in early stages of AD, a symptom that has yet to be defined on a cellular or biochemical level. A regional hot spot of rod formation was observed in slice cultures treated with 1-2 μM Aβ, and with 0.5X AβDT. This hot spot localizes to a region just adjacent to the blade of the dentate gyrus and appears to be centered in the molecular layer. This result is intriguing in that the molecular layer of the hippocampus is the site of acetylcholinesterase (AchE)-positive axon innervation from cholinergic cell bodies in the septum (Amaral & Kurz, 1985; Guthrie *et al.,* 2005). Rod formation disrupts vesicle transport (Maloney *et al.,* 2005) and synaptic functioning (Jang *et al.,* 2006). The presence of rods in Aβ-sensitive cells in the molecular layer of the hippocampus may help explain the loss of basal forebrain cholinergic neurons due to deficits in retrograde NGF transport from the hippocampus, as is observed in AD and DS (Cooper *et al.,* 2001).

In addition to the regional sensitivity for rod formation, our preliminary findings that rods form in response to treatment with AβDT but not AβM provides clues as to which fraction of soluble Aβ (monomers vs. dimer-trimers) possesses the greatest biological activity linked to rod formation. Soluble species of Aβ called ADDLs (Aβ derived diffusible ligands) bind specifically to synaptic sites on cultured hippocampal

neurons (Lacor *et al.*, 2004). In addition ADDLs are toxic to cultured neurons at nanomolar concentrations (Lambert *et al.*, 1998) and at 500 nM they prevent high frequency stimulation-induced long term potentiation (LTP) measured from the dentate gyrus in acute hippocampal slices (Wang *et al.*, 2002). I.C.V. injection of 1.5 μL of 7PA2 conditioned medium into rats disrupted LTP (Walsh *et al.*, 2002a). I.C.V. injection of 7PA2-conditioned medium also blocked recall of complex learned behavior in rats (Cleary *et al.*, 2005). The Aβ-induced block of LTP can be reversed by injection of monoclonal antibodies to Aβ (Klyubin *et al.*, 2005). Fractionation by size exclusion chromatography determined that the LTP disruption and memory impairments are caused by low-*n* oligomers of Aβ and not to monomers (Walsh et al, 2005; Cleary *et al.*, 2005). The inactivity of the Aβ monomers and the rod generation by dimer-trimer fractions suggests that rod formation may mediate some of the neurodegeneration and LTP impairment seen in the whole animals.

Slice cultures provide a unique perspective from which to explore the relationships between rod formation and ischemic injury whether modeled with anoxia, ATP depletion or oxygen-glucose deprivation. Additionally slice cultures provide a platform from which to study the effects of soluble and fibrillar forms of Aβ with regard to rod formation and AD and to be able to localize the sensitive population of responding neurons. The utility of a slice culture system for addressing the connection between rods and neurodegeneration is immense.

Chapter Four

Cofilin-mediated neurodegeneration in Alzheimer's disease, and other amyloidopathies

Preface and Acknowledgement

The work presented in this chapter will be submitted to Molecular Neurobiology. The order and list of the authors will be Michael T. Maloney and James R. Bamburg. The article was written in response to an invitation following the publication of (Maloney *et al.*, 2005) and summarizes the current literature regarding cofilin pathology (rods) and Alzheimer's disease.

Abstract

Transport defects may arise in a variety of neurodegenerative diseases from failures in molecular motors, microtubule abnormalities, and the chaperone/proteasomal degradation pathway leading to aggresomal-lysosomal accumulations. These defects clearly represent an important step in the neurodegenerative cascade, although in many cases a clear consensus has yet to be reached as to their causal relationship to the disease. A growing body of evidence supports a relationship between neurite transport defects in the very early stages of many neurodegenerative diseases and alterations in structural organization of the actin cytoskeleton initiated by the misregulation of cofilin. Here we focus on involvement of the actin depolymerizing factor ADF/cofilin family of proteins in initiating the formation of rod-shaped actin bundles (rods) that inhibit transport and contribute to the pathology of Alzheimer's disease. Because these rods form rapidly in

response to anoxia, they could also contribute to synaptic deficits associated with ischemic brain injury (e.g. stroke). Understanding initiators of rod formation, rod structure, composition, stability and persistence, and rod effects on synaptic function and survival of the neurons in which they form are essential for determining how rods contribute to disease pathology.

Introduction

The cytoskeleton is a dynamic array of proteins creating a critical framework upon which many cellular functions rely. Misregulation of the neuronal cytoskeleton can lead to improper growth cone path-finding, dendritic spine abnormalities, transport defects, protein aggregation and cell death. The three major classes of cytoskeletal elements are actin filaments, intermediate filaments and microtubules. A few of the more common pathological hallmarks of neurodegeneration include the extracellular senile plaque, composed primarily of insoluble aggregates of amyloid peptides, and neurofibrillary tangles, composed of the microtubule binding protein tau. More recently actin aggregates in the form of cofilin-actin rods have been identified in postmortem brains of Alzheimer's disease (AD) patients (Minamide *et al.*, 2000) (Fig 4.1). Significantly, these aggregates are also present in perfusion fixed transgenic mice (Tg2576) expressing a mutant human amyloid precursor protein (APP) (Maloney *et al.*, 2005). The misregulation of actin and cofilin proteins can be linked to a wide range of human neurodegenerative disorders including corticobasal degeneration, William's syndrome, fragile X syndrome, AD, dystonia with dementia and spinal muscular atrophy. Though these diseases ultimately result from a range of defects including dendritic spine

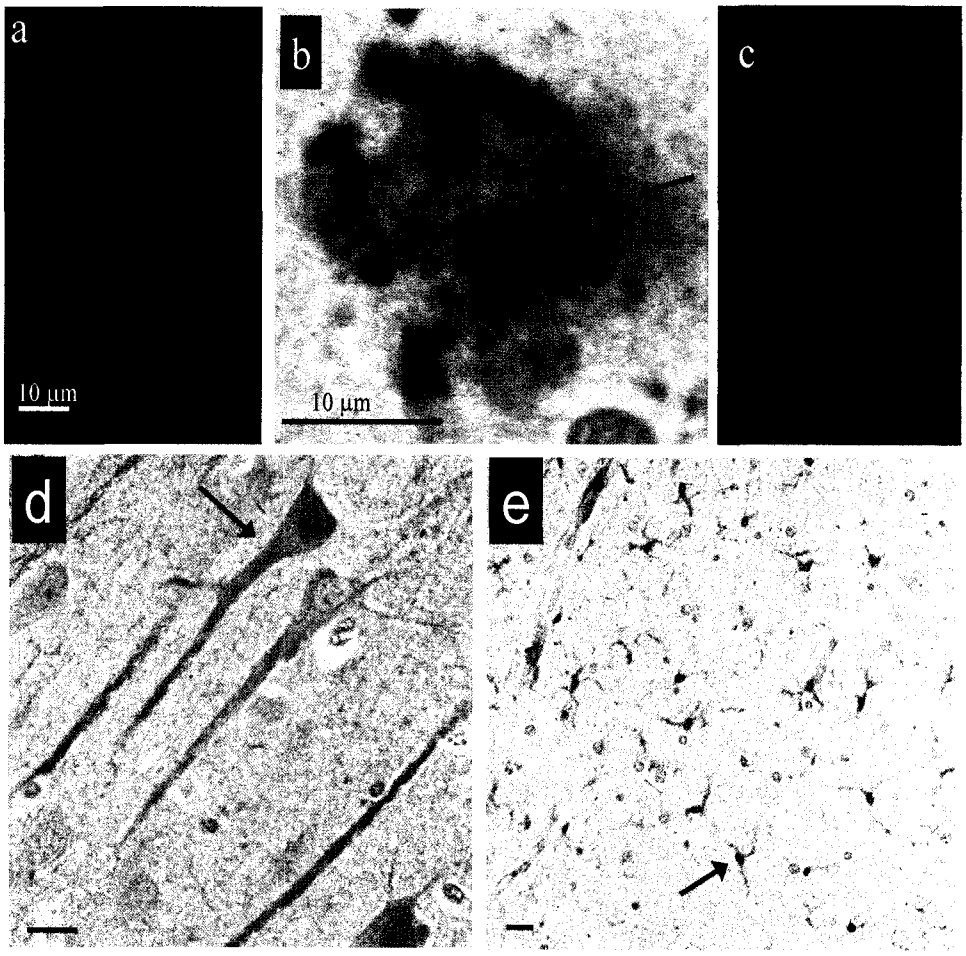

Figure 4.1: Cofilin staining in normal human brain (d, e) shows apical dendrites of pyramidal neurons and microglia contain the most cofilin, IC (b) and IF (c) cofilin staining in AD brain shows linear array of rod-like structures similar in length to rods observed in neurites of cultured cells (a) (From Minamide *et al.*, 2000).

abnormalities, loss of long term potentiation and long term depression (LTP/LTD), alterations in specific mRNA transport and translation, they are all related to processes involving the actin cytoskeleton (Maloney *et al.*, 2006).

Ischemia, oxidative stress and excitotoxic insults, key factors driving neurodegeneration, result from stroke, trauma, mitochondrial dysfunction, or genetic risk factors (Bazan *et al.*, 2002). With upstream initiating factors and final stage pathology well defined, the focus of current research lies in deciphering which biochemical pathways are involved in the disease process and to what extent. These investigations are defined in part by the necessity and, in many cases, the inability to connect cellular and biochemical aspects of neurodegeneration with the behavioral consequences and cognitive decline observed in the associated human diseases. One example of this disparity is a failure to define the biochemical and cellular basis for cognitive decline associated with early stages of AD. During the period of mild to moderate memory impairment, neuronal loss is minimal, however the number and strength of synaptic connections begins to decline. Transport defects arising from misregulation of the neuronal cytoskeleton present a promising model not only for explaining early cognitive decline, but also for bringing together key features driving progressive neurodegeneration.

Down syndrome and Alzheimer's disease

Down syndrome (DS), a.k.a. trisomy 21, is a genetic disorder arising from the triplication of chromosome 21. Among the genes on chromosome 21 are those encoding APP and the β-amyloid cleavage enzyme (BACE). Children affected with DS suffer

from impaired learning and cognitive development (i.e. mental retardation) and are recognizable by stereotypic cranio-facial deformities. Life expectancy averages around 40 years due to a multiplicity of complications arising from the presence of additional genomic DNA. One common feature associated with DS is the development of all of the pathological hallmarks of AD in 100% of the DS patients living to age 40 or beyond (Glenner & Wong, 1984a).

AD is a neurodegenerative disorder currently diagnosed post mortem by the presence of senile plaques and neurofibrillary tangles in the brain. AD presents clinically as a steady decline in cognitive ability beginning with the loss of short-term memory and progressing through stages of increasing dementia. Cognitive decline continues as a precipitous loss of the ability to recall common names, dates, and places, and inability to perform increasingly simple tasks requiring planning. Late stages of AD are characterized by hallucinations, paranoia, loss of verbal communication, loss of fine and later gross motor control often resembling Parkinson's disease, incontinence, and finally the patient falls into a vegetative state where they remain until death. Progression through these stages may take anywhere from months to years and symptoms can vary greatly from case to case, however the pathology found in post mortem brains is largely stereotypical. Nearly 95% of AD occurs in the elderly, whereas early onset familial cases of AD (FAD) account for the remaining 5% of cases. FAD mutations have been identified in genes encoding APP, and in presenilins 1 and 2 (enzymatic component of the γ-secretase complex). Additionally a common polymorphism (ε4) found in the apolipoprotein-E (ApoE) is highly associated with increased risk for a later onset AD. These mutations all lead to increased cerebral amyloid beta levels ($A\beta_{1-42}$) either via

increased production and aggregation or via decreased clearance or degradation of this internal peptide derived from sequential β- and γ-secretase cleavage of APP.

Actin and cofilin in neurodegenerative disease

Actin is a 42 kDa cytoskeletal protein expressed ubiquitously in eukaryotes. Monomeric, globular (G-actin) actin readily polymerizes into filaments (F-actin). Actin filaments are dynamic biopolymers that continually undergo cycles of assembly and disassembly. Monomers of actin can be added to or removed from a filament at both ends, however a polarity exits which influences the on/off rate of G-actin. This polarity is caused by the ability of an actin monomer to bind to adenine nucleotides, ATP and ADP. ATP-actin has a higher affinity for filament assembly than ADP-actin. Following the addition of an ATP-actin monomer to the plus end of a growing filament the γ-phosphate is rapidly hydrolyzed allowing for the release of inorganic phosphate (P*i*). Loss of P*i* induces a conformational change in the ADP-actin subunit within the filament. ATP hydrolysis associated with actin dynamics can consume up to 50% of the total ATP used by growing neurons (Bernstein & Bamburg, 2003).

Under steady state conditions actin filaments are non-equilibrium polymers and undergo treadmilling during which ATP-actin monomers polymerize on to the filament plus end and ADP-actin depolymerizes from the minus end.

Actin depolymerizing factor (ADF) and cofilin are members of a 13-19 kDa family of actin binding proteins. The ADF/cofilin family proteins share high sequence homology and are regulated, in large part, by phosphorylation of a conserved Ser3 residue. Because in human brain the cofilin:ADF expression ratio is >10:1 (Minamide *et*

al., 2000), we will just refer to cofilin hereafter. Phosphorylation, by LIM or TES kinases, inactivates cofilin and dephosphorylation, by slingshot (Niwa *et al.*, 2002) and chronophin (Ghola *et al.*, 2005; Huang *et al.*, 2006) phosphatase, increases cofilin's actin dynamizing activity. Dephosphorylated cofilin binds cooperatively (Hawkins *et al.*, 1993; Hayden *et al.*, 1993) along regions of ADP-actin (Carlier *et al.*, 1997) resulting in enhanced filament severing (Bobkov *et al.*, 2006) and minus end depolymerization. Cofilin aggregates and actin bundles have been observed in AD brain, providing a link between oxidative stress and cofilin pathology, both of which are prominent characteristics in AD (Minamide *et al.*, 2000).

Transient cellular stress can cause a sharp decline in the local ATP concentrations, especially within domains of neurites where mitochondria are not uniformly distributed. Loss of ATP produces a rapid rise in the concentrations of both ADP-actin and activated (dephosphorylated) cofilin. Under these conditions cofilin and actin readily associate to form cylindrical aggregates with tapered ends (rods). Rods form in variety of cell lines in response to ischemia, oxidative stress, excitotoxicity, 10% DMSO (Mann, 1894; Iida *et al*, 1986; Nishida *et al.*, 1987; Ohta *et al.*, 1989; Iida *et al.*, 1992; Ono *et al.*, 1993; Moriyama *et al.*, 1996; Aizawa *et al.*, 1997; Sameshima *et al.*, 2000; Minamide *et al.*, 2000), and form in neurons treated with soluble and fibrillar forms of the amyloid beta peptide ($A\beta_{1\text{-}42}$) (Maloney *et al.*, 2005). In addition rod-like cofilin immunostaining is found in both human AD brain (Minamide *et al.*, 2000), and in brain of transgenic AD mice (Maloney *et al.*, 2005; Zhao *et al.*, 2006; Gonzalez-Bilault, unpublished observations) in close proximity to amyloid plaques. Thus, rods are a

stereotypic cellular response to a wide range of stress factors modeling common mediators of neurodegeneration.

Rods can be uniquely characterized by their immunoreactivity to antibodies against both actin and cofilin and inability to label with phalloidin, a mushroom toxin with F-actin binding properties (Minamide *et al.* 2000). The absence of phalloidin binding suggests that the actin in rods is saturated with cofilin; subunits in cofilin-saturated actin filaments are slightly rotated with respect to normal F-actin, eliminating the phalloidin binding site (McGough *et al.*, 1997). In cultured neurons rods typically appear either as single structures or in linear arrays within neurites and can enlarge to completely occlude the neurite, sometimes observed by phase microscopy as a swelling of the neurite caliber. Although the entire neurite remains intact when rods are present, microtubules are often disrupted in neurites distal to rods, especially if rods are occluding the neurite (Minamide *et al.*, 2000). The persistence of rods has been observed for as long as 72 hours without loss of the neuron, although neurites distal to the rod undergo withering. Thus, formation of rods represent a promising model to explain the loss of synaptic connections and cognitive decline without associated loss of neurons as is often reported in early stages of neurodegenerative diseases, and can explain disruption of microtubule based transport.

The presence of "cofilin pathology" is a prominent feature found in AD brains. In Alzheimer's brains >97% of dense core amyloid plaques are associated with cofilin aggregates and rods (cofilin pathology), while ~45% of cofilin aggregates are found isolated from amyloid plaques (Minamide *et al.*, 2000). Rod-like cofilin staining associated with diffuse cofilin pathology often is remarkably similar in size, spacing and

appearance to rods observed in cultured neurons. The high spatial correlation between amyloid plaques and cofilin pathology has sparked investigations into the relationship between Aβ and cofilin regulation.

Amyloid precursor protein processing

APP can be divided into three domains: a large extra-cellular N-terminal domain, a single transmembrane domain, and a short cytoplasmic C-terminal tail. Multiple isoforms of APP are expressed ranging in size from 695 to 770 amino acids with APP695 being the most abundant in brain. In humans the APP gene is found on chromosome 21 and in mice on chromosome 16. Proteolytic processing of full length APP occurs via one of two pathways. The non-amyloidogenic pathway, which dominates APP processing in most cell types, begins with cleavage by α-secretase (Vetrivel & Thinakaran, 2006). α-Secretase is a protein resembling the TNF-α cleavage enzyme (TACE) and belonging to the ADAM (a disintegrin and metalloproteinase domain) family. This cleavage releases the soluble APP N-terminus (sAPPα) extracellularly and leaves the membrane bound 83 amino acid C-terminus (C83). C83 undergoes subsequent cleavage by γ-secretase to release the transcriptionally active APP intracellular domain (AICD) and the soluble P3 fragment. γ-Secretase is multi-subunit complex composed of nicastrin, Pen2, Aph-1, and presenilin. Presenilin, an aspartyl protease, is the enzymatically active component of the γ-secretase complex. In Chinese hamster ovarian cells stably expressing γ-secretase only ~6% of total γ-secretase resides at plasma membrane where it also maintains full functional activity (Chyung *et al.*, 2005).

APP can alternatively undergo amyloidogenic processing initialized by β-amyloid cleavage enzyme (BACE), a metalloprotease commonly referred to as β-secretase. Much like the α-cleavage of APP, β-cleavage releases a soluble extracellular N-terminal fragment (sAPPβ) and leaves behind a membrane bound 99 amino acid C-terminal peptide (C99). BACE is enriched within membrane lipid raft domains, and thus the β-cleavage event occurs primarily during endocytosis or within early endosomal compartments. C99 subsequently undergoes sequential cleavage by the γ-secretase to produce the 40-43 amino acid amyloid beta peptide (Aβ). The endosomal Aβ will either become liberated into the extracellular space upon endosomal fusion with the plasma membrane or may be trafficked back to the soma where lysosomal fusion can help degrade the peptide produced. Aβ is a 4 kDa peptide dominated by β-sheet secondary structures predisposing it to polymerize into soluble small oligomers and eventually into long fibrils and insoluble aggregates. Fibrils of the extracellularly released Aβ peptide eventually precipitate to form deposits known as senile plaques, a hallmark of AD, the presence of which is a characteristic for the diagnosis of AD.

The Amyloid Hypothesis

Amyloidopathies are a class of degenerative diseases arising from the accumulation of amyloid-like protein aggregates. Some common neuronal amyloidosis includes spongiform encephalopathies (a.k.a. prion diseases), AD, Parkinson's disease, DS, and Huntington's disease. The common features of neuropathology, senile plaques and cerebral atrophy, shared by late onset AD, early onset FAD, and DS has shed light on the mechanism at work in these amyloidopathies. The "amyloid hypothesis" states that

increasing cerebral accumulation of Aβ over years to decades is responsible for cognitive decline, neurodegeneration, and senile plaque deposition associated with AD. This hypothesis found its roots in the characterization of the Aβ peptide as the major component of senile plaques (Glenner & Wong, 1984b), and has since been strengthened by genetic and biochemical data. The identification of inherited genetic mutations with high penetrance in early onset familial AD has led to the development of transgenic mouse models that display neurodegeneration with similarities to human AD. *In vitro* studies of the Aβ peptide have demonstrated acute toxicity against cultured neurons as well as depressive effects on long-term potentiation (LTP), transient cognitive impairment, loss of cellular homeostasis and impaired transport.

APP trafficking

Following its translation APP is trafficked from the endoplasmic reticulum (ER) though the constitutive secretory pathway, becoming modified by N- and O-glycosylation, phosphorylation, and tyrosine sulfation along its transit to the plasma membrane (Vetrivel & Thinakaran, 2006). APP remains at the plasma membrane briefly before being internalized into endosomes (Vetrivel & Thinakaran, 2006). Early endosomes are protease rich membrane compartments in which the processing and function of many key players of AD pathogenesis occurs, including APP, Aβ peptide, ApoE, Low-density lipoprotein (LDL) and the LDL-receptor, BACE and γ-secretases (Cataldo *et al*, 2004). Following endocytosis APP is delivered to late endosomes then and on to the late Golgi/trans Golgi network (TGN) (Koo & Squazzo, 1994). The γ-secretase complex is found localized within several compartments including late

endosomes, Golgi, and TGN (Vetrivel *et al.*, 2004). Intracellular Aβ localized to Rab5 positive early endosomes and is prominent in enlarged endosomes from AD brain. These findings suggest that Aβ overproduction and accumulation in AD and DS may signify earlier disease related disturbances of endosomal signaling or transport (Cataldo *et al.*, 2004).

In neurons vesicles containing APP, PS1 and BACE all undergo kinesin I mediated fast anterograde axonal transport (Kamal *et al.*, 2000; Kamal *et al.*, 2001; Papp *et al.*, 2002; Sheng *et al.*, 2003). Evidence has been presented for both direct interactions between APP and kinesin (Kamal *et al.*, 2000; Inomata *et al.*, 2003) and indirect coupling via c-Jun NH2-terminal kinase-interacting protein (JIP1) (Matsuda *et al.*, 2003). APP, BACE and PSI all accumulate in axonal swellings, associated with increased levels of Aβ, that form during normal brain aging or after head trauma (Kawarabayashi *et al.*, 1993; Roberts *et al.*, 1994; Smith *et al.*, 2003; Chen *et al.*, 2004; Maloney *et al.*, 2005, Stokin & Goldstein, 2006). $A\beta_{1-42}$ accumulates within endosomal vesicles where it also aggregates into oligomers in the brains of Tg2576 mice, in primary neuronal cultures from these mice and in human AD brain (Takahashi *et al.*, 2004; Gouras *et al.*, 2005). Accumulations are associated with pathological alteration within the process and synaptic compartment of mouse and human AD brains (Takahashi *et al.*, 2004; Gouras *et al.*, 2005). Vesicles containing APP, BACE, PSI and β-cleaved APP all accumulate at rods in cultured neurons (Maloney *et al.*, 2005). It has been proposed that transport defects may stimulate proteolytic processing of APP or allow it to assemble into more toxic oligomers, thereby exacerbating the formation of senile plaques in AD (Borchelt *et al.*, 1997; Stokin *et al.*, 2005, Maloney *et al.*, 2005).

Aβ induces formation of cofilin-actin rods

Treatment of cultured rat hippocampal neurons with $A\beta_{1-42}$ induces rod formation in ~18% of the total population (Maloney *et al.*, 2005). Rods form rapidly, reaching 50% of the maximum response within 6 hours, in neurons treated with 1 μM soluble $A\beta_{1-42}$ oligomers (Maloney *et al.*, 2005), and with concentrations as low as 10 nM (Maloney *et al.*, 2005). $A\beta_{1-42}$ treatment causes the dephosphorylation (activation) of AC only within soma and neurites of those neurons that form rods (Maloney *et al.*, 2005) suggesting that a subpopulation of neurons is sensitive to $A\beta_{1-42}$. Labeling of a subpopulation (30 to 50%) of the total neurons with $A\beta_{1-42}$ oligomers extracted from AD brain or prepared from synthetic peptides has also been reported (Lacor *et al.*, 2004). Together these studies suggest that that soluble $A\beta_{1-42}$ can induce rod formation by activating cofilin in a neuronal subpopulation with high specificity for Aβ-binding.

p21-Activated kinase (PAK) is an important modulator of AC activity. PAK phosphorylates and activates LIM kinase (LIMK), which then phosphorylates and inactivates cofilin (p-cofilin). The PAK-cofilin signaling axis is important for dendritic spine morphogenesis, and consequently PAK mutations have been linked to several human developmental mental retardation syndromes characterized by dendritic spine abnormalities (Meng *et al.*, 2002; Bamburg & Wiggan, 2002; Bellugi *et al.*, 1999). Cofilin pathology in both AD and DS is spatially and temporally associated with marked reduction of PAK protein levels and activity (Zhao *et al.*, 2006). In postmortem human and Tg2576 mice brains, activated phospho-PAK (pPAK) immunostaining was reported to resemble staining of intraneuronal $A\beta_{1-42}$ that accumulates along with APP-carboxy-

terminal fragments (APP-CTF) within enlarged endosomal and lysosomal structures (Yang *et al.*, 1995). Similar observations were found in brains from Tg2576 mice (Zhao *et al.*, 2006). Antibody depletion of $A\beta_{1-42}$ in Tg2576 mice led to a recovery (increase) in pPAK levels (Zhao *et al.*, 2006). Persistent reduction in pPAK was observed as early as two hours following treatment of dissociated rat hippocampal neurons with soluble $A\beta_{1-42}$ oligomers and occurred with oligomer concentrations as low as 10 nM (Zhao *et al.*, 2006). Application of a PAK specific inhibitory peptide to cultured neurons induced the formation of cofilin rods and infusion of this peptide into wild type mouse brains induced CA1 hippocampal cofilin pathology and adult-onset memory deficits (Zhao *et al.*, 2006). Taken together these findings have prompted the hypothesis that a loss of pPAK may lead to local pathology related to the formation of cofilin aggregates similar to those observed in human AD and Tg2576 mouse brain, and may contribute to impaired cognitive functioning (Zhao *et al.*, 2006).

Aβ, cofilin, and cognitive decline

Synaptic dysfunction is the most established correlate of cognitive decline in AD (Masliah, 2000; Mucke *et al.*, 2000). In cultured rat hippocampal neurons, rods disrupt neurite function (Minamide *et al.*, 2000) as observed by diminished microtubule immunostaining distal to rods. Recent studies using *Aplysia kurodai* neurons found that cofilin over expression led to rod formation, synapse loss and, distal to the rod, impairment of synaptic plasticity measured by electrophysiological methods (Jang *et al.*, 2005). While cofilin expression did not affect the gross morphology of the neuron, a decrease in the number of pre-synaptic varicosities was observed (Jang *et al.*, 2005). In

addition, cofilin over-expression impaired both basal synaptic transmission and LTP. Neither cell death nor induction of an apoptotic cascade was found to be responsible for these effects (Jang *et al.*, 2005).

Synapse failure has been attributed to soluble Aβ oligomers (Hartmann *et al.*, 2004) in part due to their ability to disrupt LTP (Lambert *et al.*, 1998; Walsh *et al.*, 2002; Wang *et al.*, 2002). Following treatment of cultured hippocampal neurons with soluble oligomers, greater than 90% of the punctate oligomer binding sites co-localized with the synaptic marker PSD95 (Hartmann *et al.*, 2004). Natural human Aβ is secreted from CHO cells stably expressing a mutant form of human APP found in AD (Walsh *et al.*, 2005). When injected intracerebroventricullarly (i.c.v.) into rats these cell derived soluble Aβ oligomers consistently produced significant but transient disruption of a complex learned behavior (Cleary *et al.*, 2005). Taken together with the ability of Aβ to induce rods, these findings support a molecular mechanism where rods play a pivotal role in producing the underlying memory and cognitive dysfunction of neurodegenerative disease.

Cytoskeleton, transport defects, and AD

Axonopathy and transport defects have been reported in Tg-swAPP^{prp} mouse brains (Stokin *et al.*, 2005). The formation of blockages, resembling axonal swellings and dystrophic neurites, is one of the earliest reported degenerative phenotypes, occurring as early as one year prior to the formation of senile plaques in the mouse model of AD (Stokin *et al.*, 2005). These swellings are often found in areas lacking amyloid deposition in early stage human AD suggesting that they precede, and may play a role in,

amyloid deposition (Stokin *et al.*, 2005). Swellings in the neurites of hippocampal cultures harvested from mice contain aberrant accumulation of oligomeric Aβ (Takahashi *et al.*, 2004). Swellings have also been reported to form within cholinergic axons of the nucleus basalis magnocellularis in early stage human AD brain (Stokin *et al.*, 2005). The reduction of kinesin expression enhances the frequency of axonal defects as well as increases Aβ levels and amyloid deposition in the transgenic mouse model (Stokin *et al.*, 2005). APP over expression is proposed to be responsible for the AD pathology observed in DS (Prasher *et al.*, 1998). A cycle of local increased APP processing causing additional vesicle stalling further stimulating additional APP processing (Stokin *et al.*, 2005) could result in a positive feed-back spiral in which axonal blockages and Aβ production become mutually stimulatory leading to early synaptic loss (Minamide *et al.*, 2000; Stokin *et al.*, 2005; Maloney *et al.*, 2005).

Glutamate and Aβ treatment disrupt anterograde and retrograde fast axonal transport in cultured neurons by formation of actin bundles (Hiruma *et al.*, 2003). Excessive glutamate in extra cellular space is recognized as an excitotoxin playing a role in the development of AD and other neurodegenerative diseases (Arias *et al.*, 1998; Lancelot *et al.*, 1998). A decline in the ability of glia to take up and process glutamate to glutamine may be a contributing factor to age-related cognitive decline. Application of $A\beta_{25\text{-}35}$, to cultured rat hippocampal neurons slowed axonal transport within a few minutes, and did so in a dose dependent manner from 200 nM to 20 μM. Although transport was restored within 30 min following washout of 2 μM $A\beta_{25\text{-}35}$ after 26 min exposure (Hiruma *et al.*, 2003), washout of 20 μM $A\beta_{25\text{-}35}$ was not reversible and resulted in continuous decline in transport. Interestingly, treatment with 20 μM $A\beta_{1\text{-}42}$ incubated

under aggregating conditions (pre-incubated) reproduced the effects observed with $A\beta_{25-35}$, however treatments with the same concentration of freshly prepared $A\beta_{1-42}$ or with pre-incubated $A\beta_{1-40}$, failed to impair transport (Hiruma *et al.*, 2003). Among others, these findings highlight the importance of Aβ peptide composition (sequence and length), species (monomers, oligomers, fibrils), and solubility (soluble vs. insoluble) relating to its biological activity. In the studies of Hiruma *et al.* (1993) actin aggregates were observed by phalloidin staining, but fixation was mild (4% paraformaldehyde for 3 min) and certainly would have resulted in the loss of cofilin from actin rods, allowing some phalloidin binding. Fixation of rods requires 45 min in paraformaldehyde (Maloney *et al.*, 2005). These results suggest that the inhibitory effects of $A\beta_{25-35}$, and pre-incubated $A\beta_{1-42}$ on transport and the subsequent aggregation of actin (Hiruma *et al.*, 2003) are intimately linked.

Transport defects, Down syndrome, and AD

Enlarged early neuronal endosomes develop before birth in DS brains (Cataldo *et al.*, 2003) and years before significant Aβ deposits and neurofibrillary pathology associated with AD and DS form (Cataldo *et al.*, 1997; Cataldo *et al.*, 2000; Cataldo *et al.*, 2004). Both the number and size of basal forebrain cholinergic neurons (BFCN) decreases during the progression of AD and DS (Whitehouse *et al.*, 1982; Mann *et al.*, 1984; Casanova *et al.*, 1985; Mufson *et al.*, 1989). Aβ has been proposed to act specifically on BFCN via activation of whole cell voltage-activated currents in these neurons and not in GABAergic neurons (Jhamandas *et al.*, 2001). BFCN loss is a classic feature of both AD and DS and is known to result from defective retrograde transport of

nerve growth factor (NGF) from the hippocampus (Cooper *et al.*, 2001). BFCN depend upon NGF for the normal function and development (Sofroniew et al., 2001). NGF produced in the hippocampus binds to receptors on BFCN axons and is retrogradely transported as an active signaling endosome to the cell body (Sofroniew *et al.*, 2001).

Studies using the partial trisomy 16 (Ts65Dn) mouse model of DS found reduced BFCN size and number as well as regression of their hippocampal terminal fields (Cooper *et al.*, 2001). Increased levels of NGF occur in the hippocampus of Ts65Dn mice as a result of failed retrograde transport to the BFCN (Cooper *et al.*, 2001). While the exact cause for the defect remains a mystery, NGF binding and internalization in synaptosomes prepared from Ts65Dn mice showed no impairment as compared to wild type (2N) mice suggesting that the failure lies in an axonal abnormality affecting retrograde transport (Cooper *et al.*, 2001). In Ts65Dn mice i.c.v. NGF infusion improved BFCN size as well as restored cholinergic innervation of the hippocampus (Cooper *et al.*, 2001).

Several lines of evidence place APP at the center of transport defects in both AD and DS (Kasa *et al.*, 2003). Increased expression of APP is found in DS and increased levels of APP-CTF's accumulate in AD pathology. Ts65Dn mice display enlarged neuronal early endosomes in BFCN (Cataldo *et al.*, 2004). Selective deletion of one copy of APP from Ts65Dn mice eliminated the endosomal phenotype (Cataldo *et al.*, 2003), however the over expression of APP alone did not produce endosomal phenotype. This suggests that while APP gene dosage is critical to the development of endosomal abnormalities additional genes found on the triplicated region of mouse chromosome 16 are also required (Cataldo *et al.*, 2003). Some candidate genes located on the triplicated

region of human chromosome 21 encode BACE-2 and super-oxide dismutase-1 (Sod-1) (Cataldo *et al.*, 2003).

Mitochondrial degeneration and Cofilin

Mitochondria produce much of the ATP required to power nearly every cellular function. Over a lifetime mitochondria in postmitotic cells become less efficient due in part to damage caused by increased levels of reactive oxygen species (ROS). Increased production of ROS also arises due to the lowered mitochondrial efficiency providing a feed-forward model for ROS generation. Rundown of mitochondria contributes to normal aging and has been attributed to cellular dysfunction in neurodegenerative disease. Rod formation occurs in >80% of cultured neurons within minutes of ischemia induced by treating cells with sodium azide to shut down the electron transport chain, and 2-deoxy glucose to poison glycolysis (Minamide *et al.*, 2000). Under these conditions ATP levels run down rapidly leading to large pools of ADP-actin and activated dephosphorylated cofilin (Minamide *et al.*, 2000). Upon washout and return of cells to normal culture conditions, ATP levels rapidly recover and rods vanish. Rods will reappear within ~30% of neurons after 24 hours, in regions where irreversible damage has occurred to the mitochondria (Minamide *et al.*, 2000).

Studies in yeast have demonstrated a key role for the actin cytoskeleton in aging and apoptosis (Gourlay *et al.*, 2005b). Decreased actin turnover during normal aging or induced by the application of actin stabilizing drugs, leads to accumulation of F-actin aggregates and triggers a rise in reactive oxygen species (Gourlay *et al.*, 2004; Gourlay *et al.*, 2005b). Actin filaments have been proposed by play a direct role in apoptosis

(Gourlay *et al.*, 2005a; Gourlay *et al.*, 2005c) by regulating the opening of mitochondrial voltage gated anion channels (VDAC), sites of cytochrome *c* release (Tsujimoto & Shimizu, 2000; Zalk *et al.*, 2005).

Mitochondrial membrane potential ($\Delta\Psi_m$) depends upon cellular ATP (Bernstein *et al.*, 2006), and at steady state in resting neurons actin treadmilling alone has been demonstrated to consume nearly 50% of the available ATP (Bernstein & Bamburg, 2003). For a short period immediately after initial rod formation the loss of both $\Delta\Psi_m$ and ATP in neurites with rods is slower than in neurite without them (Bernstein *et al.*, 2006). In addition, gelsolin, an F-actin severing protein, has been reported to protect cells from apoptosis by blocking both $\Delta\Psi_m$ loss and cytochrome *c* release via the closing of VDAC (Kusano *et al.*, 2000; Koya *et al.*, 2000). Thus, the formation of rods transiently protects neurites by slowing filament turnover and its associated ATP hydrolysis (Bernstein *et al.*, 2006). Because actin dynamics is such a major energy drain for neurons, the ability to turn off the actin treadmill during times of transient stress would provide the cell with additional time and ATP required for surviving transient insults. Rods provide such a mechanism by tying up nearly all-available cofilin into non-dynamic structures (Bernstein *et al.*, 2006). Taken together the ability of rods to preserve ATP levels, retard the loss of $\Delta\Psi_m$, along with their rapid appearance during stress and their disappearance following stress, suggests rods function as part of a regulated protective mechanism.

Altered mitochondrial function has been implicated in the pathogenesis of AD (Bowen *et al*, 1979; Hirai *et al.*, 2001; Swerdlow & Kish, 2002). Quantitative proteomic analysis of mitochondria isolated from rat cortical neurons treated with Aβ showed

increased association of cofilin among nine other proteins with statistically elevated protein levels (Lovell *et al.*, 2005). Another report found cofilin to be among a handful of proteins up-regulated in human AD brain compared to normal brain when screening was performed using a cDNA library from embryonic rat brains to isolate neuron specific genes (Kondo *et al*, 1996).

In the neurons of AD brain were found all the morphological features of apoptosis, including blebbing, formation of apoptotic bodies, chromatin condensation and cytoskeleton reorganization (Ostrowski *et al.*, 2003 abstract). Cofilin plays an important role in the initiation of mitochondrial-dependent apoptosis (Chua *et al.*, 2003). Activation of this apoptotic cascade causes mitochondrial release of cytochrome *c* leading to formation of the apoptosome, a committed step in apoptosis. Treatment of neuroblastoma cells with the apoptotic agent staurosporine (STS) or etoposide, induced a translocation of cofilin to the outer mitochondrial membrane within 30 min, peaking by 2 h after treatment (Chua *et al.*, 2003). Suppression of cofilin expression by siRNA resulted in cell protection from apoptosis induced by STS or etoposide. Dephosphorylation of cofilin Ser3 was required for its translocation to mitochondria. In addition, expression of a pseudophosphorylated form of cofilin (S3D) did not localize to mitochondria and inhibited staurosporine induced apoptosis (Chua *et al.*, 2003). In PC12 cells, over expression of LIMK1 protected cells from serum-induced apoptosis by inhibiting both caspase 3 and JNK activation (Yang *et al.*, 2004). Inhibition of cofilin activation by LIMK1 transiently protects cells from apoptosis (Yang *et al.*, 2004) and sequestration of cofilin into rods retards mitochondrial rundown (Bernstein *et al.*, 2006). Since the translocation of activated cofilin to mitochondria is both upstream of and

necessary for cytochrome *c* release (Chua *et al.*, 2003) rods may prevent or delay this translocation by sequestering cofilin thus protecting cells from apoptosis (Bernstein *et al.*, 2006).

The term Aβ is used to describe a spectrum of peptide species, but often the downstream effects of different Aβ peptides are lost by the generalities ascribed to Aβ effects. Investigations are beginning to elucidate differences in the biological activity of Aβ species, especially on the phosphorylation (activity) of cofilin. Soluble species of the longer $A\beta_{1\text{-}42}$ induce the activation of cofilin only in the responding subpopulation of neurons that form rods at low nanomolar concentrations (Maloney *et al.*, 2005). Fibrillar $A\beta_{1\text{-}42}$ can induced rods, deliver toxicity and produce dystrophic neurites at low micromolar concentrations (Maloney *et al.*, 2005). On the other hand treatment of cultured hippocampal neurons with 20 μM fibrillar $A\beta_{1\text{-}40}$ produces an inactivation of cofilin in neurons that develop dystrophic neurites, while the same concentration of freshly prepared soluble $A\beta_{1\text{-}40}$ displayed no adverse effects (Heredia *et al.*, 2006). Thus the amino acid length, structure, and aggregation state may greatly affect the binding of Aβ peptides to prospective receptors and therefore influence the biological activity of Aβ against cultured neurons and *in vivo*. Taken together these reports both indicate that selective populations of neurons react to different isoforms and conformers of Aβ via alterations in cofilin regulation.

Cholesterol homeostasis and transport

Epidemiological studies indicate that high serum cholesterol levels are associated with increased risk of AD and cholesterol regulation and metabolism may be altered in

AD (Knebl *et al.*, 1994; Frears *et al.*, 1999). This correlation is strengthened by the inheritance of the ε4 allele of apolipoprotein E (ApoE) as a high risk factor with familial late onset AD. Additional evidence is found in the reports of increased amyloidogenic processing of APP by increasing cellular cholesterol levels *in vitro* and converse reduction of this processing by cholesterol depletion. Sub-cellular distribution of cholesterol may influence APP cleavage because mutations and pharmacological inhibitors of Niemann-Pick complex cholesterol transport pathway alter the localization of presenilin/γ-secretase and lead to Aβ aggregate production (Sawamura *et al.*, 2000; Runz *et al.*, 2002; Burns *et al.*, 2003; Jin *et al.*, 2004). The form and distribution of cholesterol in cells may modulate APP processing in a complex fashion (Cole *et al.*, 2005; Cole & Vassar, 2006).

Cholesterol depletion by lovastatin and methyl-β-cyclodextrin extraction inhibits APP processing by BACE1 and lowers Aβ production (Simons *et al.*, 1998; Austen *et al.*, 1999; Buxbaum *et al.*, 2001; Fassbender *et al.*, 2001; Kojro *et al.*, 2001; Ehehalt *et al.*, 2003). Moderate but not complete depletion of cholesterol results in increased Aβ production (Abad-Rodriguez *et al.*, 2004), and cholesterol enrichment leads to elevated amyloidogenic APP processing (Bodovitz & Klein 1996; Racci *et al.*, 1997; Galbete *et al.*, 2000). Thus, there appears be optimal cholesterol content for activation of the BACE-APP-processing pathway.

β-Secretase has been reported to associate with lipid raft domains of the plasma membrane, areas rich in cholesterol and sphingolipids. Lipid rafts or detergent insoluble membrane regions are sites for endocytosis and the amyloidogenic processing of APP is believed to be favored in endocytic vesicles. The entire γ-secretase complex, which

includes PS1, mature nicastrin, APH1 and PEN2, has been found to associate with rafts (Vetrivel *et al.*, 2004). BACE undergoes palmitoylation targeting it to lipid rafts (Vetrivel & Thinakaran, 2006). Addition of a GPI-anchor targets BACE exclusively to rafts and increases APP processing at the β-cleavage site (Riddell *et al.*, 2001; Cordy *et al.*, 2003). Raft micro domains also have been implicated in amyloidogenic processing of APP in other studies (Ehehalt *et al.*, 2003). Early endocytic vesicles undergo retrograde transport via microtubule networks before being merged into the lysosomal or secretory pathways. Defective transport in this system may be at the heart of cholesterol and ApoE related effects in AD. Cholesterol lowering drugs, statins, are not currently prescribed in AD therapy, however statin use has been linked to a decreased risk of developing Alzheimer's disease (Jick *et al.*, 2000; Wolozin *et al.*, 2000; Yaffe *et al.*, 2002; Rockwood *et al.*, 2002).

Statins inhibit HMG-CoA reductase, an enzyme that catalyzes the rate-limiting step in cholesterol biosynthesis (Cole *et al.*, 2005). Statins have been found to enhance sAPPα ectodomain cleavage thereby reducing amyloidogenic APP processing and $A\beta_{1-42}$ production. While this effect is believed to be due in part to reduced cholesterol, recent evidence also supports a cholesterol-independent effect (Pedrini *et al.*, 2005; Cole *et al.*, 2005). Statins can modulate the association of the Rho family GTPases and other proteins with the inner leaflet of the plasma membrane (Bi *et al.*, 2004; Kato *et al.*, 2004) via effects on the isoprenoid pathway (Pedrini *et al.*, 2005; Cole *et al.*, 2005). Furthermore the Rho-ROCK pathway has been implicated in regulating γ-secretase activity towards APP proteolysis (Ryder *et al.*, 2003).

Expression of dominant negative ROCK in cultured N2a neuroblastoma cells increased sAPPα shedding while expression of constitutively active ROCK inhibited the statin stimulated shedding (Pedrini *et al.*, 2005). Statin treatment elevated intracellular levels of APP and β-cleaved fragments (Cole *et al.*, 2005) due to inhibited trafficking of APP through the secretory pathway resulting from low cellular isoprenoid levels. While cholesterol depletion does not inhibit APP cell surface trafficking, it does slow endocytosis thereby reducing the levels of intracellular Aβ (Cole *et al.*, 2005) via a different pathway than statins. It is becoming apparent that intracellular Aβ is affected by isoprenoids and secreted Aβ is affected by cholesterol (Cole *et al.*, 2005). Inhibition of isoprenylation of key G-proteins in the Rho and Rab families is associated with cytoskeletal alterations and decreased efficiency of vesicular transport (Vicent *et al.*, 2000; Ridley, 2001). These finding provide a direct link between upstream effectors of cofilin and APP processing into Aβ.

Concluding Remarks

Understanding mechanisms involved in the early stages of Alzheimer's disease progression is critical for the development of preventative strategies. Here we present evidence for the involvement of cofilin in transport defects that may lie at the root of a neurodegenerative cascade. Cofilin rods provide a link between seemingly unrelated aspects of AD such as synaptic loss and increased deposition of Aβ. Rods may also contribute to cognitive decline as well as increased production of Aβ. Furthermore a number of reports highlighted herein demonstrate direct and indirect effects of various neurodegenerative stimuli on cofilin regulation.

The opposite effects of fibrillar $A\beta_{1-40}$ and soluble $A\beta_{1-42}$ on cofilin activity could arise from their interactions with different neuronal populations, with different receptors on the same neuronal population, or through concentration effects of ligand on the same receptor that alters its intracellular signaling. Regardless of which of these mechanisms gives rise to the differences observed, it is significant that misregulation of cofilin is the common feature of these two very different effects. State and solubility, in mediating opposing end effects on cofilin *in vitro*, may also explain *in vivo* features of AD.

Chapter Five

Conclusions and Future Directions

Concluding remarks

The role of AC proteins in actin dynamics has been well studied in a myriad of biological systems. Because actin plays such a central role in most cellular processes, AC proteins do so as well. Regulating actin dynamics is a complex process involving more than just AC proteins. Studies on the function of AC protein and their upstream regulators have led to the discovery of a number of roles for actin in cells that were hitherto unknown. Among these is the release of cytochrome *c* from mitochondria. Because of the diverse functional roles for AC proteins, therapeutic intervention through their regulation/modification is probably not a realistic goal in many diseases in which AC proteins have been implicated.

One of the unique areas for AC protein involvement in disease is the formation of AC-actin rods induced in neurons by common mediators of neurodegeneration. Rod-related diseases are one area where possible therapeutic intervention might succeed because the protein-protein interface between the AC-saturated filaments that form the rod may be different from the interface between AC proteins and the actin filament that is required for the AC dynamizing functions. Developing reagents to target this interface may be a worthwhile goal for future research.

Future directions

Rods and apoptosis

A protective role for rods has been demonstrated in neurons expressing XAC-GFP (Bernstein *et al.*, 2006). The presence of rods within neurites protects local mitochondria from a loss of membrane potential $\Delta\Psi_m$ and slows the loss of ATP (Bernstein *et al.*, 2006). In resting neurons, actin turnover can consume nearly 50% of cellular ATP (Bernstein & Bamburg, 2003). Thus, it is plausible that rods are neuroprotective by forming non-dynamic aggregates with actin thereby preserving ATP. Rods are potentially neuroprotective in other ways. Chua *et al*, 2003 demonstrated that treatment of cultured cells with the apoptotic agent staurosporine (STS) induced the translocation of activated cofilin to mitochondria, an event upstream of and required for cytochrome *c* release. We have demonstrated the translocation of cofilin to mitochondria in primary neurons occurs within 2 h following treatment with 1 μM STS (Fig 5.1). Rods sequester nearly all of the activated cofilin, therefore rods may provide a mechanism to delay or prevent cofilin translocation to mitochondria during transient stress thereby protecting the cell from an apoptotic death. Because rods form rapidly in response to a variety of neurodegenerative stimuli including ischemia and $A\beta_{1-42}$, continued investigation into the neuroprotective nature of rods in neurons is imperative.

This study could be carried out in dissociated primary neuronal cultures beginning with a titration of the apoptotic inducing drugs to find the minimum effective concentration required to induce both cofilin translocation to mitochondria and apoptosis. Apoptosis can be followed by observing nuclear condensation with DAPI and by using cytochrome *c* antibodies to follow its loss from mitochondria. Mitochondrial

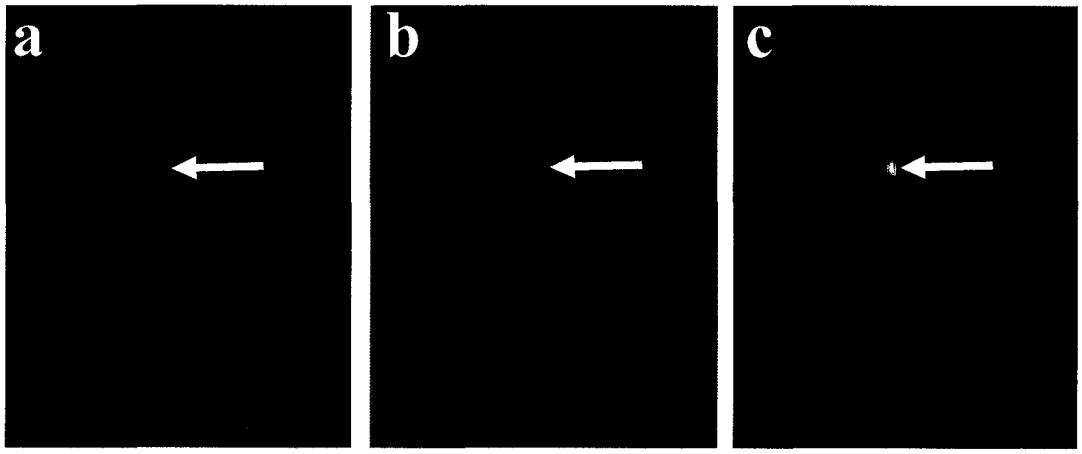

Figure 5.1: Staurosporine (STS) induces cofilin translocation to mitochondria in cultured neurons. ADF/cofilin staining (green a) and mitochondiral stain (red b) colocalized following 2 h STS treatment. Co-localization is observed in overlay (c) (white arrow a, b, c). Not all mitochondria become labeled with cofilin as shown in adjacent areas of the same neurite (blue circle). The cofilin labeled mitochondrion appears swollen, a common feature of early apoptosis.

translocation of cofilin can be observed in fixed cell by co-staining with Mito-tracker red and antibodies to cofilin to observe co-localization. Mitochondrial translocation of cofilin can also be followed by probing western blots with cofilin antibodies to follow the shift in signal intensity between cytoplasmic and mitochondrial enriched fractions from cell lysates. Next conditions will need to be optimized for inducing fluorescent rods using tet-regulated XAC-GFP adenoviruses to keep protein expression levels at a minimum. By treating cultures with STS or Etoposide and observing for apoptosis we should be able to determine if the presence of fluorescent rods protects neurons from apoptosis and also if rods prevent the translocation of cofilin to mitochondria.

Identification of the $A\beta_{1-42}$ sensitive sub-population

Treatment of dissociated cultured neurons with up to 2 μM $A\beta_{1-42}$ induces rod formation in a maximum of ~20 % of the total population. At higher $A\beta_{1-42}$ concentrations, cell viability is negatively impacted but the percent of neurons with rods does not increase (Maloney *et al.*, 2005). Lacor *et al*, 2004 demonstrated that Aβ selectively binds to an undetermined sub-population of neurons in culture, which represents only 30-50% of the total population. The identification of the sensitive population of neurons will help in the development of strategies to protect neurons from the effects of Aβ. Organotypic slice cultures will provide useful clues. By mapping the location of rods formed in slice cultures by soluble $A\beta_{1-42}$ we hope to identify whether or not rods form preferentially in a specific region such as the dentate gyrus (Fig 3.1).

No differences in rod formation were observed when dissociated hippocampal cultures enriched in CA1 or CA3 neurons were treated with soluble $A\beta_{1-42}$ suggesting that

the sensitive subpopulation may be distributed throughout the hippocampus (Maloney *et al.*, 2005). A subset of cells worth investigating are the 30-40 % of hippocampal neurons that express the p75 low affinity NGF receptor in the absence of the cognate Trk receptors (Friedman, 2000). NGF exposure induces apoptosis of this subset of neurons via unregulated activation of the p75 receptor which is also a target for $A\beta_{1-42}$ mediated toxicity (Costantini *et al.*, 2005). Other candidates include neurons expressing specific subunits of glutamate or NMDA receptors. Whatever the receptor site may be, by pre-treating dissociated cultures with inhibitory peptides or receptor blocking drugs we aim to block $A\beta_{1-42}$ mediate rod formation and identify the sensitive sub-population. Additionally we seek to co-stain fixed Aβ treated cultured neurons with antibodies against specific receptor types or subunits and with antibodies against Aβ to look for co-localization.

Transport studies

Exposure of neurons to elevated $A\beta_{1-42}$ causes rearrangement of the actin cytoskeleton and disrupts transport (Stokin *et al.*, 2005, Hiruma *et al.*, 2003, Maloney *et al.*, 2005). Transport defects are among the earliest signs of degeneration in human AD brain and in the brains of Tg-swAPP^{prp} mice (Stokin *et al.*, 2005). The accumulation of APP, BACE and PS1 occurs at rods suggesting that these may be sites for local $A\beta_{1-42}$ production (Maloney *et al.*, 2005). We have created an adenovirus for expression of APP conjugated to yellow fluorescent protein (APP-YFP), with which we can observe transport in live cultured neurons (Fig 5.2). By co-infecting with XAC-RFP we will

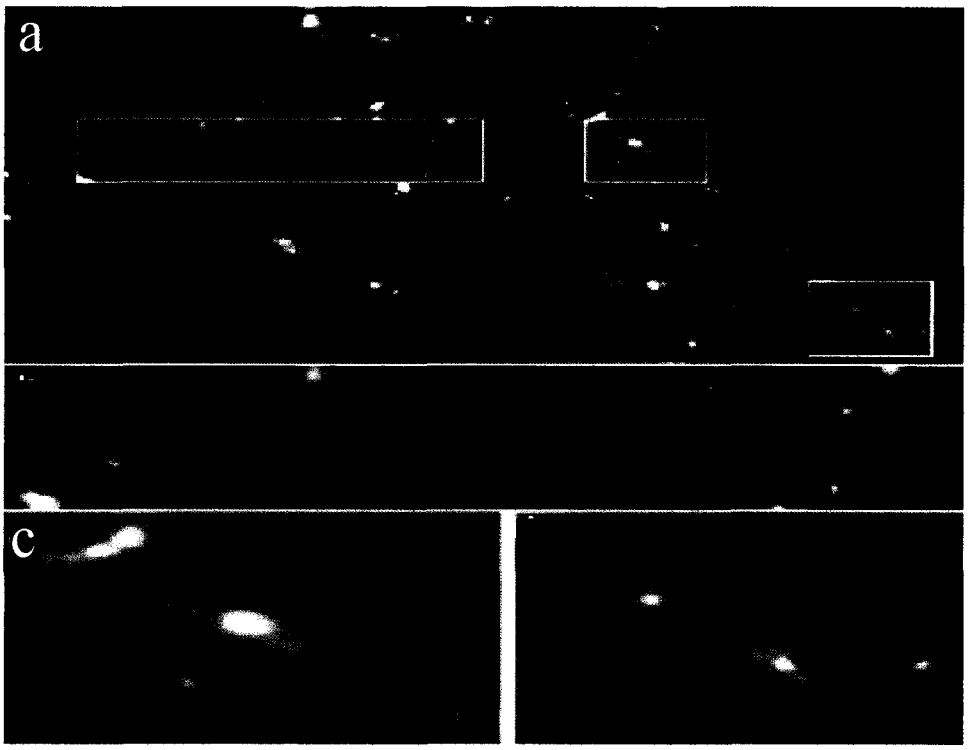

Figure 5.2: Time lapse imaging of APP-YFP in E18 Rat hippocampal neurons. Color composite image of APP-YFP trafficking. Images taken at t = 0 (red), t = 1 s (green), and t = 2 s (blue) (a). Enlarged boxes from (a) showing vesicles trafficking (b, c, d). Vesicles that don't move are white or yellow since time points would overlap in position.

induce spontaneous rod formation and observe the impact of rods on APP-YFP transport in real time.

To study whether rods lead to elevated $A\beta_{1-42}$ production we will induce rod formation in dissociated cultured neurons by ATP depletion followed by washout. Secreted $A\beta_{1-42}$ will be measured in the conditioned medium and intracellular $A\beta_{1-42}$ will be measured from cell lysates using protein dot blots probed with a specific antibody to $A\beta_{1-42}$. By comparison to untreated cultures we hope to determine if the presence of rods will lead to elevated levels of secreted or intracellular $A\beta_{1-42}$.

Reversal of $A\beta_{1-42}$ induced rods

Rods induced in cultured neurons by ATP depletion are initially reversible upon removal of ATP depletion medium (Minamide *et al.*, 2000). Cell derived Aβ induces transient cognitive deficits when injected into the brains of rats (Cleary *et al.*, 2004) and induce rod formation in organotypic slice cultures (Maloney, Minamide and Bamburg unpublished observation). PDAPP is a transgenic AD mouse model that overexpress mutant human APP V717F and progressively develop many of the neuropathological hallmarks of Alzheimer's disease in an age- and brain-region-dependent manner (Schenk *et al.*, 1999). Immunization of young PDAPP mice with $A\beta_{1-42}$ peptides essentially prevented the development of Aβ-plaque formation, neuritic dystrophy and astrogliosis and the immunization of older animals also markedly reduced the extent and progression of AD-like pathology (Schenk, *et al.*, 1999). Because rods form rapidly in response to soluble $A\beta_{1-42}$ (Maloney *et al.*, 2000) and interfere with synaptic functioning (Jang *et al.*, 2005), it is important to determine if $A\beta_{1-42}$ induced rods are reversible. Reversibility

could explain the transient cognitive effects of cell derived Aβ and would mean that immunization therapies could reverse rod formation *in-vivo*.

In a pilot experiment dissociated hippocampal neurons (5 div) were treated with 1 μM soluble $A\beta_{1-42}$ and some cultures were fixed at 24 and 48 hours while in other cultures the $A\beta_{1-42}$ was washed out at 24 h and cells were fixed at 2 h and 24 h post washout. At 24 h with $A\beta_{1-42}$ 10.4% of neurons formed rods and by 48 h the maximal response of 19.1% of neurons with rods was recorded. At 2 h and 24 h post washout only 5.2% and 5.1% of neurons maintained persistent rod formation respectively (Fig 5.3). This result suggests that $A\beta_{1-42}$ induced rods are reversible in ½ to ¾ of affected neurons. A more rigorous follow up to this experiment would help to classify $A\beta_{1-42}$ induced rods as transient or persistent.

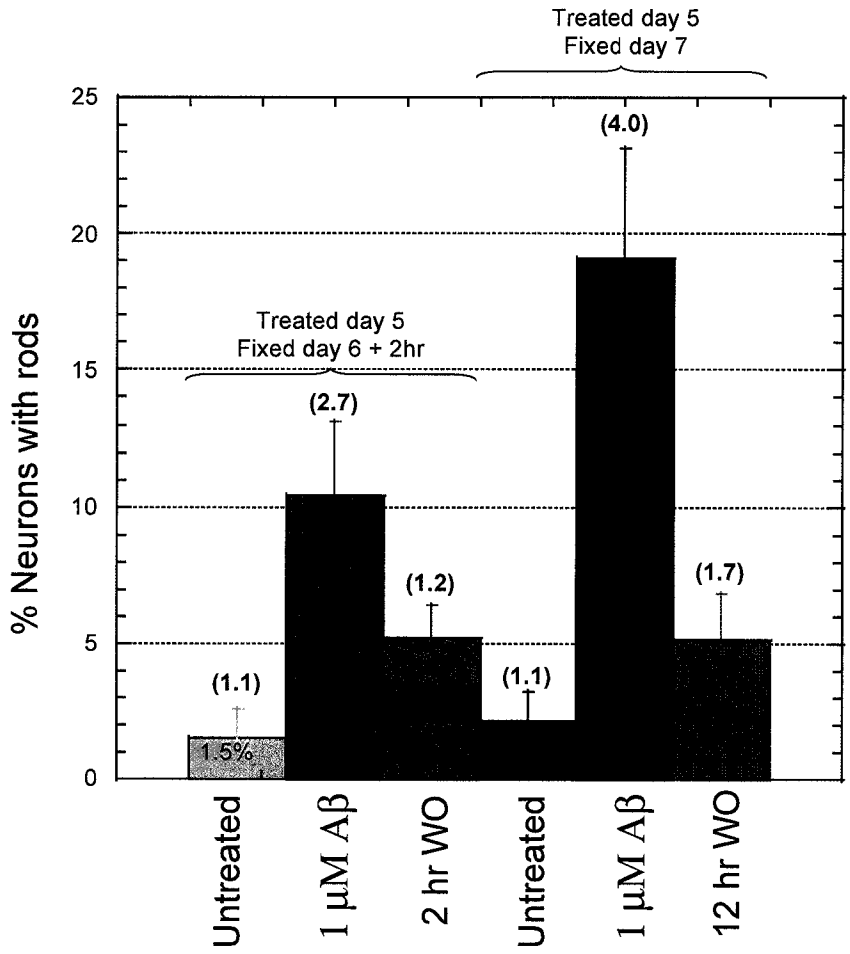

Figure 5.3: The percent of neurons with rods decline when $A\beta_{1-42}$ is removed. E-18 rat hippocampal neurons were exposure to soluble Aβ for 24 and 48 hours and the percent rod formation is compared to neurons exposed for 24 hours followed by a 2 or 12 h washout and recovery period.

Reference List

Abad-Rodriguez, J., Ledesma, M. D., Craessaerts, K., Perga, S., Medina, M., Delacourte, A., Dingwall, C., De Strooper, B., and Dotti, C. G. (2004). Neuronal membrane cholesterol loss enhances amyloid peptide generation. *J Cell Biol.* 167(5), 953-960.

Abe, H., Ohshima S., and Obinata, T. (1989). A cofilin-like protein is involved in the regulation of actin assembly in developing skeletal muscle. *J Biochem* (Tokyo), 106, 696-702.

Agnew, B., Minamide, L. and Bamburg, J. (1995). Reactivation of phosphorylated actin depolymerizing factor and identification of the regulatory site. *J Biol Chem.*, 270, 17582-17587.

Ahmed, I., Calle, Y., Iwashita, S., and Nur-E-Kamal, A. (2006). Role of Cdc42 in neurite outgrowth of PC12 cells and cerebellar granule neurons. *Mol Cell Biochem.*, 281(1-2), 17-25.

Aizawa, H., Fukui, Y., and Yahara, I. (1997). Live dynamics of Dictyostelium cofilin suggests a role in remodeling actin latticework into bundles. *J Cell Sci.*, 110 (Pt 19), 2333-2344.

Aksenov, M. Y., Aksenova, M. V., Markesbery, W. R., and Butterfield, D.A. (1998). Amyloid beta-peptide (1-40)-mediated oxidative stress in cultured hippocampal neurons. Protein carbonyl formation, CK BB expression, and the level of Cu, Zn, and Mn SOD mRNA. *J Mol Neurosci.* 10, 181-192.

Alzheimer, A., (1907). Über eine eigenartige Erkrankung der Hirnrinde. *Allgemeine Zeitschrift für Psychiatre und phychish-Gerichtlieche Medizin*, (Berlin), 64, 146-148.

Amaral, D. G., & Kurz, J. (1985). An analysis of the origins of the cholinergic and noncholinergic septal projections to the hippocampal formation of the rat. *J Comp Neurol.*, 240(1), 37-59.

Anandatheerthavarada, H. K., Biswas, G., Robin, M. A., and Avadhani, N. G. (2003). Mitochondrial targeting and a novel transmembrane arrest of Alzheimer's amyloid precursor protein impairs mitochondrial function in neuronal cells. *J Cell Biol,* 161, 41-54.

Arber, S., Barbayannis, F., Hanser, H., Schneider, C., Stanyon, C.,Bernard, O. and Caroni, P. (1998). Regulation of actin dynamics through phosphorylation of cofilin by LIM-kinase. *Nature,* 393, 805-809.

Arias, C., Becerra-Garcia, F., and Tapia, R. (1998). Glutamic acid and Alzheimer's disease. *Neurobiology (Bp)*, 6(1), 33-43. Review.

Ashenafi, S., Fuente, A., Criado, J. M., Riolobos, A. S., Heredia, M., and Yajeya, J. (2005). Beta-Amyloid peptide25-35 depresses excitatory synaptic transmission in the rat basolateral amygdala "in vitro". *Neurobiol Aging*, 26(4), 419-428.

Austen, W. G. Jr., Kyriakides, C., Favuazza, J., Wang, Y., Kobzik, L., Moore, F. D. Jr., and Hechtman, H. B. (1999). Intestinal ischemia-reperfusion injury is mediated by the membrane attack complex. *Surgery*, 13(2), 343-348.

Bahr, B. A., Hoffman, K. B., Yang, A. J., Hess, U. S., Glabe, C. G., and Lynch, G. (1998). Amyloid beta protein is internalized selectively by hippocampal field CA1 and causes neurons to accumulate amyloidogenic carboxyterminal fragments of the amyloid precursor protein. *J Comp Neurol*, 397, 139-147.

Bamburg, J.R. (1999). Proteins of the ADF/cofilin family: essential regulators of actin dynamics. *Annu Rev Cell Dev Biol.*, 15, 185-230.

Bamburg, J. R., & Wiggan, O. P. (2002). ADF/Cofilin and actin dynamics in disease. *Trends in Cell Bio.*, 12, 598-605.

Bamburg, J. R., Harris, H. E., and Weeds, A. G. (1980). Partial purification and characterization of an actin depolymerizing factor from brain. *FEBS Lett.*, 121(1), 178-182.

Bamburg, J. R., McGough, A., and Ono, S. (1999). Putting a new twist on actin: ADF/cofilins modulate actin dynamics. *Trends Cell Biol.*, 9, 364-370.

Bartlett, W. P., & Banker, G. A. (1984). An electron microscopic study of the development of axons and dendrites by hippocampal neurons in culture. I. Cells which develop without intercellular contacts. *J Neurosci*, 4, 1944-1953.

Bazan, N. G., Palacios-Pelaez, R., and Lukiw, W. J. (2002). Hypoxia signaling to genes: significance in Alzheimer's disease. *Mol Neurobiol.*, 26(2-3), 283-298. Review.

Bellugi, U., Lichtenberger, L., Mills. D., Galaburda, A., and Korenberg, J. R. (1999). Bridging cognition, the brain and molecular genetics: evidence from William's syndrome. *TRENDS Neuroscience*, 22, 197-207.

Berezovska, O., Frosch, M., McLean, P., Knowles, R., Koo, E., Kang, D., Shen, J., Lu, F. M., Lux, S. E., Tonegawa, S., and Hyman, B. T. (1999). The Alzheimer-related gene presenilin 1 facilitates notch 1 in primary mammalian neurons. *Brain Res Mol Brain Res.*, 69(2), 273-280.

Bernstein, B. W., & J. R., Bamburg. (2003). Actin-ATP hydrolysis is a major energy drain for neurons. *J Neurosci.*, 23(1), 1-6.

Bernstein, B. W., Chen, H., Boyle, J. A., and Bamburg, J. R. (2006). Formation of actin-ADF/cofilin rods transiently retards decline of mitochondrial potential and ATP in stressed neurons. *Am J Physiol Cell Physiol.*, (in press).

Bernstein, B. W., Painter, W. B., Chen, H., Minamide, L. S., Abe, H., and Bamburg, J. R. (2000). Intracellular pH modulation of ADF/cofilin proteins. *Cell Motil Cytoskeleton*, 47(4), 319-336.

Bershadsky, A. D., Belfand, V. I., Svitkina, T. M. & Tent, I. S. (1980). Destruction of microfilament bundles in mouse embryo fibroblasts treated with inhibitors of energy metabolism. *Exp. Cell Res.*, 127, 421-429.

Bi, X., Baudry, M., Liu, J., Yao, Y., Fu, L., Brucher, F., and Lynch, G. (2004). Inhibition of geranylgeranylation mediates the effects of 3-hydroxy-3-methylglutaryl (HMG)-CoA reductase inhibitors on microglia. *J Biol Chem.*, 279(46), 48238-48245.

Blennow, K., Vanmechelen, E., and Hampel, H. (2001). CSF total tau, Abeta42 and phosphorylated tau protein as biomarkers for Alzheimer's disease. *Mol Neurobiol,* 24, 87-97.

Bobokov, A. A., Muhlrad, A., Pavlov, D. A., Kokabi, K., Yilmaz, A., and Reisler, E. (2006). Cooperative effects of cofilin (ADF) on actin structure suggest allosteric mechanism of cofilin function. *J Mol Biol.*, 256(2), 325-334.

Bodovitz, S., & Klein, W. L. (1996). Cholesterol modulates alpha-secretase cleavage of amyloid precursor protein. *J Biol Chem.*, 271(8)., 4436-4440.

Bond, J. P., Deverin, S. P., Inouye, H., el-Agnaf, O. M., Teeter, M. M., and Kirschner, D. A. (2003). Assemblies of Alzheimer's peptides A beta 25-35 and A beta 31-35: reverse-turn conformation and side-chain interactions revealed by X-ray diffraction. *J Struct Biol.*, 141, 156-170.

Borchelt, D. R., Ratovitski, T., van Lare, J., Lee, M. K., Gonzales, V., Jenkins, N. A., Copeland, N. G., Price, D. L., and Sisodia, S. S. (1997). Accelerated amyloid deposition in the brains of transgenic mice coexpressing mutant presenilin 1 and amyloid precursor proteins. *Neuron.*, 19(4), 939-945.

Bowen, D. M., White, P., Spillane, J. A., Goodhardt, M. J., Curzon, G., Iwangoff, P., Meier-Ruge, W., and Davison, A. N. (1979). Accelerated ageing or selective neuronal loss as an important cause of dementia? *Lancet*, 1(8106), 11-14.

Brana, C., Benham, C. D., and Sundstrom, L. E. (1999). Calpain activation and inhibition in organotypic rat hippocampal slice cultures deprived of oxygen and glucose. *Eur J Neurosci.*, 11(7), 2375-2384.

Bruijn, L. I., Becher, M. W., Lee, M. K., Anderson, K. L., Jenkins, N. A., Copeland, N. G., Sisodia, S. S., Rothstein, J. D., Borchelt, D. R., Price, D. L., and Cleveland, D. W. (1997). ALS-linked SOD1 mutant G85R mediates damage to astrocytes and promotes rapidly progressive disease with SOD1-containing inclusions. *Neuron,* 18, 327-338.

Bryan, D. (1996). McKersic Dept. of Crop Science, Univ of Huelph.

Budd, S. L., & Nicholls, D. G. (1998). Mitochondria in the life and death of neurons. *Essays Biochem.,* 33, 43-52.

Burns, M., Gaynor, K., Olm, V., Mercken, M., LaFrancois, J., Wang, L., Mathews, P. M., Noble, W., Matsuoka, Y., and Duff, K. (2003). Presenilin redistribution associated with aberrant cholesterol transport enhances beta-amyloid production in vivo. *J Neurosci.*, 23(13), 5645-5649.

Buxbaum, J. D., Geoghagen, N. S., and Friedhoff, L. T. (2001). Cholesterol depletion with physiological concentrations of a statin decreases the formation of the Alzheimer amyloid Abeta peptide. *J Alzheimers Dis.*, 3(2), 221-229.

Café, C., Torri, C., Bertorelli, L., Angeretti, N., Lucca, E., Forloni, G., and Marzatico, F. (1996). Oxidative stress after acute and chronic application of beta-amyloid fragment 25-35 in cortical cultures. *Neurosci Lett,* 203, 61-65.

Carlier, M.-F. (1998). Control of actin dynamics Curr Opin Cell Biol., 10, 45-51.

Carlier, M-F., & Pantaloni, D. (1997). Control of actin dynamics in cell motility. *J Mol Biol.*, 269(4), 459-467. Review.

Carlier, M.-F., Laurent, V., Santolini, J., Melki, R., Didry, D., Xia, G. X., Hong, Y., Chua, N. H., and Pantaloni, D. (1997). Actin Depolymerizing Factor (ADF/cofilin) enhances the rate of filament turnover: implication in actin-based motility. *J Cell Biol.,* 136, 1307-1322.

Casanova, M. F., Walker, L. C., Whitehouse, P. J., and Price, D. L. (1985). Abnormalities of the nucleus basalis in Down's syndrome. *Ann Neurol.*, 18(3), 310-313.

Cataldo, A. M., Barnett, F. L., Pieroni, C., and Nixon, R. A. (1997). Increased neuronal endocytosis and protease delivery to early endosomes in sporadic Alzheimer's disease neuropathologic evidence for a mechanism of increased beta-amyloidogenesis. *J Neurosci.*, 17, 6142-6151.

Cataldo, A. M., Petanceska, S., Peterhoff, C. M., Terio, N. B., Epstein, C. J., Villar, A., Carlson, E. J., Staufenbiel, M., and Nixon, R. A. (2003). App gene dosage modulates endosomal abnormalities of Alzheimer's disease in a segmental trisomy 16 mouse model of down syndrome. *J Neurosci.*, 23(17), 6788-6792.

Cataldo, A. M., Petanceska, S., Terio, N. B., Peterhoff, C. M., Durham, R., Mercken, M., Mehta, P. D., Buxbaum , J., Haroutunian, V., and Nixon, R. A. (2004). Abeta localization in abnormal endosomes: association with earliest Abeta elevations in AD and Down syndrome. *Neurobiol Aging.*, 25(10), 1263-12672.

Cataldo, A. M., Peterhoff, C. M., Troncoso, J. C., Gomez-Isla, T., Hyman, B. T., and Nixon, R. A. (2000). Endocytic pathway abnormalities precede amyloid-β deposition in sporadic Alzheimer's disease and Down syndrome. Differential effects of ApoE genotype and presenilin mutations. *Am J Pathol.*, 157, 277-286.

Chaney, M.O., Webster, S. D., Kuo, Y. M., and Roher, A. E. (1998). Molecular modeling of the Abeta1-42 peptide from Alzheimer's disease. *Protein Eng.*, 11, 761-767.

Chartier-Harlin, M. C., Crawford, F., Hamandi, K., Mullan, M., Goate, A., Hardy, A., Backhovens, H., Martin, J. J., and Broeckhoven, C. V. (1991a). Screening for the beta-amyloid precursor protein mutation (APP717: Val----Ile) in extended pedigrees with early onset Alzheimer's disease. *Neurosci Lett.*, 129, 134-135.

Chartier-Harlin, M.C., Crawford, F., Houlden, H., Warren, A., Hughes, D., Fidani, L., Goate, A., Rossor, M., Roques, P., Hardy, J., et al. (1991b). Early-onset Alzheimer's disease caused by mutations at codon 717 of the beta-amyloid precursor protein gene. *Nature,* 353, 844-846.

Chen, H. (2001). *In vitro* analysis of the functional difference between proteins of the ADF/cofilin family. Ph.D. Dissertation Colorado State University, Fort Collins,CO.

Chen, J., Nagayama, T., Jin, K., Stetler, R. A., Zhu, R. L., Graham, S. H., and Simon, R. P. (1998). Induction of caspase-3-like protease may mediate delayed neuronal death in the hippocampus after transient cerebral ischemia. *J Neurosci.*, 18(13), 4914-4928.

Chen, X. H., Siman, R., Iwata, A., Meaney, D. F., Trojanowski, J. Q., and Smith, D. H. (2004). Long-term accumulation of amyloid-beta, beta-secretase, presenilin-1, and caspase-3 in damaged axons following brain trauma. *Am J Pathol.*, 165(2), 357-371.

Chromy, B. A., Nowak, R. J., Lambert, M. P., Viola, K. L., Chang, L., Velasco, P. T., Jones, B. W., Fernandez, S. J., Lacor, P. N., Horowitz, P., Finch, C. E., Krafft, G. A., and Klein, W. L. (2003). Self-assembly of Abeta(1-42) into globular neurotoxins. *Biochemistry,* 42, 12749-12760.

Chua, B. T., Volbracht, C., Tan, K. O., Li, R., Yu, V. C., and Li, P. (2003). Mitochondrial translocation of cofilin is an early step in apoptosis induction. *Nat Cell Biol.*, 5(12), 1083-1089.

Chyung, J. H., Raper, D. M., and Selkoe, D. J. (2005). Gamma-secretase exists on the plasma membrane as an intact complex that accepts substrates and effects intramembrane cleavage. *J Biol Chem.*, 280, 4383-4392.

Cimarosti. H., Rodnight. R., Tavares, A., Paiva, R., Valentim, L., Rocha, E., and Salbego, C. (2001). An investigation of the neuroprotective effect of lithium in organotypic slice cultures of rat hippocampus exposed to oxygen and glucose deprivation. *Neurosci Lett,* 315(1-2), 33-36.

Cleary, J. P., Walsh, D. M., Hofmeister, J. J., Shankar, G. M., Kuskowski, M. A., Selkoe, D. J., and Ashe, K. H. (2005). Natural oligomers of the amyloid-beta protein specifically disrupt cognitive function. *Nat Neurosci*, 8, 79-84.

Cobb, M. H., & Goldsmith, E. J. (1995). How MAP kinases are regulated. *J Biol Chem*, 270(25), 14843-14836.

Cole, S. L., & Vassar, R. (2006). Isoprenoids and Alzheimer's disease: A complex relationship. *Neurobiol Dis Neurobiol Dis.*, (*in press*).

Cole, S. L., Grudzien, A., Manhart, I. O., Kelly, B. L., Oakley, H., and Vassar, R. (2005). Statins cause intracellular accumulation of amyloid precursor protein, beta-secretase-cleaved fragments, and amyloid beta-peptide via an isoprenoid-dependent mechanism. *J Biol Chem.*, 280(19), 18755-18770.

Cooper, J. D., Salehi, A., Delcroix, J. D., Howe, C. L., Belichenko, P. V., Chua-Couzens, J., Kilbridge, J. F., Carlson, E. J., Epstein, C. J., and Mobley, W. C. (2001). Failed retrograde transport of NGF in a mouse model of Down's syndrome: reversal of cholinergic neurodegenerative phenotypes following NGF infusion. *PNAS U S A.*, 98(18), 10439-10444.

Cordy, J. M., Hussain, I., Dingwall, C., Hooper, N. M., and Turner, A. J. (2003). Exclusively targeting beta-secretase to lipid rafts by GPI-anchor addition up-regulates beta-site processing of the amyloid precursor protein. *Proc Natl Acad Sci U S A,* 100, 11735-11740.

Costantini, C, Rossi, F., Formaggio, E., Bernardoni, R., Cecconi, D., and Della-Bianca, V. (2005). Characterization of the signaling pathway downstream p75 neurotrophin receptor involved in beta-amyloid peptide-dependent cell death. *J Mol Neurosci.*, 25(2), 141-156.

Dahlgren, K.N., Manelli, A. M., Stine Jr., W. B., Baker, L. K., Krafft, G. A., and LaDu., M. J. (2002). Oligomeric and fibrillar species of amyloid-beta peptides differentially affect neuronal viability. *J Biol Chem.*, 277, 32046-32053.

Dickson, D.W., Crystal, H. A., Bevona, C., Honer, W., Vincent, I., and Davies., P. (1995). Correlations of synaptic and pathological markers with cognition of the elderly. *Neurobiol Aging,* 16, 285-298; discussion 298-304.

Didry, D., Carlier, M-F., and Pantaloni, D. (1998). Synergy between actin depolymerizing factor/cofilin and profilin in increasing actin filament turnover. *J Biol Chem.*, 273(40), 25602-25611.

dos Remedios, C. G., Chhabra, D., Kekic, M., Dedova, I. V., Tsubakihara, M., Berry, D. A., and Nosworthy, N. J. (2003). Actin binding proteins: regulation of cytoskeletal microfilaments. *Physiol Rev.*, 83(2), 433-473. Review.

Ehehalt, R., Keller, P., Haass, C., Thiele, C., and Simons, K. (2003). Amyloidogenic processing of the Alzheimer beta-amyloid precursor protein depends on lipid rafts. *J Cell Biol,* 160, 113-123.

Eldadah, B. A., & Faden, A. I. (2000). Caspase pathways, neuronal apoptosis, and CNS injury. *J Neurotrauma.*, 17(10), 811-829. Review.

Esler, W.P., & Wolfe, M. S. (2001). A portrait of Alzheimer secretases--new features and familiar faces. *Science,* 293, 1449-1454.

Fassbender, K., Simons, M., Bergmann, C., Stroick, M., Lutjohann, D., Keller, P., Runz, H., Kuhl, S., Bertsch, T., von Bergmann, K., Hennerici, M., Beyreuther, K., and Hartmann, T. (2001). Simvastatin strongly reduces levels of Alzheimer's disease beta -amyloid peptides Abeta 42 and Abeta 40 in vitro and in vivo. *PNAS U S A.*, 98(10), 5856-5861.

Federov, A., Lappalainen, P., Federov, E., Drubin, D. and Almo, S. (1997). Structure determination of yeast cofilin. *Nat Struct Biol.*, 4(5), 366-369.

Fluhrer, R., Friedlein, A., Haass, C., and Walter, J. (2004). Phosphorylation of presenilin 1 at the caspase recognition site regulates its proteolytic processing and the progression of apoptosis. *J Biol Chem.*, 279(3), 1585-1593.

Forloni, G., Chiesa, R., Smiroldo, S., Verga, L., Salmona, M., Tagliavini, F., and Angeretti, N. (1993). Apoptosis mediated neurotoxicity induced by chronic application of beta amyloid fragment 25-35. *Neuroreport*, 4(5), 523-526.

Frears, E. R., Stephens, D. J., Walters, C. E., Davies, H., and Austen, B. M. (1999). The role of cholesterol in the biosynthesis of beta-amyloid. *Neuroreport.*, 10(8), 1699-1705.

Friedman, W. J. (2000). Neurotrophins induce death of hippocampal neurons via the p75 receptor. *J Neurosci,* 20, 6340-6346.

Galbete, J. L., Martin, T. R., Peressini, E., Modena, P., Bianchi, R., and Forloni, G. (2000). Cholesterol decreases secretion of the secreted form of amyloid precursor protein by interfering with glycosylation in the protein secretory pathway. *Biochem J.*, 348 Pt 2, 307-313.

Gianni, D., Zambrano, N., Bimonte, M., Minopoli, G., Mercken, L., Talamo, F., Scaloni, A., and Russo, T. (2003). Platelet-derived growth factor induces the beta-gamma-secretase-mediated cleavage of Alzheimer's amyloid precursor protein through a Src-Rac-dependent pathway. *J Biol Chem.*, 278(11), 9290-9297.

Glenner, G. G., & Wong, C. W. (1984a). Alzheimer's disease and Down's syndrome: sharing of a unique cerebrovascular amyloid fibril protein. *Biochem Biophys Res Commun.,* 122(3), 1131-1135.

Glenner, G. G., & Wong, C. W. (1984b). Alzheimer's disease: initial report of the purification and characterization of a novel cerebrovascular amyloid protein. *Biochem Biophys Res Commun.*, 120(3), 885-890.

Goate, A., Chartier-Harlin, M. C., Mullan, M., Brown, J., Crawford, F., Fidani, L., Giuffra, L., Haynes, A., Irving, N., James, L., et al. (1991). Segregation of a missense mutation in the amyloid precursor protein gene with familial Alzheimer's disease. *Nature,* 349, 704-706.

Gohla, A., Birkenfield, J., and Bokoch, G. M. (2005). Chronophin, a novel HAD-type serine protein phosphatase, regulates cofilin-dependent actin dynamics. *Nature Cell Biol.*, 7(1), 21-29.

Gong, Y., Chang, L., Viola, K. L., Lacor, P. N., Lambert, M. P., Finch, C. E., Krafft, G. A., and Klein, W. L. (2003). Alzheimer's disease-affected brain: presence of oligomeric A beta ligands (ADDLs) suggests a molecular basis for reversible memory loss. *Proc Natl Acad Sci U S A*, 100, 10417-10422.

Gouras, G. K., Almeida, C.G., and Takahashi, R. H. (2005a). Intraneuronal Abeta accumulation and origin of plaques in Alzheimer's disease. *Neurobiol Aging.*, 26(9), 1235-12344. Review.

Gourlay, C. W., & Ayscough, K. R. (2005a). A role for actin in aging and apoptosis. *Biochemical Society Transactions*, 33(6), 1260-1264.

Gourlay C. W., & Ayscough, K. R., (2005b). The actin cytoskeleton in ageing and apoptosis. *FEMS Yeast Research*, 5, 1193-1198.

Gourlay, C. W., & Ayschogh, K. R. (2005c). Identification of an upstream regulatory pathway controlling actin-mediated apoptosis in yeast. *J Cell Sci.*, 118(10), 2119-2132.

Gourlay, C. W., Carpp, L. N., Timpson, P., Winder, S. J., and Ayschough, K. R. (2004). A role for the actin cytoskeleton in cell death and aging in yeast. *J Cell Biol.*, 164, 803-809.

Grace, E. A., Rabiner, C. A., and Busciglio, J. (2002). Characterization of neuronal dystrophy induced by fibrillar amyloid beta: implications for Alzheimer's disease. *Neuroscience,* 114, 265-273.

Graham, S. H., & Chen, J. (2001). Programmed cell death in cerebral ischemia. *J Cereb Blood Flow Metab.*,21(2), 99-109. Review.

Grant, S. M., Shankar, S. L., Chalmers-Redman, R. M., Tatton, W. G., Szyf, M., and Cuello, A. C. (1999). Mitochondrial abnormalities in neuroectodermal cells stably expressing human amyloid precursor protein (hAPP751). *Neuroreport,* 10, 41-46.

Grilli, M., Toninelli, G. F., Uberti, D., Spano, P., and Memo, M. (2002). Alzheimer's disease linking neurodegeneration with neurodevelopment. *Funct Neurol.*, 8(3), 145-148. Review.

Guan, J-Q., Vorobiev, S., Almo, S. and Chance, M. (2002). Mapping the G-actin binding surface of cofilin using synchrotron protein footprinting. *Biochemistry*, 41(18), 5765-5775.

Guthrie, K. M., Tran, A., Baratta, J., Yu, J., and Robertson, R. T. (2005). Patterns of afferent projections to the dentate gyrus studied in organotypic co-cultures. *Brain Res Dev Brain Res.,* 157(2), 162-171.

Hardy, J., & Selkoe, D. J. (2002). The amyloid hypothesis of Alzheimer's disease: progress and problems on the road to therapeutics. *Science,* 297, 353-356.

Harris, M.E., Hensley, K., Butterfield, D..A., Leedle, R. A., and Carney, J. M. (1995). Direct evidence of oxidative injury produced by the Alzheimer's beta-amyloid peptide (1-40) in cultured hippocampal neurons. *Exp Neurol.* 131, 193-202.

Hartley, D. M., Walsh, D. M., Ye, C. P., Diehl, T., Vasquez, S., Vassilev, P. M., Teplow, D. B., and Selkoe, D. J. (1999). Protofibrillar intermediates of amyloid beta-protein induce acute electrophysiological changes and progressive neurotoxicity in cortical neurons. *J Neurosci,* 19, 8876-8884.

Hartmann, J., Erb, C., Ebert, U., Baumann, K. H., Popp, A., Konig, G., and Klein, J. (2004). Central cholinergic functions in human amyloid precursor protein knock-in/presenilin-1 transgenic mice. *Neuroscience.*, 125(4), 1009-1017.

Hatanaka, H., Ogura, K. Moriyama, K., Ichikawa, S., Yahara, I., and Inagaki., F. (1996). Tertiary structure of destrin and structural similarity between two actin-regulating protein families. *Cell,* 85, 1047-1055.

Hawkins, M., Pope, B., Maciver, S. K. & Weeds, A. G. (1993). The interaction of human actin depolymerizing factor with actin is pH regulated. *Biochemistry,* 32, 9985-9993.

Hayden, S. M., Miller, P. S., Brauweiler, A., and Bamburg, J. R. (1993). Analysis of the interactions of actin depolymerizing factor with G- and F-actin. *Biochemistry,* 32(38), 9994-10004.

Head, E., & Lott, I. T. (2004). Down syndrome and beta-amyloid deposition. *Curr Opin Neurol,* 17, 95-100.

Hensley, K., Butterfield, D. A., Hall, N., Cole, P., Subramaniam, R., Mark, R., Mattson, M. P., Markesbery, W. R., Harris, M. E., Aksenov, M., et al. (1996). Reactive oxygen species as causal agents in the neurotoxicity of the Alzheimer's disease-associated amyloid beta peptide. *Ann N Y Acad Sci.*, 786, 120-134.

Hensley, K., Carney, J. M., Mattson, M. P., Aksenova, M., Harris, M., Wu, J. F., Floyd, R. A., and Butterfield, D. A. (1994). A model for beta-amyloid aggregation and neurotoxicity based on free radical generation by the peptide: relevance to Alzheimer disease. *Proc Natl Acad Sci U S A.*, 91, 3270-3274.

Hensley, K., Floyd, R. A., Zheng, N. Y., Nael, R., Robinson, K. A., Nguyen, X., Pye, Q. N., Stewart, C. A., Geddes, J., Markesbery, W. R., Patel, E., Johnson, G. V., and Bing, G. (1999). p38 kinase is activated in the Alzheimer's disease brain. *J Neurochem.*, 72(5), 2053-2058.

Heredia, L., Helguera, P. de Olmos, S., Kedikian, G., Sola, Vigo, F., Laferla F., Staufenbeil, M., de Olmos, J, Busciglio, J., Caceras A., and Lorenzo, A. (2006). Phosphorylation of actin-depolymerizing factor/cofilin by LIM-kinase mediates amyloid beta-induced degeneration: a potential mechanism of neuronal dystrophy in Alzheimer's disease. *J Neurosci.*, 26(24), 6533-6542.

Hewitt, K., & Corbett, D. (1992). Combined treatment with MK-801 and nicardipine reduces global ischemic damage in the gerbil. *Stroke*, 23(1), 82-86.

Hirai, K., Aliev, G., Nunomura, A., Fujioka, H., Russell, R. L., Atwood, C. S., Johnson, A. B., Kress, Y., Vinters, H. V., Tabaton, M., Shimohama, S., Cash, A. D., Siedlak, S. L., Harris, P. L., Jones, P. K., Petersen, R. B., Perry, G. , and Smith, M. A. (2001). Mitochondrial abnormalities in Alzheimer's disease. *J Neurosci.*, 21(9), 3017-3023.

Hirano, A. (1994). Hirano bodies and related neuronal inclusions. *Neuropathol Appl Neurobiol,* 20, 3-11.

Hiruma, H., Katakura, T., Takahashi, S., Ichikawa, T., and Kawakami, T. (2003). Glutamate and amyloid beta-protein rapidly inhibit fast axonal transport in cultured rat hippocampal neurons by different mechanisms. *J Neurosci.*, 23(26), 8967-8977.

Huang, T. Y., DerMardirossian, C., and Bokoch, G. M. (2006). Cofilin phosphatases and regulation of actin dynamics. *Curr Opin Cell Biol.*, 18(1), 26-31.

Iida, K., Iida, H., and Yahara, I. (1986). Heat shock induction of intranuclear actin rods in cultured mammalian cells. *Exp Cell Res.*, 165, 207-215.

Iida, K., Matsumoto, S., and Yahara, I. (1992). The KKRKK sequence is involved in heat shock-induced nuclear translocation of the 18-kDa actin-binding protein, cofilin. *Cell Struct Funct.*, 17(1), 39-46.

Inomata, H., Nakamura, Y., Hayakawa, A., Takata, H., Suzuki, T., Miyazawa, K., and Kitamura, N. (2003). A scaffold protein JIP-1b enhances amyloid precursor protein phosphorylation by JNK and its association with kinesin light chain 1. *J Biol Chem.*, 278(25), 22946-22955.

Iqbal, K., & Grundke-Iqbal, I. (1996). Molecular mechanism of Alzheimer's neurofibrillary degeneration and therapeutic intervention. *Ann N Y Acad Sci.*, 777, 132-138.

Irving, E. A., Barone, F. C., Reith, A. D., Hadingham, S. J., and Parsons, A. A. (2000). Differential activation of MAPK/ERK and p38/SAPK in neurones and glia following focal cerebral ischaemia in the rat. *Brain Res Mol Brain Res.*, 77(1), 65-75.

James, N. D., Davis, D. R., Sindon, J., Hanger, D. P., Brion, J. P., Miller, C. C., Rosenberg, M. P., Anderton, B. H., and Propst, F. (1996). Neurodegenerative changes including altered tau phosphorylation and neurofilament immunoreactivity in mice transgenic for the serine/threonine kinase Mos. *Neurobiol Aging,* 17, 235-241.

Jang, D. H., Han, J. H., Lee, S. H., Lee, Y. S., Park, H., Lee, S. H., Kim, H. , and Kaang, B. K. (2005). Cofilin expression induces cofilin-actin rod formation and disrupts synaptic structure and function in Aplysia synapses. *PNAS U S A.*, 102(44), 16072-16077.

Jhamandas, J. H., Cho, C., Jassar, B., Harris, K., MacTavish, D., and Easaw, J. (2001). Cellular mechanisms for amyloid beta-protein activation of rat cholinergic basal forebrain neurons. *J Neurophysiol.*, 86(3), 1312-1320.

Jick, H., Zornberg, G. L., Jick, S. S., Seshadri, S., and Drachman, D. A. (2000). Statins and the risk of dementia. *Lancet.*, 356(9242), 1627-1631. Erratum in: *Lancet*, 357(9255), 562.

Jin, L. W., Shie, F. S., Maezawa, I., Vincent, I., and Bird, T. (2004). Intracellular accumulation of amyloidogenic fragments of amyloid-beta precursor protein in neurons with Niemann-Pick type C defects is associated with endosomal abnormalities. *Am J Pathol.*, 164(3), 975-985. Erratum in: *Am J Pathol.*, 165(4), 1447.

Kaech, S., Fischer, M., Doll, T., Matus, M. (1997). Isoform specificity in the relationship of actin to dendritic spines. *J Neurosci.*, 17, 9565-95672.

Kamal, A., Almenar-Queralt, A., LeBlanc, J. F., Roberts, E. A., and Goldstein, L. S. (2001). Kinesin-mediated axonal transport of a membrane compartment containing beta-secretase and presenilin-1 requires APP. *Nature.*, 414(6864), 643-648.

Kamal, A., Stokin, G. B., Yang, Z., Xia, C. H., and Goldstein, L. S. (2000). Axonal transport of amyloid precursor protein is mediated by direct binding to the kinesin light chain subunit of kinesin-I. *Neuron.*, 28(2), 449-459.

Kamenetz, F., Tomita, T., Hsieh, H., Seabrook, G., Borchelt, D., Iwatsubo, T., Sisodia, S., and Malinow, R. (2003). APP processing and synaptic function. *Neuron*, 37(6), 925-937.

Kaneko, I., Yamada, N., Sakuraba, Y., Kamenosono, M., and Tutumi, S. (1995). Suppression of mitochondrial succinate dehydrogenase, a primary target of beta-amyloid, and its derivative racemized at Ser residue. *J Neurochem.*, 65, 2585-2593.

Kasa, P., Papp, H., Zombori, J., Mayer, P., and Checler, F. (2003). C-terminal fragments of amyloid-beta peptide cause cholinergic axonal degeneration by a toxic effect rather than by physical injury in the nondemented human brain. *Neurochem Res.*, 28(3-4), 493-498.

Kato, T., Hashikabe, H., Iwata, C., Akimoto, K., and Hattori, Y. (2004). Statin blocks Rho/Rho-kinase signalling and disrupts the actin cytoskeleton: relationship to enhancement of LPS-mediated nitric oxide synthesis in vascular smooth muscle cells. *Biochim Biophys Acta.*, 1689(3), 267-272.

Kawarabayashi, T., Shoji, M., Yamaguchi, H., Tanaka, M., Harigaya, Y., Ishiguro, K., and Hirai, S. (1993). Amyloid beta protein precursor accumulates in swollen neurites throughout rat brain with aging. *Neurosci Lett.*, 153(1),73-76.

Kayed, R., Head, E., Thompson, J. L., McIntire, T. M., Milton, S. C., Cotman, C. W., and Glabe, C. G. (2003). Common structure of soluble amyloid oligomers implies common mechanism of pathogenesis. *Science,* 300, 486-489.

Kim, H. J., Chae, S. C., Lee, D. K., Chromy, B., Lee, S. C., Park, Y. C., Klein, W. L., Krafft, G. A., and Hong S. T., (2003). Selective neuronal degeneration induced by soluble oligomeric amyloid beta protein. *Faseb J.*, 17, 118-120.

Kim, T. W., & Tanzi, R. E. (1997). Presenilins and Alzheimer's disease. *Curr Opin Neurobiol.*, 7, 683-688.

Klyubin, I., Walsh, D. M., Lemere, C. A., Cullen, W. K., Shankar, G. M., Betts, V., Spooner, E. T., Jiang, L., Anwyl, R., Selkoe, D. J, and Rowan, M. J. (2005). Amyloid beta protein immunotherapy neutralizes Abeta oligomers that disrupt synaptic plasticity in vivo. *Nat Med.,* 11(5), 556-561.

Knebl, J., DeFazio, P., Clearfield, M. B., Little, L., McConathy, W. J., McPherson, R., and Lacko, A. G. (1994). Plasma lipids and cholesterol esterification in Alzheimer's disease. *Mech Ageing Dev.*, 73(1), 69-77.

Koistinaho, M., & Koistinaho, J. (2002). Role of p38 and p44/42 mitogen-activated protein kinases in microglia. *Glia*, 40(2), 175-183.

Kojro, E., Gimpl, G., Lammich, S., Marz, W., and Fahrenholz, F. (2001). Low cholesterol stimulates the nonamyloidogenic pathway by its effect on the alpha - secretase ADAM 10. *PNAS U S A.*, 98(10), 5815-5820.

Kondo, T., Shirasawa, T., Itoyama, Y., and Mori, H. (1996). Embryonic genes expressed in Alzheimer's disease brains. *Neurosci Lett.*, 209(3), 157-160.

Koo, E. H., & Squazzo, S. L. (1994). Evidence that production and release of amyloid beta-protein involves the endocytic pathway. *J Biol Chem,* 269, 17386-17389.

Korn, E. (1982). Actin polymerization and its regulation by proteins from non-muscle cells. *Physio. Rev.,* 62, 672-737.

Koya, R. C., Fujita, H., Shimizu, S., Ohtsu, M., Takimoto, M., Tsujimoto, Y. and Kuzumaki, N. (2000). Human gelsolin prevents apoptosis by inhibiting apoptotic mitochondrial changes via closing VDAC. *Oncogene*, 19, 4807-4814.

Kuhn, T. B., Meberg P. J., Brown, M. D., Bernstein, B. W., Minamide, L. S., Jensen, J. R., Okada, K., Soda, E. A., and Bamburg, J. R. (2000). Regulating actin filament dynamics in neuronal growth cones by ADF/cofilin and Rho family GTPases. *J Neurobiology,* 44, 126-144.

Kusanno, H., Schimuzu, S., Koya, R. C., Fujita, H., Kamada, S., Kuzumaki, N., and Tsujimoto, Y. (2000). Gelsolin inhibits apoptosis by blocking mitochondrial membrane potential loss and cytochrome c release. *J Biol Chem.*, 275, 15343-15349.

Lacor, P. N., Buniel, M. C., Chang, L. , Fernandez, S. J., Gong, Y., Viola, K. L., Lambert, M. P., Velasco, P. T., Bigio, E. H., Finch, C. E., Krafft, G. A., and Klein, W. L. (2004). Synaptic targeting by Alzheimer's-related amyloid beta oligomers. *J Neurosci.*, 24(45), 10191-10200.

LaLonde, D. P., Brown, M. C., Bouverat, B. P., and Turner, C. E. (2005). Actopaxin interacts with TESK1 to regulate cell spreading on fibronectin. *J Biol Chem.*, 280(22), 21680-21688.

Lambert, M.P., Barlow, A. K., Chromy, B. A., Edwards, C., Freed, R., Liosatos, M., Morgan, T. E., Rozovsky, I., Trommer, B., Viola, K. L., Wals, P., Zhang, C., Finch, C. E., Krafft, G. A., and Klein, W. L. (1998). Diffusible, nonfibrillar ligands derived from Abeta1-42 are potent central nervous system neurotoxins. *Proc Natl Acad Sci U S A.*, 95, 6448-6453.

Lancelot, E., & Beal, M. F. (1998). Glutamate toxicity in chronic neurodegenerative disease. *Prog Brain Res.*, 116, 331-347. Review.

Lappalainen, P., Federov, E., Federov, A., Almo, S. and Drubin, D. (1997). Essential functions and actin-binding surfaces of yeast cofilin revealed by systematic mutagenesis. *EMBO J.*, 16, 5520-5530.

Lee, J. P., Stimson, E. R., Ghilardi, J. R., Mantyh, P. W., Lu, Y. A., Felix, A. M., Llanos, W., Behbin, A., Cummings, M., Van Criekinge, M., et al. (1995). 1H NMR of A beta amyloid peptide congeners in water solution. Conformational changes correlate with plaque competence. *Biochemistry,* 34, 5191-5200.

Lee, K. S., Brooks, P., and Lowenkopf, T. (1991). Transient ischemia attenuates neuronal afterdischarges induced in the absence of synaptic transmission. *Brain Res.*, 553(1), 171-174.

Lenaz, G. (1998). Role of mitochondria in oxidative stress and ageing. *Biochim Biophys Acta.*, 1366, 53-67.

Levy-Lahad, E., Wasco, W., Poorkaj, P., Romano, D. M., Oshima, J., Pettingell, W. H., Yu, C. E., Jondro, P. D., Schmidt, S. D., Wang, K. et al. (1995). Candidate gene for the chromosome 1 familial Alzheimer's disease locus. *Science,* 269, 973-977.

Li, F., Chong, Z. Z., and Maiese, K. (2006). Winding through the WNT pathway during cellular development and demise. *Histol Histopathol.*, 21(1), 103-124. Review.

Li, L., Darden, T. A., Bartolotti, L, Kominos, D., and Pedersen, L. G. (1999). An atomic model for the pleated beta-sheet structure of Abeta amyloid protofilaments. *Biophys J.*, 76, 2871-2878.

Lim, G. P., Calon, F., Morihara, T., Yang, F., Teter, B., Ubeda, O., Salem, N., Jr., Frautschy, S. A., and Cole, G. M. (2005). A diet enriched with the omega-3 fatty acid docosahexaenoic acid reduces amyloid burden in an aged Alzheimer mouse model. *J Neurosci,* 25, 3032-3040.

Loo, D. T., Copani, A., Pike, C. J., Whittemore, E. R., Walencewicz, A. J., and Cotman, C. W. (1993). Apoptosis is induced by beta-amyloid in cultured central nervous system neurons. *Proc Natl Acad Sci U S A.*, 90(17), 7951-7955.

Lovell, M. A., Xiong, S., Markesbery, W. R., and Lynn, B. C. (2005). Quantitative proteomic analysis of mitochondria from primary neuron cultures treated with amyloid beta peptide. *Neurochem Res.*, 30(1), 113-122.

Lue, L. F., Kuo, Y. M., Roher, A. E., Brachova, L, Shen, Y., Sue, L, Beach, T., Kurth, J. H., Rydel, R. E., and Rogers, J. (1999). Soluble amyloid beta peptide concentration as a predictor of synaptic change in Alzheimer's disease. *Am J Pathol.*, 155, 853-862.

Lushnikova, I. V., Voronin, K. Y., Malyarevskyy, P. Y., and Skibo, G. G. (2004). Morphological and functional changes in rat hippocampal slice cultures after short-term oxygen-glucose deprivation. *J Cell Mol Med.*,8(2), 241-248.

Lustbader, J. W., Cirilli, M., Lin, C., Xu, H. W., Takuma, K., Wang, N., Caspersen, C., Chen, X., Pollak, S., Chaney, M., Trinchese, F., Liu, S., Gunn-Moore, F., Lue, L. F., Walker, D. G., Kuppusamy, P., Zewier, Z. L., Arancio, O., Stern, D., Yan, S. S., and Wu, H. (2004). ABAD directly links Abeta to mitochondrial toxicity in Alzheimer's disease. *Science,* 304, 448-452.

Maciver, S. K., &Harrington, C. R. (1995). Two actin binding proteins, actin depolymerizing factor and cofilin, are associated with Hirano bodies. Neuroreport, 6, 1985-1988.

Maloney, M. T., Kinley, A. W., Pak, C. W., and Bamburg, J. R. (2006). ADF/cofilin, Actin Dynamics and Disease in "Disorders Caused by Actin and Actin-binding Proteins" Cris dos Remedos and Deepak Chhabra (Eds.), Wiley, New York, (in press).

Maloney, M. T., Minamide, L. S., Kinley, A. K., Boyle, J. A., and Bamburg, J. R. (2005). βeta-secretase-cleaved amyloid precursor protein accumulates at actin inclusions induced in neurons by stress or amyloid beta: a feedforward mechanism for Alzheimer's disease. *J Neurosci.,* 25(49), 11313-11321.

Mann, D. M., Yates, P. O., and Marcyniuk, B. (1984). Alzheimer's presenile dementia, senile dementia of Alzheimer type and Down's syndrome in middle age form an age related continuum of pathological changes. *Neuropathol Appl Neurobiol.*, 10(3), 185-207.

Mann, G., (1894). Histochemical changes induced in sympathetic, motor, and sensory nerve cells by functional activity. *J Anat Physiol. London*, 19, 100-108.

Mark, R. J., Hensley, K., Butterfield, D. A., and Mattson, M. P. (1995). Amyloid beta-peptide impairs ion-motive ATPase activities: evidence for a role in loss of neuronal Ca2+ homeostasis and cell death. *J Neurosci.*, 15, 6239-6249.

Marshall, C. J. (1994). MAP kinase kinase kinase, MAP kinase kinase and MAP kinase. *Curr Opin Genet Dev.*, 4(1), 82-89.

Marshall, C. J. (1995). Specificity of receptor tyrosine kinase signaling: transient versus sustained extracellular signal-regulated kinase activation. *Cell*, 80(2), 179-185.

Masliah, E. (2000). The role of synaptic proteins in Alzheimer's disease. *Ann N Y Acad Sci.*, 924, 68-75. Review.

Matsuda, S., Matsuda, Y., and D'Adamio, L. (2003). Amyloid beta protein precursor (AbetaPP), but not AbetaPP-like protein 2, is bridged to the kinesin light chain by the scaffold protein JNK-interacting protein 1. *J Biol Chem.*, 278(40), 38601-38606.

Mattila, P. K., Quintero-Monzon, O., Kugler, J., Moseley, J. B., Almo, S. C., Lappalainen, P., and Goode, B. L. (2004). A high-affinity interaction with ADP-actin monomers underlies the mechanism and in vivo function of Srv2/cyclase-associated protein. *Mol Biol Cell*, 15(11), 5158-5171.

Mattson, M. P. (2004). Pathways towards and away from Alzheimer's disease. *Nature,* 430, 631-639.

Mattson, M. P., & Kater, S. B. (1988). Isolated hippocampal neurons in cryopreserved long-term cultures: development of neuroarchitecture and sensitivity to NMDA. Int J Dev *Neurosci,* 6, 439-452.

Mattson, M.P., Cheng, B., Davis, D., Bryant, K., Lieberburg, I., and Rydel, R. E. (1992). beta-Amyloid peptides destabilize calcium homeostasis and render human cortical neurons vulnerable to excitotoxicity. *J Neurosci.*, 12, 376-389.

McGough, A., Pope, B., Chiu, W., and Weeds, A. (1997). Cofilin changes the twist of F-actin: implications for actin filament dynamics and cellular function. *JCell Biol.*, 138, 771-781.

McLean, C.A., Cherny, R. A., Fraser, F. W., Fuller, S. J., Smith, M. J., Beyreuther, K., Bush, A.I., and Masters, C. L. (1999). Soluble pool of Abeta amyloid as a determinant of severity of neurodegeneration in Alzheimer's disease. *Ann Neurol.*, 46, 860-866.

Meberg, P. J., & Bamburg, J. R. (2000). Increase in neurite outgrowth mediated by overexpression of actin depolymerizing factor. *J Neurosci*, 20, 2459-2469.

Meberg, P. J., & Miller, M. W. (2003). Culturing hippocampal and cortical neurons. *Methods Cell Biol,* 71, 111-127.

Meberg, P. J., Ono, S., Minamide, L. S., Takahashi, M., and Bamburg, J. R. (1998). Actin depolymerizing factor and cofilin phosphorylation dynamics: response to signals that regulate neurite extension. *Cell Motil Cytoskeleton,* 39, 172-190.

Meng, Y., Zhang, Y., Tregoubov, V., Janus, C., Cruz, L., Jackson, M., Lu, W. Y., MacDonald, J. F., Wang, J. Y., Falls, D. L., and Jia, Z. (2002). Abnormal spine morphology and enhanced LTP in LIMK-1 knockout mice. *Neuron.*, 35(1), 121-133.

Minamide, L.S., Striegl, A. S., Boyle, J. A., Meberg, P. J., and Bamburg, J. R. (2000). Neurodegenerative stimuli induce persistent ADF/cofilin-actin rods that disrupt distal neurite function. *Nat Cell Biol.*, 2, 628-636.

Morgan, T.E., Lockerbie, R. O., Minamide, L. S., Browning, M. D., and Bamburg, J. R. (1993). Isolation and characterization of a regulated form of actin depolymerizing factor. *J Cell Biol.*, 122, 623-633.

Moriyama, K., Iida, K., and Yahara, I. (1996). Phosphorylation of Ser-3 of cofilin regulates its essential function on actin. *Genes Cells.*, 1(1), 73-86.

Moriyama, K., Yonezawa, N., Sakui, H., Yahara, I., and Nishida, E. (1992). Mutational analysis of an actin-binding site of cofilin and characterization of chimeric proteins between cofilin and destrin. *J Biol Chem.*, 267, 7240-7244.

Mucke, L., Masliah, E., Yu, G. Q., Mallory, M., Rockenstein, E. M., Tatsuno, G., Hu, K., Kholodenko, D., Johnson-Wood, K., and McConlogue, L. (2000). High-level neuronal expression of abeta 1-42 in wild-type human amyloid protein precursor transgenic mice: synaptotoxicity without plaque formation. *J Neurosci.*, 20(11), 4050-4058.

Mufson, E. J., Bothwell, M., and Kordower, J. H. (1989). Loss of nerve growth factor receptor-containing neurons in Alzheimer's disease: a quantitative analysis across subregions of the basal forebrain. *Exp Neurol.*, 105(3), 221-232.

Murrell, J., Farlow, M., Ghetti, B., and Benson, M. D. (1991). A mutation in the amyloid precursor protein associated with hereditary Alzheimer's disease. *Science,* 254, 97-99.

Nagata-Ohashi, K., Ohta, Y., Goto, K., Chiba, S., Mori, R., Nishita, M., Ohashi, K., Kousaka, K., Iwamatsu, A., Niwa, R., Uemura, T., and Mizuno, K. (2004). A pathway of neuregulin-induced activation of cofilin-phosphatase Slingshot and cofilin in lamellipodia. *J Cell Biol.*, 165(4), 465-471.

Nicholls, D.G., & Budd, S. L. (1998). Mitochondria and neuronal glutamate excitotoxicity. *Biochim Biophys Acta.*, 1366, 97-112.

Nikolic, M., Chou, M. M., Lu, W., Mayer, B. J., and Tsai, L. H. (1998). The p35/Cdk5 kinase is a neuron-specific Rac effector that inhibits Pak1 activity. *Nature*, 395(6698), 194-198.

Nishida, E. (1984). Actin-regulatory proteins--regulators of cytoskeleton. *Seikagaku.*, 56, 1251-1265.

Nishida, E., Iida, K., Yonezawa, N., Koyasu, S., Yahara, I., and Sakai, H. (1987). Cofilin is a component of intranuclear and cytoplasmic actin rods induced in cultured cells. *Proc Natl Acad Sci U S A.*, 84, 5262-5266.

Niwa, R., Nagata-Ohashi, K., Takeichi, M., Mizuno, K., Uemura, T. (2002). Control of Actin Reorganization by Slingshot, a family of phosphatases that dephosphorylate ADF/Cofilin. *Cell,* 108, 233-246.

Nixon, R. A. (2005). Endosome function and dysfunction in Alzheimer's disease and other neurodegenerative diseases. *Neurobiol Aging,* 26, 373-382.

Ohm, T. G., Treiber-Held, S., Distl, R., Glockner, F., Schonheit, B., Tamanai, M., and Meske, V. (2003). Cholesterol and tau protein--findings in Alzheimer's and Niemann Pick C's disease. *Pharmacopsychiatry*, 36 Suppl 2, S120-S126.

Ohta, Y., Nishida, E., Sakai, H., and Miyamoto, E. (1989). Dephosphorylation of cofilin accompanies heat shock-induced nuclear accumulation of cofilin. *J Biol Chem.*, 264(27), 16143-16148.

Ono, S., Abe, H., Nagaoka, R., and Obinata, T. (1993). Colocalization of ADF and cofilin in intranuclear actin rods of cultured muscle cells. *J Muscle Res Cell Motil.*, 14(2), 195-204.

Ono, S., McGough, A., Pope, B., Tolbert, V., Bui, A., Pohl, J., Benian, G., Gernert, K., and Weeds, A. (2001). The C-terminal tail of UNC-60B (actin depolymerizing factor/cofilin) is critical for maintaining its stable association with F-actin and is implicated in the second actin-binding site. *J Biol Chem.*, 276(8), 5952-5958.

Ostrowski, M., Grzanka, A., and Izdebska, M. (2005). The role of actin in Alzheimer's disease. *Postepy Hig Med Dosw.*, 3,59, 224-228. (Abstract)

Paavilainen, V. O., Bertling, E., Falck, S., and Lappalainen, P. (2004). Regulation of cytoskeletal dynamics by actin-monomer-binding proteins. *Trends Cell Biol.*, 14(7), 386-394. Review.

Papp, H., Pakaski, M., and Kasa, P. (2002). Presenilin-1 and the amyloid precursor protein are transported bidirectionally in the sciatic nerve of adult rat. *Neurochem Int.*, 41(6), 429-435.

Pedrini, S., Carter, T. L., Prendergast, G., Petanceska, S., Ehrlich, M. E., and Gandy, S. (2005). Modulation of statin-activated shedding of Alzheimer APP ectodomain by ROCK. *PLoS Med.*, 2(1):e18. (*in press*).

Perini, G., Della-Bianca, V., Politi, V., Della valle, G., Dal-Pra, I., Rossi, F., and Armato, U. (2002). Role of p75 neurotrophin receptor in the neurotoxicity by beta-amyloid peptides and synergistic effect of inflammatory cytokines. *J Exp Med,* 195, 907-918.

Petkova, A.T., Y. Ishii, J.J. Balbach, O.N. Antzutkin, R.D. Leapman, F. Delaglio, and R. Tycko. 2002. A structural model for Alzheimer's beta -amyloid fibrils based on experimental constraints from solid state NMR. *Proc Natl Acad Sci U S A.* 99:16742-7. Epub 2002 Dec 12.

Pike, C. J., Burdick, D., Walencewicz, A. J., Glabe, C. G., and Cotman, C. W. (1993). Neurodegeneration induced by beta-amyloid peptides in vitro: the role of peptide assembly state. *J Neurosci.*, 13, 1676-1687.

Pike, C. J., Cummings, B. J., and Cotman, C. W. (1992). beta-Amyloid induces neuritic dystrophy in vitro: similarities with Alzheimer pathology. *Neuroreport.*, 3, 769-772.

Pike, C. J., Cummings, B. J., and Cotman, C. W. (1995a). Early association of reactive astrocytes with senile plaques in Alzheimer's disease. *Exp Neurol.*, 132, 172-179.

Pike, C. J., Overman, M. J., and Cotman, C. W. (1995b). Amino-terminal deletions enhance aggregation of beta-amyloid peptides in vitro. *J Biol Chem.*, 270, 23895-23898.

Pike, C. J., Walencewicz, A. J., Glabe, C. G., and Cotman, C. W. (1991a). Aggregation-related toxicity of synthetic beta-amyloid protein in hippocampal cultures. *Eur J Pharmacol.*, 207, 367-368.

Pike, C. J., Walencewicz, A. J., Glabe, C. G., and Cotman, C. W. (1991b). In vitro aging of beta-amyloid protein causes peptide aggregation and neurotoxicity. *Brain Res.*, 563, 311-314.

Podlisny, M. B., Ostaszewski, B. L., Squazzo, S. L., Koo, E. H., Rydell, R. E., Teplow, D. B., and Selkoe, D. J. (1995). Aggregation of secreted amyloid beta-protein into sodium dodecyl sulfate-stable oligomers in cell culture. *J Biol Chem.*, 270(16), 9564-9570.

Pollard, T. D., Blanchoin, L., and Mullins, R. D. (2005). Molecular mechanisms controlling actin filament dynamics in nonmuscle cells. *Annu Rev Biophys Biomol Struct.*, 29, 545-576. Review.

Prasher, V. P., Farrer, M. J. Kessling, A. M., Fisher, E. M. West, R. J., Barber, P. C., and Butler, A. C. (1998). Molecular mapping of Alzheimer-type dementia in Down's syndrome. *Ann Neurol.*, 43(3), 380-383.

Price, D. L., Sisodia, S. S., and Gandy, S. E. (1995). Amyloid beta amyloidosis in Alzheimer's disease. *Curr Opin Neurol,* 8, 268-274.

Racchi, M., Baetta, R., Salvietti, N., Ianna, P., Franceschini, G., Paoletti, R., Fumagalli, R., Govoni, S., Trabucchi, M., and Soma, M. (1997). Secretory processing of amyloid precursor protein is inhibited by increase in cellular cholesterol content. *Biochem J.*, 322 (Pt 3), 893-898.

Rami, A., Jansen, S., Giesser, I.., and Winckler, J. (2003). Post-ischemic activation of caspase-3 in the rat hippocampus: evidence of an axonal and dendritic localisation. *Neurochem Int.,* 43(3), 211-223.

Rapoport, M., & Ferreira, A. (2000). PD98059 prevents neurite degeneration induced by fibrillar beta-amyloid in mature hippocampal neurons. *J Neurochem.*, 74(1), 125-133.

Renbaum, P., & Levy-Lahad, E. (1998). Monogenic determinants of familial Alzheimer's disease: presenilin-2 mutations. *Cell Mol Life Sci.*, 54(9), 910-919. Review.

Richardson, J.S. (1997). Cerebral microischemia as a potential precipitant of the neurodegenerative cascade of Alzheimer's disease. *Ann N Y Acad Sci.*, 826, 437-439.

Riddell, D. R., Christie, G., Hussain, I., and Dingwall, C. (2001). Compartmentalization of beta-secretase (Asp2) into low-buoyant density, noncaveolar lipid rafts. *Curr Bio.*, 11(16), 1288-1293.

Ridley, A. J. (2001). Rho proteins: linking signaling with membrane trafficking. *Traffic.*, 2(5), 303-310. Review.

Roberts, G. W., Gentleman, S. M., Lynch, A., Murray, L., Landon, M., and Graham, D. I. (1994). Beta amyloid protein deposition in the brain after severe head injury: implications for the pathogenesis of Alzheimer's disease. *J Neurol Neurosurg Psychiatry*, 57(4), 419-425.

Rockwood, K., Kirkland, S., Hogan, D. B., MacKnight, C., Merry, H., Verreault, R., Wolfson, C., and McDowell, I. (2002). Use of lipid-lowering agents, indication bias, and the risk of dementia in community-dwelling elderly people. *Arch Neurol.*, 59(2), 223-227.

Rogaev, E. I., Sherrington, R., Rogaeva, E. A., Levesque, G., Ikeda, M., Liang, Y., Chi, H., Lin, C., Holman, K., Tsuda, T. et al. (1995). Familial Alzheimer's disease in kindreds with missense mutations in a gene on chromosome 1 related to the Alzheimer's disease type 3 gene. *Nature,* 376, 775-778.

Rossiter, J. P., Anderson, L. L., Yang, F., and Cole, G. M. (2000). Caspase-cleaved actin (fractin) immunolabelling of Hirano bodies. *Neuropathol Appl Neurobiol.*, 26(4), 342-346.

Runz, H., Rietdorf, J., Tomic, I., de Bernard, M., Beyreuther, K., Pepperkok, R., and Hartmann, T. (2002). Inhibition of intracellular cholesterol transport alters presenilin localization and amyloid precursor protein processing in neuronal cells. *J Neurosci.*, 22(5), 1679-1689.

Russ, C., Lovestone, S., and Powell, J. F. (2002). Identification of genomic organisation, sequence variants and analysis of the role of the human dishevelled 1 gene in late onset Alzheimer's disease. *Mol Psychiatry*, 7(1), 104-109.

Ryder, J., Su, Y., Liu, F., Li, B., Zhou, Y., and Ni, B. (2003). Divergent roles of GSK3 and CDK5 in APP processing. *Biochem Biophys Res Commun.*, 312(4), 922-929.

Sameshima, M., Kishi, Y., Osumi, M., Mahadeo, D., and Cotter, D. A. (2000). Novel actin cytoskeleton: actin tubules. *Cell Struct Funct.*, 25(5), 291-295.

Saunders, A. J., K, T.-W., Tanzi, R. E., Fan, W., Bennett, B. D., Babu-Kahn, S., Lou, Y., Louis, J.-C., McCaleb, M., Citron, M., Vassar, R., and G, R. W. (1999). BACE maps to Chromosome 11 and BACE Homolog, BACE2, Reside in the Obligate Down Syndrome Region of Chromosome 21. *Science,* 286.

Sawamura, N., Morishima-Kawashima, M., Waki, H., Kobayashi, K., Kuramochi, T., Frosch, M. P., Ding, K., Ito, M., Kim, T. W., Tanzi, R. E., Oyama, F., Tabira, T., Ando, S., and Ihara, Y. (2000). Mutant presenilin 2 transgenic mice. A large increase in the levels of Abeta 42 is presumably associated with the low density membrane domain that contains decreased levels of glycerophospholipids and sphingomyelin. *J Biol Chem.*, 275(36), 27901-27908.

Schenk, D., Barbour, R., Dunn, W., Gordon, G., Grajeda, H., Guido, T., Hu, K., Huang, J., Johnson-Wood, K., Khan, K., Kholodenko, D., Lee, M., Liao, Z., Lieberburg, I., Motter, R., Mutter, L., Soriano, F., Shopp, G., Vasquez, N., Vandevert, C., Walker, S., Wogulis, M., Yednock, T., Games, D., and Seubert, P. (1999). Immunization with amyloid-beta attenuates Alzheimer-disease-like pathology in the PDAPP mouse. *Nature*, 400(6740), 173-177.

Selkoe, D. J. (2001). Presenilin, Notch, and the genesis and treatment of Alzheimer's disease. *Proc Natl Acad Sci U S A.*, 98(20), 11039-11041. Review.

Sheng, J. G., Price, D.L., and Koliatsos, V. E. (2003). The beta-amyloid-related proteins presenilin 1 and BACE1 are axonally transported to nerve terminals in the brain. *Exp Neurol.*, 184(2), 1053-1057.

Sherrington, R., Rogaev, E. I., Liang, Y., Rogaeva, E. A., Levesque, G., Ikeda, M., Chi, H., Lin, C., Li, G., Holman, K. et al. (1995). Cloning of a gene bearing missense mutations in early-onset familial Alzheimer's disease. *Nature,* 375, 754-760.

Simons, M., Keller, P., De Strooper, B., Beyreuther, K., Dotti, C. G., and Simons, K. (1998). Cholesterol depletion inhibits the generation of beta-amyloid in hippocampal neurons. *PNAS U S A.*, 95(11), 6460-6464.

Sisodia, S. S., & Price, D. L. (1995). Role of the beta-amyloid protein in Alzheimer's disease. *FASEB J*, 9, 366-370.

Smith, D.H., Chen, X. H., Iwata, A., and Graham, D. I. (2003). Amyloid beta accumulation in axons after traumatic brain injury in humans. *J Neurosurg.*, 98(5), 1072-1077.

Smith, M. A., Sayre, L. M., Anderson, V. E., Harris, P. L., Beal, M. F., Kowall, N. K., and Perry, G. (1998). Cytochemical demonstration of oxidative damage in Alzheimer disease by immunochemical enhancement of the carbonyl reaction with 2,4-dinitrophenylhydrazine. *J Histochem Cytochem.*, 46, 731-735.

Sofroniew, M. V., Howe, C. L., and Mobley, W. C. (2001). Nerve growth factor signaling, neuroprotection, and neural repair. *Annu Rev Neurosci.*, 24, 1217-1281. Review.

Soosairajah, J., Maiti, S., Wiggan, O., Sarmiere, P., Moussi, N., Sarcevic, B., Sampath, R., Bamburg, J. R., and Bernard, O. (2005). Interplay between components of a novel LIM kinase-slingshot phosphatase complex regulates cofilin. *EMBO J.*, 24(3), 473-486.

Strasser, U., & Fischer, G. (1995). Quantitative measurement of neuronal degeneration in organotypic hippocampal cultures after combined oxygen/glucose deprivation. *J Neurosci Methods.* 57(2), 177-186.

Stine, W. B., Jr., Dahlgren, K. N., Krafft, G. A., and LaDu, M. J. (2003). In vitro characterization of conditions for amyloid-beta peptide oligomerization and fibrillogenesis. *J Biol Chem*, 278, 11612-11622.

Stokin, G. B., & Goldstein, L. S. (2006). Linking molecular motors to Alzheimer's disease. *J Physiol Paris.*, 99(2-3), 193-200.

Stokin, G. B., Lillo, C., Falzone, T. L., Brusch, R. G., Rockenstein, E., Mount, S. L., Raman, R., Davies, P., Masliah, E., Williams, D. S., and Goldstein, L. S. (2005). Axonopathy and transport deficits early in the pathogenesis of Alzheimer's disease. *Science,* 307, 1282-1288.

Stoppini, L., Buchs, P. A., and Muller, D. (1991). A simple method for organotypic cultures of nervous tissue. *J Neurosci Methods*, 37(2), 173-182.

Sugden, P. H., & Clerk, A. (1997). Regulation of the ERK subgroup of MAP kinase cascades through G protein-coupled receptors. *Cell Signal.*, 9(5), 337-351.

Sutton, K., & Mabuchi, I., (1989). End-label fingerprintings show that an N-terminal segment of depactin participates in interaction with actin. *Biochemistry*, 28(1), 102-106.

Swerdlow, R. H., & Kish, S. J. (2002). Mitochondria in Alzheimer's disease. *Int Rev Neurobiol.*, 53, 341-385. Review.

Takahashi, R. H., Almeida, C. G., Kearney, P. F., Yu, F., Lin, M. T., Milner, T. A., and Gouras, G. K. (2004). Oligomerization of Alzheimer's beta-amyloid within processes and synapses of cultured neurons and brain. *J Neurosci,* 24, 3592-3599.

Tanzi, R. E., & Bertram, L. (2005). Twenty years of the Alzheimer's disease amyloid hypothesis: a genetic perspective. *Cell,* 120, 545-555.

Taru, H., Iijima, K., Hase, M., Kirino, Y., Yagi, Y., and Suzuki, T. (2002). Interaction of Alzheimer's beta -amyloid precursor family proteins with scaffold proteins of the JNK signaling cascade. *J Biol Chem.*, 277(22), 20070-20078.

Terry, R. D., Masliah, E., Salmon, D. P., Butters, N., DeTeresa, R., Hill, R., Hansen, L. A., and Katzman, R. (1991). Physical basis of cognitive alterations in Alzheimer's disease: synapse loss is the major correlate of cognitive impairment. *Ann Neurol.*, 30, 572-580.

Tikka, T. M., & Koistinaho, J. E. (2001). Minocycline provides neuroprotection against N-methyl-D-aspartate neurotoxicity by inhibiting microglia. *J Immunol.*, 166(12), 7527-7533.

Torok, M., Milton, S. Kayed, R., Wu, P., McIntire, T., Glabe, C. G., and Langen, R. (2002). Structural and dynamic features of Alzheimer's Abeta peptide in amyloid fibrils studied by site-directed spin labeling. *J Biol Chem.*, 277, 40810-40815.

Toshima, J., Ohashi, K., Okano, I., Nunoue, K., Kishioka, M., Kuma, K., Miyata, T., Hirai, M., Baba, T., and Mizuno, K. (1995). Identification and characterization of a novel protein kinase, TESK1, specifically expressed in testicular germ cells. *J Biol Chem.*, 270(52), 31331-31337.

Toshima, J., Toshima, J. Y., Amano, T., Yang, N., Narumiya, S., and Mizuno, K. (2001). Cofilin phosphorylation by protein kinase testicular protein kinase 1 and its role in integrin-mediated actin reorganization and focal adhesion formation. *Mol Biol Cell.*, 12(4), 1131-1145.

Tsuda, T., Chi, H., Liang, Y., Rogaeva, E. A., Sherrington, R., Levesque, G., Ikeda, M., Rogaev, E. I., Pollen, D., Freedman, M., et al. (1995). Failure to detect missense mutations in the S182 gene in a series of late-onset Alzheimer's disease cases. *Neurosci Lett.*, 201, 188-190.

Tsujimoto, Y. & Shimizu, S. (2000). The voltage-dependent anion channel: an essential player in apoptosis. *Biochimie*, 84, 187-193.

Ueda, K., Shinohara, S., Yagami, T., Asakura, K., and Kawasaki, K. (1997). Amyloid beta protein potentiates Ca2+ influx through L-type voltage-sensitive Ca2+ channels: a possible involvement of free radicals. *J Neurochem.*, 68, 265-271.

Valentim, L. M., Rodnight, R., Geyer, A. B., Horn, A. P., Tavares, A., Cimarosti, H., Netto, C. A., and Salbego, C. G. (2003). Changes in heat shock protein 27 phosphorylation and immunocontent in response to preconditioning to oxygen and glucose deprivation in organotypic hippocampal cultures. *Neuroscience*, 118(2), 379-386.

Vetrivel, K. S., & Thinakaran, G. (2006). Amyloidogenic processing of beta-amyloid precursor protein in intracellular compartments. *Neurology.*, 66(2 Suppl 1), S69-S73. Review.

Vetrivel, K. S., Cheng, H., Lin, W., Sakurai, T., Li, T., Nukina, N., Wong, P. C., Xu, H., and Thinakaran, G. (2004). Association of gamma-secretase with lipid rafts in post-Golgi and endosome membranes. *J Biol Chem.*, 279(43), 44945-44954.

Vicent, D., Maratos-Flier, E., and Kahn, C. R. (2000). The branch point enzyme of the mevalonate pathway for protein prenylation is overexpressed in the ob/ob mouse and induced by adipogenesis. *Mol Cell Biol.*, 20(6), 2158-2166.

Walsh, D.M., Hartley, D. M., Kusumoto, Y. K., Fezoui, Y., Condron, M. M., Lomakin, A., Benedek, G. B., Selkoe, D. J., and Teplow, D. B. (1999). Amyloid beta-protein fibrillogenesis. Structure and biological activity of protofibrillar intermediates. *J Biol Chem.*, 274, 25945-25952.

Walsh, D. M., Klyubin, I., Fadeeva, J. V., Cullen, W. K., Anwyl, R., Wolfe, M. S., Rowan, M. J., and Selkoe, D. J. (2002a). Naturally secreted oligomers of amyloid beta protein potently inhibit hippocampal long-term potentiation in vivo. *Nature*, 416, 535-539.

Walsh, D. M., Klyubin, I., Fadeeva, J. V., Rowan, M. J., and Selkoe, D. J. (2002b). Amyloid-beta oligomers: their production, toxicity and therapeutic inhibition. *Biochem Soc Trans,* 30, 552-557.

Walsh, D. M., Klyubin, I., Shankar, G. M., Townsend, M., Fadeeva, J. V., Betts, V., Podlisny, M. B., Cleary, J. P., Ashe, K. H., Rowan, M. J., and Selkoe, D. J. (2005). The role of cell-derived oligomers of Abeta in Alzheimer's disease and avenues for therapeutic intervention. *Biochem Soc Trans.*, 33(Pt 5), 1087-1090.

Wang, H. W., Pasternak, J. F., Kuo, H., Ristic, H., Lambert, M. P., Chromy, B., Viola, K. L., Klein, W. L., Stine, W. B., Krafft, G. A., and Trommer, B. L. (2002). Soluble oligomers of beta amyloid (1-42) inhibit long-term potentiation but not long-term depression in rat dentate gyrus. *Brain Res.*, 924(2), 133-140.

Wang, Y., Shibasaki, F., and Mizuno, K. (2005). Calcium signal-inducing dephosphorylation is mediated by Slingshot via calcineurin. *J Biol Chem.*, 280(13), 12683-12689.

Wegner, A. (1976). Head to tail polymerization of actin. *J Mol Biol.,* 108, 139-150.

Whitehouse P. J., Struble, R. G., Clark, A. W., and Price, D. L. (1982). Alzheimer disease: plaques, tangles, and the basal forebrain. Ann Neurol., 12(5), 494.

Wisniewski, H. M., & Wegiel, J. (1992). Alzheimer's disease neuropathology. Current status of interpretation of lesion development. *Ann N Y Acad Sci.*, 673, 270-284.

Wolfe, M. S., De Los Angeles, J., Miller, D. D., Xia, W., and Selkoe, D. J. (1999). Are presenilins intramembrane-cleaving proteases? Implications for the molecular mechanism of Alzheimer's disease. *Biochemistry*, 38(35), 11223-11230. Review.

Wolozin, B., Kellman, W., Ruosseau, P., Celesia, G. G., and Siegel, G. (2000). Decreased prevalence of Alzheimer disease associated with 3-hydroxy-3-methyglutaryl coenzyme A reductase inhibitors. *Arch Neurol.*, 57(10), 1439-1443.

Wu, D. C., Ye, W., Che, X. M., and Yang, G. Y. (2000). Activation of mitogen-activated protein kinases after permanent cerebral artery occlusion in mouse brain. *J Cereb Blood Flow Metab.*, 20(9), 1320-1330.

Xu, G. P., Dave, K. R., Vivero, R., Schmidt-Kastner, R., Sick, T. J., and Perez-Pinzon, M. A. (2002). Improvement in neuronal survival after ischemic preconditioning in hippocampal slice cultures. *Brain Res.*, 952(2), 153-158.

Yaffe, K., Barrett-Connor, E., Lin, F., and Grady, D. (2002). Serum lipoprotein levels, statin use, and cognitive function in older women. *Arch Neurol.*, 59(3), 378-384.

Yamazaki, T., Koo, E. H., and Selkoe, D. J. (1996). Trafficking of cell-surface amyloid beta-protein precursor. II. Endocytosis, recycling and lysosomal targeting detected by immunolocalization. *J Cell Sci,* 109, 999-1008.

Yamazaki, T., Selkoe, D. J., and Koo, E. H. (1995). Trafficking of cell surface beta-amyloid precursor protein: retrograde and transcytotic transport in cultured neurons. *J Cell Biol,* 129, 431-442.

Yang, A. J., Knauer, M., Burdick, D.A., and Glabe, C. (1995). Intracellular A beta 1-42 aggregates stimulate the accumulation of stable, insoluble amyloidogenic fragments of the amyloid precursor protein in transfected cells. *J Biol Chem.*, 270(24), 14786-14792.

Yang, E., Kim, H., Lee, J., Shin, J. S., Yoon, H., Kim, S. J., and Choi, I. H. (2004). Overexpression of LIM kinase 1 renders resistance to apoptosis in PC12 cells by inhibition of caspase activation. *Cell Mol Neurobiol.*, 24(2), 181-192.

Yang, N., Higuchi, O., Ohashi, K., Nagata, K., Wada, A., Kanagawa, K., Nichida, E., and Mizuno, K. (1998). Cofilin phosphorylation by LIM-kinase 1 and its role in Rac-mediated actin reorganization. *Nature,* 393, 809-812.

Yankner, B.A., Caceres, A., and Duffy, L. K. (1990a). Nerve growth factor potentiates the neurotoxicity of beta amyloid. *Proc Natl Acad Sci U S A.*, 87, 9020-9023.

Yankner, B.A., Duffy, L. K., and Kirschner, D. A. (1990b). Neurotrophic and neurotoxic effects of amyloid beta protein: reversal by tachykinin neuropeptides. *Science,* 250, 279-282.

Ye, C., Walsh, D. M., Selkoe, D. J., and Hartley, D. M.(2004). Amyloid b-protein induced electrophysiological changes are dependent on aggregation state: N-

methyl-D-aspartate (NMDA) versus non-NMDA receptor/channel activation. *Neuroscience Letts,* 366, 320-325.

Yrjanheikki, J., Keinanen, R. Pellikka, M., Hokfelt, T., and Koistinaho, J. (1998). Tetracyclines inhibit microglial activation and are neuroprotective in global brain ischemia. *Proc Natl Acad Sci U S A*, 95(26), 15769-15774.

Zalk, R., Israelson, A., Garty, E. S., Azoulay-Zohar, H., and Shoshan-Barmatz, V. (2005). Oligomeric states of the voltage-dependent anion channel and cytochrome c release from mitochondria. *Biochem J.*, 386(Pt 1), 73-83.

Zechel, K., & Weber, K. (1978). Actins from mammals, bird, fish and slime mold characterized by isoelectric focusing in polyacrylamide gels. *Eur J Biochem.*, 89(1), 105-112.

Zhang, Z., Rydel, R. E., Drzewiecki, G. J., Fuson, K., Wright, S., Wogulis, M., Audia, J. E., May, P. C., and Hyslop, P. A. (1996). Amyloid beta-mediated oxidativeand metabolic stress in rat cortical neurons: no direct evidence for a role for H2O2 generation. *J Neurochem.* 67, 1595-1606.

Zhao, L., Ma, Q. L., Calon, F., Harris-White, M. E., Yang, F., Lim, G. P., Morihara, T., Ubeda, O. J., Ambegaokar, S., Hansen, J. E., Weisbart, R. H., Teter, B., Frautschy, S. A., and Cole, G. M. (2006). Role of p21-activated kinase pathway defects in the cognitive deficits of Alzheimer disease. *Nat Neurosci.*, 9(2), 234-242.